

SUPERVISORY BOARD

Head of Chemistry Department, Faculty of Mathematics and Natural Sciences, Lambung Mangkurat University

PUBLISHER

Chemistry Department, Faculty of Mathematics and Natural Sciences, Lambung Mangkurat University

MAILING ADDRESS

Jl. A. Yani Km. 36 Banjarbaru, Kalimantan Selatan , Indonesia 70714
Phone: 0511-4773112, 0511-4782899
Email: jstk@ulm.ac.id

FIRST EDITION: 2007

EDITOR IN CHIEF

Utami Irawati, S.Si., MES., Ph.D.

EDITORIAL BOARD

Head of Editorial Board : Prof. Rodiansono, S.Si., M.Si., PhD

Associate Editors : Dahlena Ariyani, S.Si., M.S.
Dewi Umaningrum, S.Si., M.Si.

Section Editors : Noer Komari, S.Si., M.Kes (*regular section*)
Kholifatu Rosyidah, S.Si., M.Si. (*SN-STPK section*)
Maria Dewi Astuti, S.Si., M.Si. (*Sainstek 5 section*)

Editorial Board Members:

Prof. Dr. Rer.nat Drs. Karna Wijaya, M.Eng (UGM, Yogyakarta)
Dr. Hendrik Oktendy Lintang (Universitas Ma Chung, Malang)
Yuana Nurulita, S.Si, M.Si, Ph.D (Universitas Riau, Riau)
Prof. Dr. Abdullah, S.Si, M.Si (Universitas Lambung Mangkurat, Banjarbaru)
Dr. Arnida, S.Si. M.Si. Apt. (Universitas Lambung Mangkurat, Banjarbaru)
Dr. Rahadian Zainul, S.Pd., M.Si. (Universitas Negeri Padang, Padang)
Prof. Sunardi, S.Si., M.Sc., Ph.D. (Universitas Lambung Mangkurat, Banjarbaru)
Edi Mikrianto, S.Si., M.Si. (Universitas Lambung Mangkurat, Banjarbaru)

SITE EDITOR AND ADMINISTRATOR

Ahmad Rusadi Arrahimi, S.Kom., M.Kom.
Shofia Qolby, S.Si.

ABOUT US

(Jurnal Ilmiah Berkala) Sains dan Terapan Kimia publishes scientific articles in the Chemistry field which include, but not limited to, research in chemistry, theoretical chemistry, chemistry education, and applied chemistry. This journal also publishes review articles about the development of chemistry. All the articles in this journal will go through a peer-review process to ensure that the quality of the article meets our standard before being published. Each article submitted to our journal will be reviewed by a reviewer having the expertise in the field. Shall the article submitted is deemed acceptable to be published in our journal, it is the writer's responsibility to make the necessary change and revision as recommended by the reviewer.

This journal is open access journal which means that all content is freely available without charge to users or / institution. Users are allowed to read, download, copy, distribute, print, search, or link to full text articles in this journal without asking prior permission from the publisher or author.

Sains dan Terapan Kimia (Jurnal Ilmiah Berkala) is published twice a year on January and July. There is no fee for authors to submit their manuscripts to be considered for publication in this journal. When the article is accepted for the publication. The publication fee is IDR 500.000,00 that covers article processing and DOI processing charge, and one copy of the printed out edition of the journal. The publication fee is for articles being submitted in English. You can still submit the article in Bahasa Indonesia, however, there will be additional IDR 250.000,00 charge for the translation service. The publication fee does not cover shipping fee. If required, authors can ask for additional printed out edition which cost IDR. 60.000,00 per copy. Payment should be made by bank transfer to this account below

Bank : BNI Banjarmasin
Account Number : **0201041846**
Account Name : Dahlena Ariyani

Please send a confirmation of your proof of payment to dariyani@ulm.ac.id

TABLE OF CONTENTS

The Effect of Drying Method on Potential Antioxidants in Ethanol Extract of <i>Sungkai</i> Leaf (<i>Parenoma Canescens</i> Jack.) Simplicia from Kalimantan	1-8
Fahrina Kasumawati, Siti Hasnah	
Isolation and Characterization of Compounds from Cinnamon Oil (<i>Cinnamomum burmanii</i>) Distillation Residu	9-17
Maria Dewi Astuti, Latifah Fauzi, Kamilia Mustikasari	
Toxicity Testing of White Kapul Fruit Rind Extract (<i>Baccaurea macrocarpa</i>) and Component Analysis using Chromatography Method	18-27
Kholifatu Rosyidah, Lisda Karmila, Maria Dewi Astuti	
The Effect of Hydrolysis Time Using Microwave on Bioethanol Production from Sorghum Waste (<i>Sorghum Bicolor</i> L.)	28-38
Sefrinus Maria Dolfi Kolo, Lukas Pardosi, Anita Ensiana Baru	
Study on Adsorption Kinetics of Methylene Blue by Modified Sago Frond Waste	39-48
Seniman Gempur Tirani, Sunardi	
The Effect Activated Charcoal Coffee Grounds (<i>Coffea</i> Sp.) as an Adsorbent on the Quality of the Liquid Sugar of Siwalan	49-56
Eufronius Darius, Imanuel Gauru, Febri O. Nitbani, Philiphi De Rozari	
Design of Vaccine Candidate Based on Ebola Virus Epitop With In-Silico Approach	57-63
Erwin Prasetya Toepak, Sari Namarito Simarmata, Sudarman Rahman, Stevin Carolius Angga	
Moringa Leaf (<i>Moringa oleifera</i> L) Flavonoids Utilization in Suppressing Growth of <i>Aedes aegypti</i> Larvae	64-74
Vinsensius Manek Ati, Ermelinda D. Meye, Refli, Alfred O. M. Dima, Djeffry Amalo, Ursula Luhur Jebatu	

The Effect of Drying Method on Potential Antioxidants in Ethanol Extract of *Sungkai* Leaf (*Parenoma Canescens* Jack.) Simplicia from Kalimantan

Pengaruh Pengeringan Simplicia Terhadap Potensi Antioksidan Ekstrak Etanol Daun Sungkai (*Parenoma Canescens* Jack.) Asal Kalimantan

Fahrina Kasumawati^{1,*}, Siti Hasnah²

¹Pharmacy Laboratory, Lambung Mangkurat University, Banjarbaru, Indonesia

²Chemistry Laboratory, Lambung Mangkurat University, Banjarbaru, Indonesia

*Email: fahrinakasumawati@gmail.com

ABSTRACT

Sungkai (*P. canescens*) is a medicinal plant whose leaves are used to alleviate fever and strengthen the body's immune system. This study aimed to determine the effect of the simplicia drying technique on the antioxidant potential of the ethanol extract of *Sungkai* leaves from Kalimantan. The drying method employed was oven drying at 70°C, oven drying at 50°C, sun drying, and wind drying. The study's findings indicated that the antioxidant activity of all drying techniques was in the very active category. The drying method with the lowest antioxidant potential was oven drying at 50°C with IC₅₀ value of 13.340 ppm, wind drying with IC₅₀ value of 14.610 ppm, sun drying with IC₅₀ value of 16.799ppm, and oven drying at 70°C with IC₅₀ value of 17.034 ppm.

Keywords: *Sungkai* leaf ; IC₅₀; antioxidant

ABSTRAK

Tanaman daun Sungkai (*P. canescens*) merupakan tanaman obat yang digunakan untuk mengobati demam dan meningkatkan imun tubuh. Tujuan dalam penelitian ini mengetahui pengaruh pengeringan simplicia terhadap potensi antioksidan ekstrak etanol daun sungkai (*P. canescens* Jack.) dari Kalimantan. Metode pengeringan yang digunakan adalah pengeringan oven 70°C, oven 50°C, matahari dan kering angin. Hasil penelitian didapatkan bahwa aktifitas antioksidan untuk semua metode pengeringan pada tanaman daun sungkai (*P. canescens*) ini memiliki aktifitas antioksidan termasuk dalam kategori sangat aktif. Metode pengeringan dilihat berdasarkan potensi antioksidan yang paling rendah adalah oven 50°C nilai IC₅₀ 13,340 ppm, kering angin nilai IC₅₀ 14,610 ppm, matahari nilai IC₅₀ 16,799 ppm dan oven 70°C nilai IC₅₀ 17,034 ppm

Kata kunci: daun *Sungkai*; IC₅₀; antioksidan

Submitted: October 6, 2021; **Accepted:** February 4, 2022; **Available online:** March 8, 2022

1. INTRODUCTION

Sungkai (*P. canescens* Jack.) is a common plant. The Katingan Dayak tribes have traditionally employed the leaves of the *P. canescens* plant to allivate fever and boost overall immunity. Several studies have been conducted to confirm the efficacy of *Peronema canescens* scientifically.

Biologically, antioxidants are substances that can counteract or inhibit the antagonistic activity of oxidant compounds in the body. Antioxidants work by donating electrons to free radical molecules, inhibiting the action of free radical compounds. The balance of oxidants is crucial for the body. Excessive oxidant levels will compromise cell membrane integrity and affect the organelles and activity of body cells. Therefore, antioxidants are crucial for the body (Winarso, 2007). Based on practical use by the community, *P. canescens* leaves have been used to increase body immunity. According to several studies, antioxidants have been shown to increase the body's immunity (Sayuti & Yenrina, 2015).

The drying technique strongly influences the content of active ingredients in plants. Each plant reacts differently. Some plants are susceptible to direct sunlight and excessive heat. Proper drying results in high-quality *simplicia* with a long shelf life and no change in the active components (Manoi, 2006). Based on this description, this study aimed to investigate the effect of the *simplicia* drying technique on *Sungkai* leaf (*Peronema canescens* Jack.) from Kalimantan by employing the oven drying method at 50°C, oven drying method at 70°C, sun drying, and wind drying. This study examined the *simplicia* of *Sungkai* leaf (*P. canescens* Jack.) to determine the ideal drying technique for obtaining the highest antioxidant quality.

2. MATERIALS AND METHODS (Times New Roman 12 pts, bold, all capital letters)

2.1. Materials

The materials used were *Sungkai* leaf (*Peronema canescens* Jack.), filter paper, 96% ethanol, aquadest, DPPH (1.1-diphenyl-1-picrylhydrazil), and methanol (p.a). The tools used were analytical balance, oven, porcelain dish, glass beaker, test tube, macerator, water bath, spectrophotometer, vortex, drying cabinet, and rotary evaporator.

2.2. Material processing and drying of *simplicia*

Samples were taken from the Banjarbaru Botanical Gardens, South Kalimantan Province. The leaves of *P. canescens* taken were mature leaves. The fresh leaves were then sorted to separate other plant parts and impurities. Next, the *P. canescens* leaves were rinsed with running water to keep them clean and dirt-free. *P. canescens* leaves were chopped to reduce the size and facilitate the drying and size reduction process. Samples were dried in an oven at 50°C, 70°C, wind-dried, and under the sunlight. Next, the dried *P. canescens* leaves were sorted to separate the remaining impurities.

2.3. Production of Ethanol Extract from *Sungkai* Leaf (*Peronema canescens* Jack.)

The maceration method was used to extract *P. canescens* leaf using ethanol as the solvent. A total of 35 g of fresh samples of *P. canescens* leaf were dried and ground into *simplicia* powder, then put into a macerator, added with 600 mL of ethanol until the *simplicia* was submerged, and then stirred every 6-8 hours at room temperature. Extraction was carried out for 3 days (re-maceration) with solvent replacement every 1 x 24 hours. The liquid extract was filtered through filter paper to separate the powdered *simplicia* from the liquid extract. The liquid extract of *P. canescens* leaves was concentrated using a waterbath at 50°C to obtain a constant weight

(Leksono et al., 2018). Next, the percentage of extract obtained was calculated. The yield percentage is calculated using the following equation:

$$\text{Yield} = \frac{\text{weight of extract obtained}}{\text{weight of simplicia}} \times 100\%$$

2.4. Moisture Content (Drying Loss)

Two grams of *P. canescens* leaf simplicia powder was weighed in a silica crucible that had been heated at 105°C and calibrated. The simplicia was flattened by shaking the silica crucible. The open silica crucible was put into the oven and then dried at 105°C to a constant weight. The moisture content is calculated using the equation:

$$\text{moisture content} = \frac{\text{initial weight of sample} - \text{final weight of sample}}{\text{initial weight of sample}} \times 100\%$$

2.5. Antioxidant Activity Test

a. Preparation of DPPH solution

A total of 4 mg of DPPH powder was dissolved with 25 mL of methanol (p.a) in a 25 mL flask and stirred until homogeneous to obtain a DPPH solution with a concentration of 0.4 mM (Mardiah et al., 2017).

b. Determination of the maximum wavelength of DPPH

A total of 1 mL of 0.4 mM DPPH solution was added with 4 mL of methanol (p.a). The solution mixture was then vortexed and left in the dark for 30 minutes. The absorption of the solution was measured at a wavelength of 500-550 nm (Mardiah et al., 2017).

c. Preparation of sample solution

A total of 2.5 mg of *P. canescens* leaf ethanol extract was dissolved with sufficient methanol, then put into a 25 mL volumetric flask, and methanol was added until it reached the limit mark. This process produced a sample solution of 100 ppm. The sample solution of 100 ppm was diluted into series with concentrations of 5, 10, 15, 20, and 25 ppm using a 10 mL volumetric flask. A total of 4 mL of each sample solution with concentrations of 5, 10, 15, 20, and 25 ppm

were taken, then added with 1 mL of 0.4 mM DPPH solution. The sample solution was vortexed and allowed to stand in the dark for a predetermined time.

d. Determination of IC50 Value

The antioxidant activity of the ethanol extract of *P. canescens* leaves was expressed in the percentage of inhibition. The % inhibition value was calculated using the equation:

$$\% \text{ inhibition} = \frac{(A_{\text{blank}} - A_{\text{sample}})}{A_{\text{sample}}} \times 100\%$$

The IC₅₀ value was obtained from a linear curve with the equation $y = a + bx$, resulting from the regression between concentration and % inhibition. The formula for calculating the IC₅₀ value is:

$$IC_{50} = \frac{50 - a}{b}$$

2.6. Data Analysis

Data were analyzed using SPSS statistical test for oven drying at 70°C, oven drying at 50°C, wind drying, and sun-drying. The analysis determined the best simplisa drying technique of the four methods employed.

3. RESULTS AND DISCUSSION

3.1. Sample preparation and leaf drying of *P. canescens*

The sample used in this study was the leaf part of the *P. canescens* plant obtained from the Banjarbaru Botanical Garden, South Kalimantan. Samples were gathered from the same location to ensure uniform chemical composition. Furthermore, wet sorting was carried out to separate dirt, or foreign material from *P. canescens* leaf. The material was washed with clean water to eliminate any remaining contaminants, and the simplicia was drained to remove any remaining water. Furthermore, chopping was carried out to increase the surface area to facilitate the drying process. Four ways

of drying were used: oven drying at 50°C, oven drying at 70°C, sun drying, and wind drying.

The drying method employed an oven drying at 50°C for 6 hours, an oven drying at 70°C for 4 hours, sun drying for 3 days (hot conditions), and wind drying for 10 days (hot weather conditions). After drying, the sample was sorted to separate the remaining impurities. After that, the sample was ground using a blender and sieved with a mesh size of 25.

3.2. Extraction process

P. canescens leaf was extracted by cold method, namely maceration. This approach was chosen because it does not involve heating to avoid possible damage to the active compound (Wikanta et al., 2012). Additionally, the procedure is quick, simple, and ideal for the extraction of high amount of samples (Mailoa et al., 2013).

Extraction of *P. canescens* powder was carried out by soaking 35 g of powder from the drying methods in 96% ethanol solvent for 3×24 hours at room temperature and stirring every 6 hours. Maceration was carried out for 3×24 hours. More than three days of maceration might lead to over-saturation of the powder, preventing its compounds from being extracted optimally. *P. canescens* leaf powder obtained by oven drying at 50°C yielded a 6.39 g thick extract with an 18.257% yield. It means that there are 18.257 g of extract in every 100 grams of *P. canescens* leaf. *P. canescens* leaf powder from oven drying at 70°C produced a thick extract of 7.4 g or a yield of 21.142%. *P. canescens* leaf powder from sun drying produced a thick extract of 6.91 g or

a yield of 19.742%. *P. canescens* leaf powder from wind drying resulted in a thick extract of 5.77 g or a yield of 16.485%.

The organic solvent used in the extraction process was 96% ethanol. The resulting extract was filtered through Whatman filter paper to remove any remaining powder grains in the liquid extract. The maceration product was concentrated using a rotary evaporator. The results of the rotary evaporator were re-evaporated using a water bath at 50°C to obtain a thick extract with a constant weight.

The yield value is needed to estimate the amount of extract obtained during the extraction process. In addition, the yield data also has a relationship with the active compounds contained in the sample. So that if the amount of yield increases, the number of active compounds contained in it is also increasing.

3.3. Moisture content (drying loss)

Determination of drying loss aims to provide a limit or range of the amount of water and volatile compounds lost during the drying process. Measurement of residual substances was carried out by drying at 105°C for 30 minutes to constant weight. The results of determining the drying loss of *P. canescens* leaf simplicia with several drying methods are presented in Table 1. From Table 1, it can be seen that from the oven drying method at 70°C, oven drying at 50°C, sun drying, and wind drying, the drying loss values differ, which is not more than 10%. According to the Indonesian Ministry of Health (1995), the drying loss value range is not more than 10%.

Table 1. Moisture content of *P. canescens* leaves simplicia

Method	Drying Loss (%)		
	Replication 1	Replication 2	Replication 3
Oven 50°C	5,5	5,5	5,5
Oven 70°C	5,5	6	6
Sun-dry	6	6,5	6,5
Wind-dry	6	6,5	6,5

It indicates that all the simplicia of the four drying methods meet the requirements. The replication results obtained the same value because the measurements were carried out 3 times in the same solution. The quality of the drying process is said to be getting better if the drying shrinkage value is getting smaller.

3.4. Determination of the maximum wavelength of DPPH

The maximum wavelength is determined to ascertain the wavelength of the substance that delivers the greatest absorbance and sensitivity at each concentration (Robinson et al., 2005). Measurement at the maximum wavelength produces linear findings, increases instrument sensitivity, and minimizes measurement errors (Sadeli, 2016). The DPPH approach was chosen due to the compounds' higher stability than other methods.

The antioxidant activity of *P. canescens* extract was determined using the DPPH radical absorption method on a UV-Vis spectrophotometer, which quantifies the amount of antioxidant activity present in the extract to reduce free radicals. The maximum wavelength used was 516 nm. This maximum wavelength range follows the literature mentioned by Molyneux (2004) between 515 – 520 nm. The maximum range was reached with DPPH in its complementary purple color. The IC₅₀ value expresses the DPPH method. The IC₅₀ value is the concentration of the sample required to inhibit DPPH free radicals by 50%. Antioxidant capabilities are enhanced by a lower IC₅₀ value (Molyneux, 2004).

3.5. Determination of IC₅₀ value of quercetin comparison solution

Determination of the IC₅₀ value of quercetin is needed as a positive control in the antioxidant activity test of the sample. Positive control was used as a comparison to determine the amount of antioxidant activity possessed. Quercetin was chosen due to its high antioxidant activity

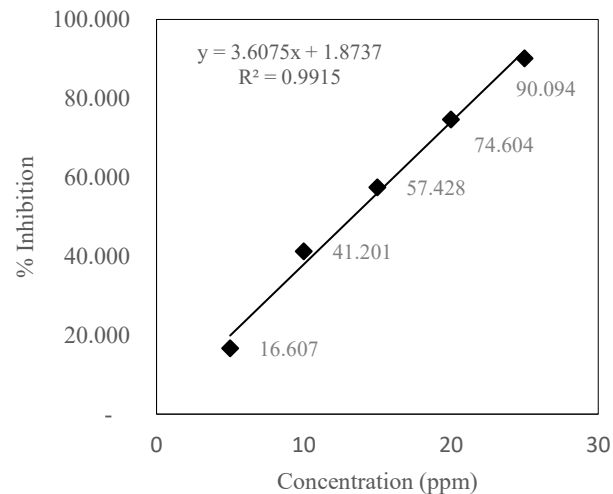
(Adawiyah & Rizki, 2018). According to Yulistati, F.R (2021), a study of the IC₅₀ measurement of quercetin as a positive control used 5 concentrations series (1, 2, 3, 4, 5 ppm). The IC₅₀ value of quercetin obtained was 2.754 ppm. The anticoagulant activity of quercetin was classified as very strong based on its IC₅₀ value.

3.3. Determination of IC₅₀ value of ethanol extract from *P. canescens* leaves

The IC₅₀ value of the ethanol extract of *P. canescens* leaf from oven drying at 70°C, oven drying at 50°C, sun drying, and wind drying was obtained by preparing 5 concentrations, namely 5, 10, 15, 20, 25 ppm in methanol (p.a). One ml of DPPH solution was added to each concentration and incubated for 30 minutes. Furthermore, measurements were taken at a maximum wavelength of 516 nm (Maulina, 2014; Sumaryanto, 2019). The absorbance value was measured to determine the percent inhibition. This percentage of inhibition indicates the free radical activity of each sample (Jatmika et al., 2015). Percent inhibition refers to a sample's ability to block the activity of free radicals in proportion to its concentration. The percentage of inhibition obtained from the difference in absorption between the control absorbance and the sample was measured using a UV-Vis Spectrophotometer (Anggresani et al., 2017). The IC₅₀ value of each sample concentration was calculated using the linear regression equation formula, which states the relationship between the concentration expressed by the x-axis and the percentage of inhibition expressed by the y-axis of the measurement replication series. The results of the percentage inhibition of the ethanol extract of *P. canescens* leaves from oven drying at 70°C, oven drying at 50°C, sun drying, and wind drying are presented in Table 2. The graph of the relationship between concentration and % inhibition of the oven drying at 50°C is presented in Fig. 1.

Table 3. Percentage of inhibition and IC₅₀ of ethanol extract of *P. canescens* leaves from oven drying at 70°C, oven drying at 50°C, sun drying, and wind drying

Concentration (ppm)	Percent Inhibition (%) of Replication			Regression Equation	IC ₅₀ (ppm)
	1	2	3		
5	12.539	12.539	12.539	Y = 2.843 x + 1.5697 R = 0.9831	17.034
10	34.562	34.562	34.562		
15	43.414	43.414	43.414		
20	59.325	59.325	59.325		
25	71.232	71.232	71.232		
Oven drying 50°C					
5	16.607	16.607	16.607	Y = 3.6075 x + 1.8737 R = 0.9915	13.340
10	41.201	41.201	41.201		
15	57.428	57.428	57.428		
20	74.604	74.604	74.604		
25	90.094	90.094	90.094		
Sun drying					
5	11.380	11.380	11.380	Y = 3.2898x - 5.2024 R = 0.9782	16.779
10	25.289	25.289	25.289		
15	44.573	44.573	44.151		
20	66.701	66.701	66.701		
25	72.918	72.918	72.918		
Wind drying					
5	17.555	17.555	17.555	Y = 3.2472x + 2.5583 R = 0.9939	14.610
10	34.773	34.773	34.773		
15	54.794	54.794	54.794		
20	66.174	66.174	66.174		
25	83.034	83.034	83.034		

**Figure 1.** The relationship between concentration and % inhibition of oven drying method at 50°C

Based on the IC₅₀ value, all *P. canescens* leaf extract drying methods were categorized as very active due to their IC₅₀ values ranging between 50 and 100 ppm. The IC₅₀ value is used to measure a sample's antioxidant capacity.

The results indicate that all extracts obtained by the drying technique had good antioxidant activity. The ethanol extract of the oven drying at 50°C has a lower IC₅₀ value than other drying techniques. The best drying technique based on the IC₅₀ was oven drying at 50°C, wind drying, sun drying, and oven drying at 70°C. The smaller the IC₅₀ value, the higher the antioxidant activity. The statistical test showed that the four drying methods were not significantly different. Based on the Uses Harmonic Mean Sample Size = 5,000, less than the significance level ($\alpha=0.05$).

4. CONCLUSIONS

From the findings of this study, it can be concluded that ethanol extract from the drying of *Sungkai* leaf (*P. canescens*) by oven drying at 50°C resulted in a lower IC₅₀ value than the oven drying at 70°C, sun drying, and wind drying. The antioxidant potential of the ethanol extract of *Sungkai* leaf (*P. canescens*) based on the drying technique was assessed based on the IC₅₀ value, and the lowest was oven drying at 50°C, wind drying, sun drying, and oven drying at 70°C.

ACKNOWLEDGMENT

Funding: This work was supported by Education Laboratory Institution Competency Research Grant.

LIST OF REFERENCES

- Adawiyah, R & M. I. Rizki. (2018). Aktivitas Antioksidan Ekstrak Etanol Akar Kalakai (*Stenochlaena palustris* Bedd) Asal Kalimantan Tengah. *Jurnal Pharmascience*, 5, 71-77.
- Anggraeni, Y., E. Hendradadi & T. Purwanti. (2012). Karakteristik Sediaan dan Pelepasan Natrium Diklofenak dalam Sistem Niosom dengan Basis Gel Carbomer 940. *Pharmascientia*, 1(1), 1-10.
- Leksono, W.B., R. Pramesti, G.W. Santoso & W.A. Setyati. (2018). Jenis Pelarut Metanol dan n-Hexane terhadap Aktivitas Antioksidan Ekstrak Rumput Laut *Gelidium* sp. Dari Pantai Drini Gunungkidul-Yogyakarta. *Jurnal Kelautan Tropis*. 21, 9-16.
- Mailoa, M. N., Mahendradatta, A. Laga & N. Djide. (2013). Tannin Extarct of Guava Leaves (*P. guajava* L). Variation with Concentration Organic Solvents. *International Journal of Scientific & Technology Research*, 2, 106-110.
- Manoi, F. (2006). Pengaruh Cara Pengeringan Terhadap Mutu Simplisia Sambiloto. *Bull Littro*, 17 (1), 1-5.
- Mardiah, N., C. Mulyanto, A. Amelia, Lisnawati, D. Anggraeni & D. Rahmawaty. (2017). Penentuan Aktivitas Antioksidan dari Ekstrak Kulit Bawang Merah (*Allium ascalonium* L.) dengan Metode DPPH. *Jurnal Pharmascience*, 4, 147-154.
- Maulina, R. (2014). *Penentuan Nilai Sun Protection Factor (SPF) dan Aktivitas Antioksidan Ekstrak Kulit Batang Bangkal (N. subdita) secara in vitro*. Skripsi. Fakultas Matematika dan Ilmu Pengetahuan Alam, Universitas Lambung Mangkurat. Banjarbaru.

- Molyneux, P. (2004). The Use of Stable Free Radical Diphenylpicrylhydrazyl (DPPH) for Estimating Antioxidant Activity. *Songklanakarin Journal of Sciences*. 26, 211-219.
- Robinson, J. W., E. M. S. Frame, G. M., Frame II. (2005). *Undergraduate Instrumental Analysis 6th Edition*. Marcel Dekker. New York.
- Sadeli, R. A. (2016). *Uji Aktivitas Antioksidan dengan Metode DPPH (1,1 diphenil-2-picrylhydrazyl Ekstrak Bromelain Buah Nanas Ananas comosus (L.) Merr.)*. Skripsi. Fakultas Farmasi Universitas Sanata Dharma.
- Sayuti, K., & R. Yenrina. (2015). *Antioksidan Alami dan Sintetik*. Andalas University Press, Padang.
- Winarso, H. (2007). *Antioksidan alami dan radikal bebas*. Kanisius, Yogyakarta
- Wikanta, T., D. Gusmita, L. Rahayu, E. Marraskuranto. (2012). Kajian awal Bioaktivitas Ekstrak Etanol dan Fraksinya dari Spons *Callyspongia* sp. Terhadap Sel Lestari Tumor Hela. *JPB Perikanan*, 1, 1-10.
- Yulistati, F.R. (2021). *Uji Farmakognostik dan Antioksidan Ekstrak Metanol Daun Sungkai (Peronema canescens Jack.) Asal Kalimantan Selatan*. Skripsi. Program Studi Farmasi. Universitas Lambung Mangkurat.

Isolation and Characterization of Compounds from Cinnamon Oil (*Cinnamomum burmanii*) Distillation Residu

Isolasi dan Karakterisasi Senyawa dari Residu Distilasi Minyak Kayu Manis (*Cinnamomum burmanii*)

Maria Dewi Astuti^{1,*}, Latifah Fauzi¹, Kamilia Mustikasari¹

¹Chemistry Study Program, Faculty of Mathematics and Natural Sciences, Lambung Mangkurat
University, Banjarbaru, Indonesia

*Email: mdastuti@ulm.ac.id

ABSTRACT

This study aimed to isolate and characterize compounds from the distillation residue of cinnamon oil from Loksado, South Kalimantan. Cinnamon (*Cinnamomum burmanii*) distillation residue was extracted with methanol as solvent. The methanol extract was fractionated by liquid vacuum chromatography to obtain fractions A, B, C, and D. The crystals contained in fraction C were washed with cold *n*-hexane to obtain 5.4 mg of yellow isolate (FC1). FC1 isolates were characterized by UV-Vis, IR, ¹H-NMR, and ¹³C-NMR spectrophotometers. UV spectra showed a maximum wavelength at 307, 316, and 321 nm indicating the presence of a conjugated or aromatic system. The infrared spectra showed -C=O, -OH, C-O, C-H, C-N, and C=N groups. The ¹H-NMR spectra showed the presence of aromatic protons at 6.38 ppm (1H, d, J=9.5 Hz), 7.67 ppm (1H, d, J=9.5 Hz), 7.29 ppm (1H, d, J=8 Hz), 7.44 ppm (1H, d, J=8 Hz), and 7.49 ppm (1H, t) and there was a methyl proton (acetyl group) at H 2.13 ppm (3H,s). The ¹³C-NMR spectra showed the presence of a C=O ketone group at 207.26 ppm and there were 9 C-sp² at 116.9; 119.0; 124.6; 128.1; 132.0; 143.7; 154.3; 161.0 ppm, which δ_C 161.0 ppm was C-oxyaryl. Based on UV, IR, ¹H and ¹³C-NMR spectra data, FC1 isolate was suggested as an isoquinoline alkaloid substituted by OH and acetyl groups.

Keywords: distillation residu, *Cinnamomum burmanii*, alkaloid, isoquinoline.

ABSTRAK

Penelitian ini bertujuan untuk mengisolasi dan mengkarakterisasi senyawa dari residu distilasi minyak kayu manis asal Loksado, Kalimantan Selatan. Residu distilasi kayu manis (*Cinnamomum burmanii*) diekstraksi dengan pelarut metanol. Ekstrak metanol difraksinasi secara kromatografi vakum cair sehingga diperoleh fraksi A, B, C, dan D. Kristal yang terdapat pada fraksi C dicuci dengan *n*-heksana dingin sehingga diperoleh isolat berwarna kuning (disebut FC1) sebanyak 5,4 mg. Isolat FC1 dikarakterisasi dengan spektrofotometer UV-Vis, IR, ¹H-NMR dan ¹³C-NMR. Spektra UV menunjukkan terdapat panjang gelombang maksimum pada 307, 316, dan 321 nm menunjukkan adanya sistem terkonjugasi atau aromatis. Spektra infra merah menunjukkan terdapat gugus -C=O, -OH, C-O, C-H, C-N dan C=N. Spektra ¹H-NMR memperlihatkan adanya proton aromatis pada pergeseran kimia δ_H 6,38 ppm (1H, d, J=9,5 Hz), 7,67 ppm (1H, d, J=9,5 Hz), 7,29 ppm (1H, d, J=8 Hz), 7,44 ppm (1H, d, J=8 Hz), dan 7,49 ppm (1H, t) serta terdapat proton metil (gugus asetil) pada δ_H 2,13 ppm (3H,s). Spektra ¹³C-NMR menunjukkan adanya gugus C=O keton pada pergeseran δ_C 207,26 ppm dan terdapat 9 C-sp² pada δ_C 116,9; 119,0; 124,6; 128,1; 132,0; 143,7; 154,3; 161,0 ppm, dimana δ_C 161,0 ppm merupakan C-oksiaril. Berdasarkan data spektra UV, IR, ¹H dan ¹³C-NMR maka isolat FC1 disarankan sebagai senyawa alkaloid isokuinolin yang tersubstitusi oleh gugus OH dan asetil.

Kata Kunci: residu distilasi, kayu manis, alkaloid, isokuinolin.

Submitted: December 10, 2021; **Accepted:** February 18, 2022; **Available online:** March 8, 2022

1. INTRODUCTION

Cinnamon (*Cinnamomum burmanii*) belongs to the Lauraceae family and is one of the leading commodities of South Kalimantan, particularly the South Hulu Sungai area. The productivity of cinnamon from the Loksado sub-district was 1,184.43 tons, and the Haruyan sub-district was 0.9 tons. Another cinnamon producer area was the Kotabaru district, with 24 tons (BPS South Kalimantan, 2014).

Cinnamon enhances the food and beverages flavor and is a raw material in cosmetics. Additionally, cinnamon is used in traditional medicine for various purposes, including treating toothache, cough, diarrhea, malaria, eliminating bad breath, preventing bleeding, and improving intestinal health (Al-Dhubiab, 2012; Rao & Gan, 2014). Several studies have shown that cinnamon has various activities such as antioxidant (Matthew & Abraham, 2006; Choi & Hwang, 2005; Prasad et al., 2009), antibacterial (Shan et al., 2007; Prasetyaningrum et al., 2012), anti-inflammatory (Khatib et al., 2005), antidiabetic (Kim et al., 2006), and anticancer (Lu et al., 2010).

These various bioactivities and the distinctive aroma of cinnamon are caused by the various compounds, such as essential oils, consisting of various compounds from the monoterpenoid, sesquiterpenoid, or phenylpropanoid groups. In addition to essential oils, cinnamon contains other compounds such as flavonoids, saponins, tannins, alkaloids, steroids, and lignans (Safratilofa, 2016; Yuan et al., 2017).

Cinnamon essential oil from Loksado contains 9 compounds, namely cinnamaldehyde (75.59%), cinnamyl acetate (17.40%), bornyl acetate (1.74%), copaene (1.63%), 1,8-cineol (1.35%), -terpineol (0.77%), limonene (0.59%), pinene (0.48%), and bicyclo 3.1.1 heptane (0.44%) (Astuti et al., 2018). Prasetyaningrum et al. (2012) stated a total phenol content of 28.563 mg/mL in cinnamon extract (*C. burmanii*),

while in the residual distillation, there was a total phenol content of 15.975 mg/mL. Several phenolic compounds are identified in *Cinnamomum*, namely 5-hydroxyethyl salicylate, syringaldehyde, p-hydroxybenzoic acid, isovanylic acid, protocatechuic acid, protocatechuic aldehyde, vanillin, vanillic acid, trans-cinnamaldehyde, cinnamyl alcohol, cinnamic acid, sinapaldehyde, litseachromolaevanes A, 4-hydroxy-1,10-seco-muurool-5-ene-1,10-dione, pinoresinol (PRO), syringaresinol, coumarin, 4-hydroxymelein, kaempferol, (-)-(2R,3R)-5,7-dimethoxy-3',4'-methylenedioxyflavan-3-ol (MFO), and decumabic acid (Li et al., 2018). Several glycosides flavonoid, including quercetin 3-O-(3",4"-di-trans-p-kumaroyl)- α -L-rhamnopyranoside and kaempferol 3-O-(3",6"-di-trans-p-coumaroyl)- β -D-glucopyranoside has been isolated from *C. cassia* (Liu et al., 2018). A lignan compound, namely cinnaburmanin A, has been isolated from the roots of *C. burmanii* (Yuan et al., 2017). The benzylisoquinoline alkaloid, cinnamolauryl, has been isolated from the *Cinnamomum* plant (Gellert & Summons, 1969). The alkaloids cinnaretamine, crykonisine, corydaldina, glaziovina, and zenkerina have been isolated from *C. philippinense* (Li et al., 2012).

Cinnamon essential oil (cinnamon oil) can be obtained by distillation. The distillation process produces dregs or residues that most likely still contain non-volatile chemical compounds such as flavonoids, saponins, tannins, or alkaloids. These compounds have various bioactivities. Flavonoids have antioxidant, anti-inflammatory, antimutagenic, and anticancer activities (Panche et al., 2016). Alkaloids act as an antibacterial, anti-inflammatory, antifungal, analgesic, and antiviral (Bribi, 2018). Saponins have anticancer and anticholesterol activity (Thakur et al., 2011). Tannins are used as lung anticancer therapy (Rajasekar et al.,

2021). Based on the description above, it can be seen that flavonoid compounds, alkaloids, saponins, and tannins have various bioactivities, and it is suspected that these compounds are still present in the cinnamon distillation residue. Therefore, it is necessary to isolate and characterize the chemical compounds from the cinnamon distillation residue from Loksado.

2. MATERIALS AND METHODS

2.1. Materials

The materials used were the distillation residue of cinnamon bark from Loksado Hulu Sungai Selatan District, silica gel 60 (Merck.), silica gel 60G (Merck.), TLC plate Silica gel GF254 (Merck.), methanol p.a (Merck.), chloroform p.a (Merck), and redistilled technical quality solvents such as methanol, n-hexane, and ethyl acetate. The tools used were glassware (measuring glass, Erlenmeyer, beaker (Pyrex), Liquid Vacuum Chromatography (KVC) column, Buchner funnel d=2 cm, porcelain dish, filter paper, analytical balance, rotary evaporator, UV-Vis spectrophotometer (Hitachi u-2100), FTIR Spectrophotometer (Thermo Nicolet IS 10), NMR spectrometer (Jeol Type JNM-ECA 500)).

2.2. Extraction

One kilogram of chopped cinnamon bark distillation residue was air-dried and then ground into a coarse powder. Cinnamon residue was macerated with methanol for 24 hours and filtered. Maceration was repeated three times. The filtrate was concentrated with a rotary evaporator and continued by heating on a waterbath until 39.79 g of methanol extract was obtained.

2.3. Search for eluent

A small amount of methanol extract was dissolved in methanol and then spotted on a Silica Gel GF254 TLC (Thin Layer Chromatography) plate and then eluted in various eluent compositions. The eluents were n-hexane:chloroform (1:9; 1:4; 3:7, 1:1) and n-hexane:ethyl acetate (2:3; 1:1).

2.4. Isolation and purity analysis.

Fractionation of cinnamon methanol extract was carried out by Vacuum Liquid Chromatography (KVC) with 60G silica gel as stationary phase (t=5 cm and column d=7 cm). The mobile phase used a gradient elution system, namely n-hexane with increased polarity with chloroform, then continued with ethylacetate single eluent. A total of 10 g of methanol extract was fractionated by KVC, obtained 4 combined fractions, namely fractions A (vials 1), B (vials 2-3), C (vials 5-10), and D (vials 11-12). There were yellow crystals in the evaporator flask at fraction C when concentrated with a rotary evaporator. Crystals were collected and washed with cold n-hexane. The washed crystal was called FC1. The rotary evaporator flask containing fraction C was rinsed with chloroform and then concentrated with a rotary evaporator, called fraction FC2. Furthermore, the FC2 fraction (60 mg) was fractionated by gravity column chromatography with n-hexane:chloroform (1:1) as eluent to produce 2 fractions, namely FC2a and FC2b fractions. FC1 and FC2b fractions were spotted on the same TLC plate with n-hexane:chloroform (1:1) eluent and showed the same R_f value. The FC1 fraction purity test was carried out by TLC in various eluents, namely n-hexane:chloroform (1:1); n-hexane:ethylacetate (1:1) and chloroform:ethylacetate (1:1), and 2-dimensional TLC with eluent 1, namely n-hexane:ethylacetate (1:1).and eluent 2, namely n-hexane:chloroform (1:1).

2.5. Structure characterization

The structural characterization of FC1 isolates was carried out using spectrophotometer UV, infrared, ¹H-NMR, and ¹³C-NMR.

3. RESULTS AND DISCUSSION

3.1. Isolation of FC1 Compound

The yield of methanol extract of cinnamon distillation residue was 3.98%. The eluent selection was carried out before fractionating the methanol extract. TLC chromatograms of methanol extracts in various eluent compositions are presented in Fig. 1.

Fig. 1f reveals that n-hexane:chloroform (1:1) TLC eluent produces better separation than n-hexane:ethyl acetate (1:1) (Fig. 1e) so that n-hexane:chloroform eluent was used as eluent for fractionation of methanol extract using KVC. Fig. 1a, 1b, 1c, and 1d show that the methanol extract was not separated properly.

Fractionation of methanol extract by KVC method employed a gradient elution system. The elution process started with a single eluent of n-hexane, followed by n-hexane:chloroform (9:1), (8:2), (7:3), and ended with ethyl acetate.

Fig. 2 shows the chromatogram of the methanol extract fractionated by KVC. Based on the TLC chromatogram pattern, the resulting fractions were grouped into 4 combined fractions, namely Fraction A, Fraction B, Fraction C, and D. There were crystals on the walls of the flask at the concentration of fraction C with a rotary evaporator, then separated and washed with cold n-hexane, called FC1. A total of 5.4 mg of FC1 isolate in the form of a yellow crystalline solid was obtained.

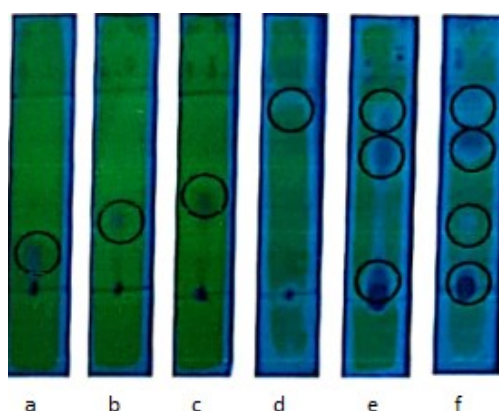


Figure 1. Chromatogram of methanol extract of cinnamon distillation residue, viewed under UV light 254 nm, stationary phase TLC silica gel GF254, mobile phase TLC (a) n-hexane:chloroform (1:9), (b) n-hexane:chloroform (1:4), (c) n-hexane:chloroform (3:7), (d) n-hexane:ethylacetate (2:3), (e) n-hexane:ethylacetate (1:1), (f) n-hexane:chloroform (1:1)

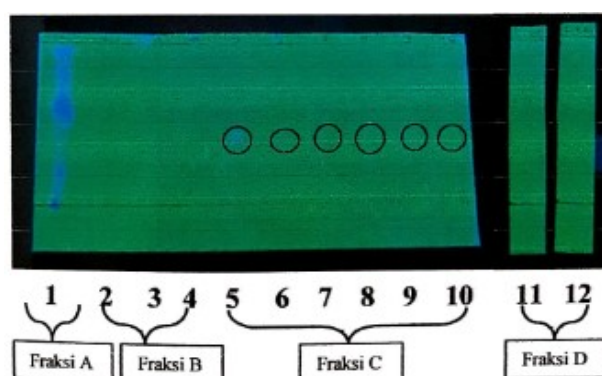


Figure 2. Chromatogram of the fractionated methanol extract of cinnamon distillation residue, viewed under UV light 254 nm, the stationary phase was Silica Gel TLC GF254, the mobile phase was n-hexane:chloroform (1:1)

The remaining fraction C in the evaporator flask was dissolved with chloroform, dried, and 60 mg FC2 was obtained. Furthermore, FC2 was fractionated by gravity column chromatography (KKG) using the fixed eluent n-hexane:chloroform (1:1) to produce 2 fractions, namely FC2(a) and FC2(b) (Fig. 3).

In Fig. 3, it can be seen that FC2(b) has one stain, so to determine whether FC2(b)

and FC1 are the same compounds, the two isolates were spotted on the same TLC plate. Fig. 4 shows that FC1 and FC2(b) have the same R_f, so it can be said that FC1 and FC2(b) are the same compounds.

The purity test was carried out on FC1 isolates in different eluents and 2-dimensional TLC. All TLC chromatograms (Fig. 5 and 6) showed one spot, so it can be stated that the FC1 isolate was pure enough to proceed with structural characterization

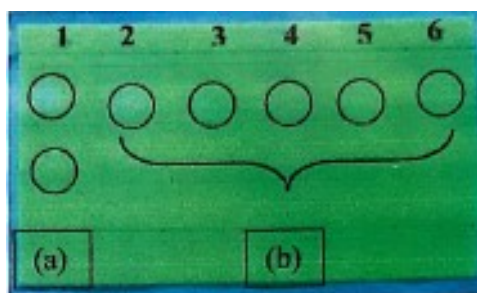


Figure 3. Chromatogram of the fractionated FC2 fraction, viewed under UV light 254 nm, the stationary phase was Silica Gel TLC GF254, the mobile phase was n-hexane:chloroform (1:1)



Figure 4. FC1 and FC2(b) TLC chromatograms, viewed under UV light at 254 nm, the stationary phase was Silica Gel TLC GF254, the mobile phase was n-hexane:chloroform TLC (1:1)

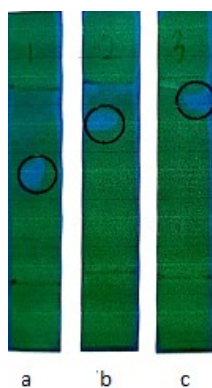


Figure 5. FC1 TLC chromatogram, viewed under UV light 254 nm, stationary phase was Silica Gel, mobile phase was GF254. (a) n-hexane:chloroform (1:1), (b) n-hexane:ethylacetate (1:1), (c) chloroform:ethylacetate (1:1)

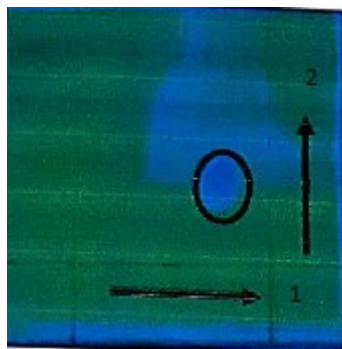


Figure 6. 2 Dimensional FC1 TLC chromatogram, viewed under UV light at 254 nm, stationary phase was Silica Gel GF254, mobile phase was 1 n-hexane:ethylacetate (1:1), 2 n-hexane:chloroform (1:1)

3.2. Compound Characterization of FC1

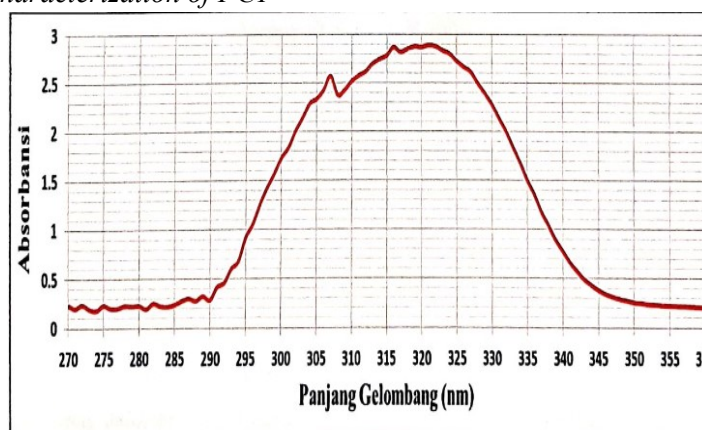


Figure 7. UV Spectra of FC1

The UV spectra of the FC1 isolate (Fig. 7) showed maximum wavelengths at 321, 316, and 307 nm. The presence of absorption at wavelengths in the UV region indicates the presence of a conjugated system chromophore or an aromatic ring, according to the simple isoquinoline framework as reported by Saidi et al. (2011). Isoquinoline alkaloid compounds, namely papralline, isolated from the *Cryptocarya rugulosa* plant (Lauraceae), showed maximum wavelengths at 325, 317, 312 nm (Saidi et al., 2011). Sulaiman et al. (2011) reported that the UV spectra of the *Litsea lancifolia* (Lauraceae) plant had a maximum wavelength at 307 nm and were a compound of N-allylaulolitsine, an alkaloid with a benzyloisoquinoline framework.

The infrared spectra show the presence of some characteristic functional group vibrations. The absorption at 3415.45 cm^{-1} is caused by the vibration of the hydroxy

functional group (-OH), which is strengthened by the presence of C-O vibrations at 1174.37 cm^{-1} . Absorption at wave number 1697.76 cm^{-1} indicates the presence of a carbonyl group (C=O). A characteristic vibration of C=C indicates the aromatic ring at 1618.95 ; 1560.62 ; 1486.74 cm^{-1} , which is also supported by the =C-H stretching vibration at a wavenumber of 3057.10 cm^{-1} and =C-H bending at 686.87 to 994.33 cm^{-1} . The aliphatic -C-H vibration appears at wave number 2954.41 cm^{-1} . Absorption at wave number 1397.20 cm^{-1} indicates the presence of C-N vibrations. The imine vibration (C=N) was found at a wavenumber of 1599.94 cm^{-1} , in accordance with the imine vibration (1599 cm^{-1}) typical of isoquinoline alkaloids as in the study of Sulaiman et al. (2011). The presence of aromatic C=C, =C-H functional groups, C-N, and C=N vibrations support the isoquinoline alkaloid framework in FC1.

The $^1\text{H-NMR}$ spectra showed several signals at a 2.13 – 7.67 ppm chemical shift. Aromatic protons appeared at a chemical shift of 6.38 – 7.67 ppm. The chemical shift H of 6.38 ppm (1H, d, $J=9.5$) and 7.67 ppm (1H, d, $J=9.5$) indicates the aromatic proton at the ortho position. Chemical shift 7.29 ppm (1H, d, $J=8$); 7.49 ppm (1H, t), and 7.44 ppm (1H, d, $J=8$) indicates the presence of 3 protons side by side. The methyl protons present in the acetyl group appear at a chemical shift of 2.13 (3H, s) (Pavia et al., 2015).

The $^{13}\text{C-NMR}$ spectra showed the presence of 9 aromatic carbon atoms (Csp^2) at the chemical shift δ_{C} 116.9; 117.1; 119.0; 124.6; 128.1; 132.0; 143.7; 154.3; 161.0

ppm. This amount of aromatic carbon (Csp^2) corresponds to the carbons in the isoquinoline skeleton alkaloids. The chemical shift δ_{C} at 161.0 ppm is oxyaryl carbon (Rodrigueza et al., 2008). The chemical shift at 31.16 ppm was an aliphatic $-\text{CH}_3$ carbon, while the ketone carbonyl carbon appeared at a chemical shift of 207.2 ppm (Pavia et al., 2015).

Based on the UV, infrared, $^1\text{H-NMR}$, and $^{13}\text{C-NMR}$ spectra data, the structure of FC1 isolate is estimated to be an alkaloid compound with an isoquinoline skeleton substituted by an OH group and an acetyl group, namely 1-(5-hydroxyisoquinoline-1-yl)ethanol, as shown in Fig. 8.

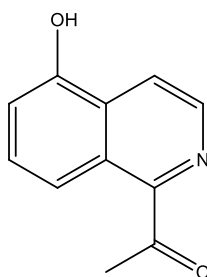


Figure 8. Structure of FC1 isolate

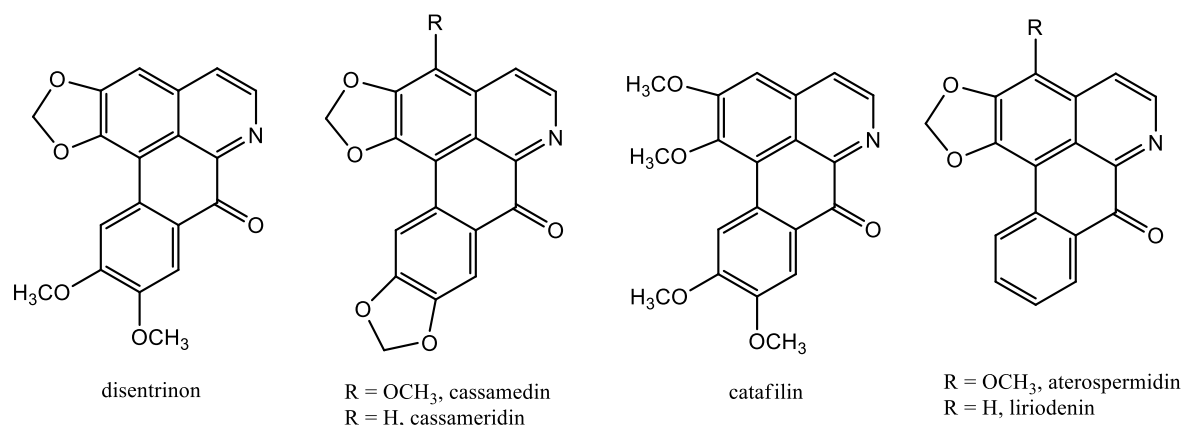


Figure 9. Structure of some isoquinoline alkaloids in the family Lauraceae (Custodio & da Veiga Jr, 2014).

Alkaloid compounds with an isoquinoline framework are commonly found in the

Lauraceae family. The structure of several alkaloid compounds that have been isolated

from plants of the Lauraceae family, namely dicentrinone, cassamedin, cassameridine, catafillin, atherospermidine, and lyriodenine are shown in Fig. 8. FC1 isolate has a simpler structure than the isoquinoline alkaloid compounds that have been reported from the Cinnamomum plant. Several Cinnamomum plant species containing isoquinoline alkaloids are *C. insularimontanum* and *C. camphora* (Custodio & da Veiga Jr, 2014).

4. CONCLUSION

FC 1 isolate was in the form of yellow crystals. FC1 isolate was an alkaloid with an isoquinoline skeleton, which was substituted by– OH and acetyl groups.

LIST OF REFERENCES

- Al-Dhubiab, B.E. (2012). Pharmaceutical applications and phytochemical profile of *Cinnamomum burmannii*. *Pharmacognosy Reviews*, 6(12), 125-131.
- Astuti, M.D., K. Mustikasari, D. Ariyani, & V. Faradilla. (2018). Distribusi Senyawa pada Fraksi Hasil Pemisahan Minyak Kayu manis Asal Loksado. *Prosiding Seminar Nasional Industri Kimia dan Sumber Daya Alam*, Universitas Lambung Mangkurat.
- Badan Pusat Statistik Provinsi Kalimantan Selatan. (2014). *Kalimantan Selatan dalam Angka 2014*. BPS Provinsi Kalimantan Selatan.
- Bribi, N. (2018). Pharmacological activity of Alkaloids: A Review. *Asian Journal of Botany*, 1, 1-5.
- Choi, E.M & J.K. Hwang. (2005). Screening of Indonesian medicinal plants for inhibitor activity on nitric oxide production of RAW264.7 cells and antioxidant activity. *Fitoterapia*, 76,194-203.
- Custodio, D.L. & D.F. da Veiga Jr. (2014). Alkaloid Lauraceae. *RSC Advance*, 4, 21864–21890.
- Gellert, E. & B. E. Summons. (1969). Alkaloid of Genus *Cinnamomum*. Isolation, Structure, and Synthesis Cinnamolaurin. *Tetrahedron Letters*, 56, 5055-5058.
- Khatib, A., M.Y. Kim & S.K. Chung. (2005). Anti-inflammatory activities of *Cinanamomum burmanni* Bl. *Food Sci Biotechnol*, 14, 223-7.
- Kim, S.H., S. H. Hyun & S. Y. Choung. (2006). Anti-diabetic effect of cinnamon extract on blood glucose in db/db mice. *Journal of Ethnopharmacology*, 104(1-2), 119–123.
- Li, A. L. , G.H. Li , Y.R. Li , X.Y. Wu , D.M Ren , H.X. Lou , X. N. Wang & T. Shen. (2018). Lignin and flavonoid support the prevention of cinnamon against oxidative stress related diseases. *Phytomedicine*, 53, 143-153.
- Li, H. T., W.J Li, H.M. Wu, C. Y. Chen. (2012). Alkaloids from *Cinnamomum philippinense*. *Natural Product Communications*, 7(12), 1581-1582.
- Liu, X., J. Yang, J. Fu, T. G. Xie, P. C. Jiang, Z. H. Jiang, G.Y. Zhu. (2018). Phytochemical and chemotaxonomic studies on the twigs of *Cinnamomum cassia* (Lauraceae). *Biochemical Systematics and Ecology*, 81, 45-48.
- Lu, J., K. Zhang, S. Nam, R. A. Anderson, R. Jove & W. Wen. (2010). Novel angiogenesis inhibitory activity in cinnamon extract blocks VEGFR2 kinase and downstream signaling. *Carcinogenesis*, 31(3), 481–488.
- Mathew, S & T. E. Abraham. (2006). Studies on the antioxidant activities of cinnamon (*Cinnamomum verum*) bark extracts, through various in vitro models. *Food Chemistry*, 94(4), 520–528.

- Panche, A.N., A. D. Diwan, & S. R. Chandra. 2016. Flavonoids: an overview. *Journal of Nutritional Science*, 5, e47.
- Pavia, D.L., G. M. Lampmann., G.S. Kriz., J.R. Vyvyan. 2015. *Introduction to Spectroscopy*, Fifth Ed., Cengage Learning, USA.
- Prasad, K.N., B. Yang, X.H. Dong, G.X. Jiang, H.Y. Zhang, H.H. Xie, Y.M. Jiang. 2009. Flavonoid contents and antioxidant activities from *Cinnamomum* species. *Innovative Food Sci. Emerg. Technol*, 10, 627–632.
- Prasetyaningrum, R. Utami., & R.B.K. Anandito. 2012. Aktivitas Antioksidan, Total Fenol, dan Antibakteri Minyak Atsiri dan Oleoresin Kayu Manis (*Cinnamomum burmanii*). *Jurnal Teknosains Pangan*, 1(1), 24-31.
- Rajasekar, N., A. Sivanantham, V. Ravikumar, S. Rajasekaran. 2021. An overview on the role of plant-derived tannins for the treatment of lung cancer. *Phytochemistry*, 188, 112799.
- Rao, P.V & S.H. Gan. 2014. Cinnamom: A Multifaced Medicinal Plant. *Evidence-Based Complementary and Alternative Medicines*, 2014, 642942.
- Rodrígueza, M., E. Bastidasa , M. Rodrígueza , E. Lucenaa , A. Castillob & M. Hasegawaa, 2008. Aporphine Alkaloids from *Guatteria stenopetala* (Annonaceae). *Natural Product Communications*, 3(4), 515-518.
- Saidi, N., H. Morita, M. Litaudon, M. R. Mukhtar, K. Awang and A. H. A. Hadi. 2011. Benzylisoquinoline Alkaloids from Bark of *Cryptocarya rugulosa*. *Indo. J. Chem.*, 11(1), 59-6.
- Safratilofa. 2016. Uji Daya Hambat Ekstrak Daun Kayu Manis (*Cinnamomum burmanii*) terhadap Bakteri *Aeromonas hydrophila*. *Jurnal Ilmiah Universitas Batanghari Jambi*, 16(1), 98-103.
- Shan, B., Y.C. Cai, J.D. Brooks, H. Corke. 2007. Antibacterial properties and major bioactive components of cinnamon stick (*Cinnamomum burmannii*): Activity against foodborne pathogenic bacteria. *J Agric Food Chem.*, 55, 5484-90.
- Sulaiman, S.N., M.P. Mukhtar., A. Hamid., A. Hadi., K. Awang., H. Hazni., A. Zahari., M. Litaudon., K. Zaima., & H. Morita. 2011. Bisbenzylisoquinoline from the Bark of *Litsea lancifolia*. *Molecules*, 16, 3119-3127.
- Thakur, M., M.F. Melzig, H. Fuchs, A. Weng. 2011. Chemistry and pharmacology of saponins: special focus on cytotoxic properties. *Botanics: Targets and Therapy*, 1,19-29.
- Yuan, L.T., C.L. Kao, C.T. Chen, H.T. Li, C.Y. Chen. 2017. A new lignan from *Cinnamomum burmanii*. *Chem. Nat. Compd*, 53, 623–625.

Toxicity Testing of White Kapul Fruit Rind Extract (*Baccaurea macrocarpa*) and Component Analysis using Chromatography Method

Uji Toksisitas Ekstrak Kulit Buah Kapul Putih (*Baccaurea macrocarpa*) dan Analisis Kandungan Senyawa dengan Metode Kromatografi

Kholifatu Rosyidah^{1,*}, Lida Karmila¹, Maria Dewi Astuti¹

¹Chemistry Study Program, Faculty of Mathematics and Natural Sciences,
Lambung Mangkurat University, Banjarbaru, Indonesia

Email: krosyidah@ulm.ac.id

ABSTRACT

White Kapul was used in this study. This study aimed to determine the toxicity of the white Kapul fruit rind extract and its chemical content analysis using TLC and GC-MS. The extraction method used was gradual maceration, namely technical n-hexane, technical ethyl acetate, and technical methanol. Toxicity test using the BSLT method with *Artemia salina* larvae at the nauplii stage. The test showed that the LC₅₀ value of ethyl acetate extract, methanol extract, and n-hexane extract was 350.87 ppm, 485.61 ppm, and 735.932 ppm, respectively. Based on LC₅₀ values, all extracts had the potential as pesticides. The third extract of white Kapul fruit rind was carried out by TLC analysis to determine the pattern of its compound content. The results of the TLC analysis showed that each extract had different polarity compounds according to the polarity of each solvent. The most active extract, ethyl acetate extract, was further analyzed using GC-MS. There were 32 peak compounds at a retention time of 25.384 to 65.725 minutes in GC-MS analysis. Four compounds with the largest percentage area were gynoloton (58.09%), 15-chloro-4-pentadesene (16.25%), 17- (acetyloxy) -2-methyl-, (2 α .,5 α ,17 β) - estra-3-on (6.07%), and methyl-11-octadesenoate (5.98%).

Keywords: *Baccaurea macrocarpa*, Euphorbiaceae, TLC, toxicity, BSLT, GC-MS

ABSTRAK

Buah kapul putih digunakan pada penelitian ini dengan tujuan mengetahui toksisitas ekstrak kulit buah kapul putih dan analisis kandungan kimianya menggunakan KLT dan GC-MS. Metode ekstraksi yang digunakan adalah maserasi bertahap dengan pelarut n-heksana teknis, etil asetat teknis, dan metanol teknis. Uji toksisitas menggunakan metode BSLT dengan larva *Artemia salina* tahap naupli. Uji toksisitas menunjukkan nilai LC₅₀ ekstrak etil asetat sebesar 350,87 ppm, ekstrak metanol sebesar 485,61 ppm, dan ekstrak n-heksana 735,932 ppm. Semua ekstrak bersifat toksik dan berdasarkan nilai LC₅₀ berpotensi sebagai pestisida. Ketiga ekstrak kulit buah kapul putih dilakukan analisis KLT untuk mengetahui pola kandungan senyawanya. Hasil dari analisis KLT menunjukkan bahwa tiap ekstrak memiliki senyawa yang berbeda kepolarannya sesuai kepolaran masing-masing pelarut. Ekstrak paling toksik yaitu ekstrak etil asetat selanjutnya dianalisis dengan GC-MS. Pada analisis GC-MS terdapat 32 puncak senyawa pada waktu retensi 25,384 sampai 65,725 menit. Empat senyawa dengan % area terbesar yaitu ginoloton (58,09 %), 15-kloro- 4-pentadesuna (16,25 %), 17-(asetiloksi)-2-metil-, (2 α .,5 α .,17 β .)-estra-3-on (6,07 %), dan metil- 11- oktadesenoat (5,98 %).

Kata Kunci: *Baccaurea macrocarpa*, Euphorbiaceae, KLT, toksisitas, BSLT, GC-MS.

Submitted: December 13, 2021; **Accepted:** February 18, 2022; **Available online:** March 8, 2022

1. INTRODUCTION

The kapul fruit is a seasonal fruit that is indigenous to Kalimantan. Kapul fruit is not farmed and is typically harvested in the wild. According to Antarlina (2009), several Kalimantan fruits naturally grow in the neighboring yards, while some are forest plants (located in the forest). Fruit can be consumed as part of a healthy lifestyle to help overcome health problems such as nutritional and vitamin deficiencies (Susi, 2014). A fruit diet can also help boost the body's immunity during pandemic, as fruit is high in vitamins and antioxidant compounds. Astuti *et al.* (2020) discovered that Kapul fruit rind contained significant antioxidant activity. Kapul fruit rind was extracted in stages with n-hexane, ethyl acetate, and methanol as solvents. The highest IC50 value in methanol extract was 22.968 ppm, ethyl acetate was 29.741 ppm, and n-hexane was 141.931 ppm, while the IC50 value for vitamin C was 5.019 ppm as a comparison compound.

Several studies have been conducted on the bioactivity of the white Kapul fruit plant (*Baccaurea macrocarpa*). Yunus *et al.* (2014) stated that the extract and methanol fraction of the rind of Kapul fruit showed antibacterial activity against *E. coli* and *S. aureus* bacteria. The diameter of the inhibition zone of the methanolic extract of the capsule fruit peel against *S. aureus* bacteria at concentrations of 5%, 10%, and 20%, respectively, was 0.0: 4.33, and 6.40 mm; the n-hexane fraction was 3.55, 6.55, and 8.77 mm; the ethyl acetate fraction was 16.55, 19.05, and 22.01 mm; and the remaining methanol fraction was 6.92, 9.78, and 12.32 mm. The antibacterial activity against *E. coli* at concentrations of 5%, 10%, and 20% was 5.01, 7.82, and 9.21 mm; the n-hexane fraction was 8.22, 11.36, and 13.66 mm; the ethyl acetate fraction was 15.41, 20.25, and 23.92 mm; and the methanol fraction was 9.78, 13.43, and 15.02 mm.

Dwijayanti (2014) showed that the bark of the Kapul stem has toxicity activity.

Toxicity test was carried out using the BSLT method, and the LC50 value of the methanol extract was 318.150 ppm. The extract was then fractionated and tested for toxicity to obtain LC50 data for the ethyl acetate fraction of 310.443 ppm, the n-hexane fraction of 500.160 ppm, the methanol fraction of 602.869 ppm, and the chloroform fraction of 640.471 ppm.

Yunus *et al.* (2017) and Tirtana *et al.* (2013) stated that Kapul fruit contains secondary metabolites, including saponins, alkaloids, and flavonoids. The results of phytochemical tests by Dwijayanti *et al.* (2014) on Kapul bark extract and ethyl acetate fraction found the presence of alkaloids, steroids, flavonoids, and polyphenols. The methanol fraction contained flavonoid compounds, alkaloids, and polyphenols, while the chloroform and n-hexane fractions contained alkaloid compounds.

This study will examine the toxicity of the white Kapul fruit rind using *Artemia salina* Leach shrimp. The toxicity testing with the BSLT method is a simple bioassay method for exploring natural products. The advantages of this method are that it can be performed quickly, is reliable, and has been used for ±30 years in toxicological studies. The extraction method used was stepwise extraction with the different polarity of solvents such as n-hexane, ethyl acetate, and methanol.

1. MATERIALS AND METHODS

2.1. Materials

The materials used were white Kapul fruit rind, technical n-hexane, technical methanol, technical ethyl acetate, cerium sulfate, dimethyl sulfoxide (DMSO), sulfuric acid, aquadest, artificial seawater, and *A. salina* Leach. The tools used were rotary evaporator, GC-MS, spatula, O'haus analytical balance, glassware, distillation apparatus, TLC, petri dish, water bath, magnifying glass, *Artemia salina* Leach hatchery equipment, vials, blender, aerator,

glass stirrer, filter paper, drip plate, and dropper.

2.2. Sample preparation of white Kapul fruit rind

The rind of the white Kapul fruit was peeled and separated from the flesh. The rind was then cut into thin strips to facilitate the drying process. The drying process was carried out by air drying for 7 days. The dried rind was then ground with a blender until it became a powder, weighed, and stored in a container.

2.3. Extraction of white Kapul fruit rind

This research employed stepwise extraction, namely the maceration method with technical n-hexane, technical ethyl acetate, and technical methanol. A total of 500 g of dry powder of Kapul fruit rind was put into a maceration vessel, soaked in a non-polar solvent, namely n-hexane, in a ratio of 1:5 for 24 hours while stirring several times. The maceration was repeated 3 times. The maceration results were filtered with Whatman paper No. 1 and evaporated using a rotary evaporator at 40-50°C. Furthermore, the extract was concentrated with a waterbath to obtain a thick extract. The n-hexane maceration residue was extracted again using ethyl acetate as solvent. The residue from the ethyl acetate extraction was re-extracted using methanol. Each extract obtained was used for further testing (Anindya, 2012).

2.4. Toxicity test of white Kapul fruit rind extract

Shrimp larvae were put into artificial seawater equipped with an aerator for 1×24 hours. Artificial seawater was made from 20 grams of salt dissolved in 1 liter of distilled water. Toxicity test solution made from n-hexane, ethyl acetate, and methanol extract was weighed as much as 6.25 mg then dissolved in 25 mL of artificial seawater. Each extract was first dissolved using 0.5 mL of DMSO solution. Each extract was pipetted 1; 1.5; 2; 2.5; 3; 3.5; 4; 4.5; 5; and

5.5 mL into the vial and added artificial seawater until the volume reached 25 mL, so that the concentration of the solution became 100, 150, 200, 250, 300, 350, 400, 450, 500, and 550 ppm. The negative control solution contained artificial seawater without the addition of sample extract with 0.5 mL of DMSO. A total of 20 shrimp larvae were added to each vial containing the test and negative control solutions. After 24 hours, the number of dead shrimp larvae was observed, and the mortality percentage was calculated.

2.5. Thin layer chromatography analysis of white Kapul fruit rind extract

A total of 2 mg of each extract was weighed and dissolved with a few drops of solvent. The diluted extract was spotted on the TLC plate at 1 cm from the bottom line and the edge. The stationary phase was a silica gel plate 60GF254. The stationary phase was then eluted using the eluent with n-hexane and ethyl acetate in a ratio of 7:3 and 9:1, while the eluents of chloroform and methanol were in a ratio of 9:1. If the eluent reached the boundary line, the elution was stopped, and the stationary phase was further dried. The stationary phase was sprayed with cerium sulfate and analyzed using 254 and 366 nm UV lamps. The resulting stain was then calculated for its R_f value.

2.6. GC-MS analysis of white Kapul fruit rind extract

GC-MS analysis following Maharani *et al.* (2016). GC-MS using Shimadzu QP 2010 with column RTx-5MS, 30 m long, the temperature of the injector and detector was 250°C, and operating temperature of 50-300°C. The temperature at 50-120°C was set to 4°C/min and held for 1 minute. The temperature of 120-300°C with a temperature increase of 6°C/minute was held for 5 minutes with a total retention time of 60 minutes. The carrier gas was helium, with a molecular weight of 50-500.

A total of 10µL of the thick extract of the white Kapul fruit rind was dissolved in

240µL of solvent. 1µL of the solution was then injected into the GC-MS. The flow rate was set at 1 mL/min with a column temperature of 70°C held for 2 minutes and then increased to 37°C/min to 250°C and held for 10 minutes (Prakash *et al.*, 2001). Compound analysis was performed using the Wiley/NIST Library software.

2.7. Data analysis

The data obtained were in the form of *A. salina* shrimp larvae mortality in each treatment/extract concentration. The mortality percentage was calculated from the data on the number of dead larvae. Data on the percentage of larval mortality was used to find the probit value in the probit table. Next, a graph of the relationship between the concentration log (X-axis) and the probit value (Y-axis) was constructed to obtain a linear regression equation $y = a + bx$. The x value was converted into antilog form so that the LC₅₀ value was obtained.

2. RESULTS AND DISCUSSION

3.1. Sample preparation

The weight of fresh Kapul fruit was 6 kg. The Kapul fruit was first separated from the pulp, then the rind of the fruit was chopped into small pieces to speed up the drying process and dried for 7 days. Drying aimed to reduce the water content in the sample, making it less susceptible to contamination by microbes or fungi (Arwan, 2017).

The weight of dry Kapul fruit rind was 2.5 kg. The rind of the kapul fruit was grounded using a blender until it became a powder, then weighed and stored in a

container. After being mashed, the weight of the dried Kapul fruit skin was 2 kg. A total of 500 grams of dried Kapul fruit peel powder was then used for the maceration process.

3.2. Extract of white Kapul fruit rind

Gradual maceration was used to extract the rind of the Kapul fruit (*B. macrocarpa*). The solvent was changed daily throughout the maceration process to maximize the extraction of secondary metabolites from the rind.

Kapul fruit rind powder was soaked with a non-polar solvent, namely n-hexane, semipolar, namely ethyl acetate, and polar, namely methanol, for 3×24 hours gradually. The sample powder was soaked with n-hexane as a solvent to extract non-polar compounds. The dregs extracted with n-hexane were then soaked with ethyl acetate to extract semipolar compounds. The dregs from ethyl acetate extraction were then soaked with methanol to extract polar compounds.

The white Kapul fruit rind extract was then evaporated using a rotary evaporator. Evaporation is the process of separating the sample from the solvent. The temperature of the rotary evaporator was kept between 40 and 50°C to avoid decomposition of the compounds contained in the macerate owing to excessive heating. The evaporated extract was then concentrated with a waterbath. The yield of white Kapul fruit rind extract is presented in Table 1.

Table 1. The result of maceration extraction of white Kapul fruit rind

Solvent	Powder	Extract	Yield (%)
n-heksana	500 gram	0.07 gram	0.014%-b/b
etil asetat		1.20 gram	0.240%-b/b
metanol		13.57 gram	2.714%-b/b
Total		14.84 gram	2.968%-b/b

Based on Table 1, it is known that the highest yield was obtained from extraction with methanol. The yield stated the number of compounds in the Kapul fruit rind extract dissolved in methanol. Kapul fruit rind has different yield values, indicating that polar secondary metabolites' content is high. It means that the methanol extract has a higher yield value compared to the ethyl acetate and n-hexane extracts. The total yield obtained was 2.968%. The difference in yield resulting from the gradual extraction is higher than Dwijayanti (2014). It may occur because the extraction was carried out with methanol solvent first and then continued with other fractions. Dwijayanti (2014) extracted Kapul bark with methanol as a solvent. Extraction of 3.3 kg of Kapul bark with methanol as a solvent resulted in 58.28 grams of methanol extract and 1.76% yield. Thus, the rind of the Kapul fruit contains a higher concentration of secondary metabolites than the bark.

3.3. Toxicity Test of White Kapul Fruit Rind Extract

The toxicity test was carried out with three variations: n-hexane extract, ethyl acetate, and methanol. The solubility of extracts in artificial seawater often causes problems because of the different levels of polarity. Extracts are difficult to dissolve in artificial seawater, so Dimethyl sulfoxide (DMSO) needs to be added. In general, DMSO is used as a surfactant to dissolve extracts in artificial seawater. A total of 0.5 mL of DMSO was added to 25 mL of mother liquor for each extract. The results of the toxicity test of the white Kapul fruit peel extract is presented in Table 2.

Meyer (1982) stated that the extract is toxic to the BSLT test if it resulted in the death of 50% of the test animals at a concentration of $LC_{50} < 1000$ ppm, which indicates that the sample has potential as an anticancer, antibacterial, anti-fungal, pesticides and so on. Rizqillah (2013) stated that compounds that have the potential as anticancer are found at an LC_{50} value of 0-30 ppm, compounds that have the potential as an antibacterial is at an LC_{50} of 30-200 ppm, and compounds that have the potential as pesticides are at an LC_{50} value of 200-1000 ppm.

Table 2. Toxicity test results of white Kapul fruit rind extract

Extract	Concentration (ppm)	% Mortality	Concentration Log	Probit	LC_{50} (ppm)
n-heksana	100	10.0	2.00	3.72	735.932 ppm
	200	17.5	2.30	4.07	
	300	25.0	2.48	4.33	
	400	30.0	2.60	4.48	
	500	41.3	2.70	4.78	
Etil Asetat	100	10.0	2.00	3.72	350.87 ppm
	150	17.5	2.18	4.07	
	200	25.0	2.30	4.33	
	250	35.0	2.40	4.61	
	300	43.8	2.48	4.84	
Methanol	350	16.3	2.54	4.02	485.61 ppm
	400	25.0	2.60	4.33	
	450	30.0	2.65	4.48	
	500	56.3	2.70	5.16	
	550	71.3	2.74	5.56	
Control	0	0	-	-	-

*Note: - = No value

The extract with the highest toxicity was ethyl acetate extract with an LC_{50} value of 350.87 ppm, methanol extract of 485.61 ppm, and n-hexane extract with an LC_{50} value of 735.932 ppm. Dwijayanti (2014) stated that the bark of the Kapul fruit has the toxicity power of methanol extract with an LC_{50} value of 318.150 ppm. While the

ethyl acetate fraction with an LC_{50} of 310.443 ppm, the n-hexane fraction of 500.160 ppm, the remaining methanol fraction of 602.869 ppm, and the chloroform fraction of 640.471 ppm. The toxicity test showed that Kapul fruit rind and bark extract has potential pesticides.

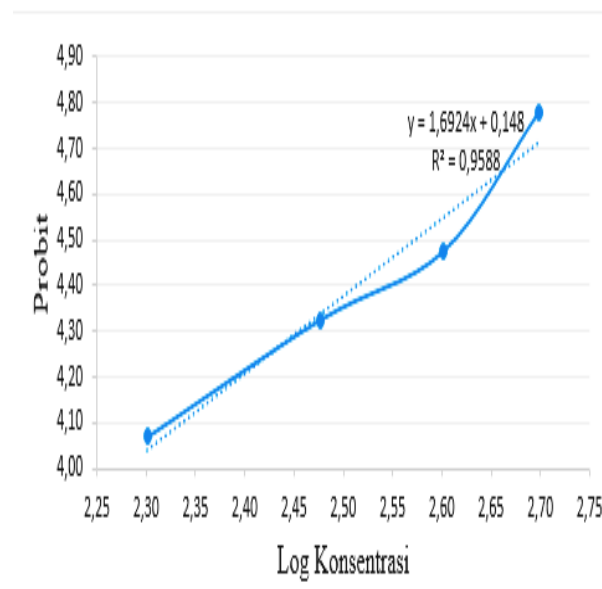


Figure 1. The Relationship Graph between Concentration and Probit of n-hexane of Kapul Fruit Rind Extract

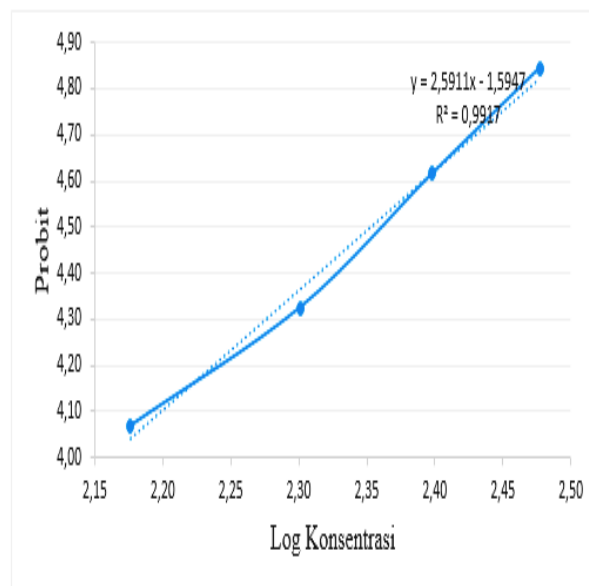


Figure 2. The Relationship Graph between Concentration and Probit of Ethyl Acetate Extract of Kapul Fruit Rind

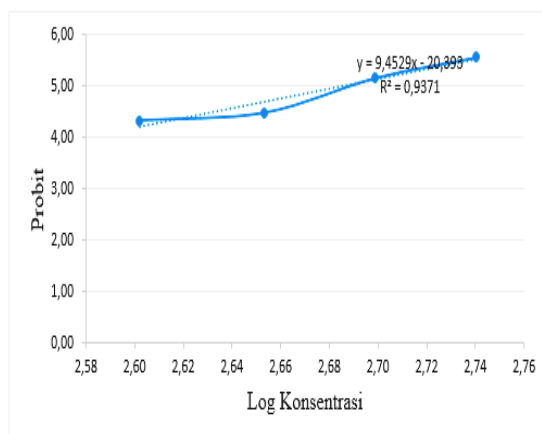


Figure 3. The Relationship Graph between Concentration and Probit of Methanol Extract of Kapul Fruit Rind

3.3. Thin layer chromatography analysis of white Kapul fruit rind extract

TLC analysis was carried out on the Kapul fruit rind extract to determine the pattern of the stains. Extracts from each sample were analyzed by TLC method using eluents with specific ratios, namely n-hexane:ethyl acetate (7:3), (9:1), and chloroform:methanol (9:1) eluents. The stationary phase was silica gel 60GF254, coated on an aluminum plate. The TLC chromatogram was sprayed using a 2% cerium sulfate solution. The stain contains

phenolics if the resulting stain is yellow after being sprayed with a 2% cerium sulfate solution.

Based on Fig. 4a, the n-hexane extract had four separation spots with an Rf1 value of 0.476 faded purple, Rf2 0.714 dark purple, Rf3 0.793 yellow, and Rf4 0.888 faded purple. The ethyl acetate extract had four separation spots with an Rf1 value of 0.079 yellow, Rf2 0.476 yellow, Rf3 0.555 dark purple, and Rf4 0.746 yellow. The methanol extract did not have a separation pattern or no elution (higher polarity).

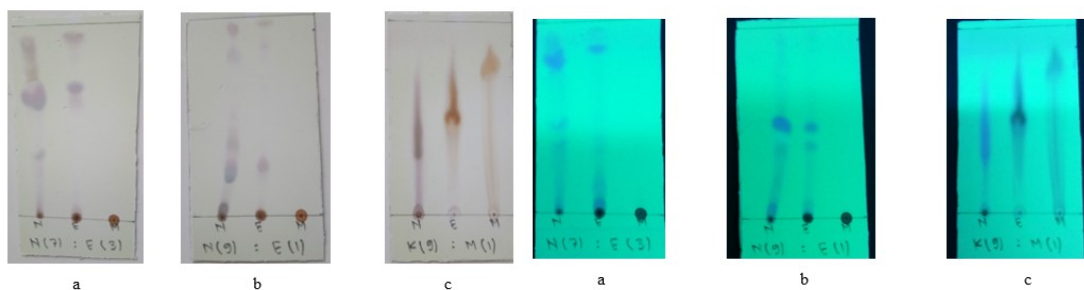


Figure 4. TLC chromatogram of white Kapul fruit rind extract with eluents of n-hexane:ethyl acetate (7:3) (a), (9:1) (b) and chloroform:methanol (9:1) (c) with 2% cerium sulfate stain (left) and 254 nm UV light (right)

Based on Fig. 4b, the n-hexane extract had five separation spots with Rf1 value of 0.079 black (terpene), Rf2 0.138 blue (steroid), Rf3 0.238 yellow (phenolic), Rf4 0.634 faded purple (terpene), and Rf5 0.714 colored yellow (phenolic). The ethyl acetate extract had three stains with an Rf1 value of 0.317, which was deep purple (terpene), Rf2 of 0.714 was pale purple (terpene), and Rf3 of 0.793 was yellow (phenolic). The

ethyl acetate extract was visible due to the presence of compounds that had not been eluted. The separation pattern was not found in the methanol extract, meaning that no compound was eluted (higher polarity). It proves that the compound content of each extract varies based on the polarity of the solvent. Based on Fig. 4c, the n-hexane extract only had one stain with an Rf1 value of 0.555, black (terpene). The ethyl acetate

extract with an Rf1 value of 0.428 was dark brown (phenolic), while the methanol extract had an Rf1 value of 0.650 faded brown (phenolic).

3.4. Compounds identification using the GC-MS instrument

Ethyl acetate extract from white Kapul fruit rind, which had the highest activity in the toxicity test, was analyzed using GC-MS SHIMADZU QP2010S with a 5 ms restex column, 30 m long, and ID 0.25 mm. The GC-MS analysis of the components of ethyl acetate extract of white Kapul fruit rind is presented in Fig. 5.

GC-MS analysis showed 32 peaks at retention times from 25,384 to 65,725. The four prominent compound peaks with the largest percentage area, namely 58.09%, were identified as ginoluton compounds with SI (Similarity index) 83, compounds 15-chloro-4-pentadesuna (16.25 %) with SI 81, compounds 17-(acetyloxy)- 2-methyl-, (2.α.,5. .,17. .)-estra-3-one (6.07%) with SI 80, and the compound methyl-11-octadesenoate (5.98 %) with SI 93. Compound components with SI values close to 100% indicate that the identified compounds are getting closer to the comparison compounds (Rasyid, 2016).

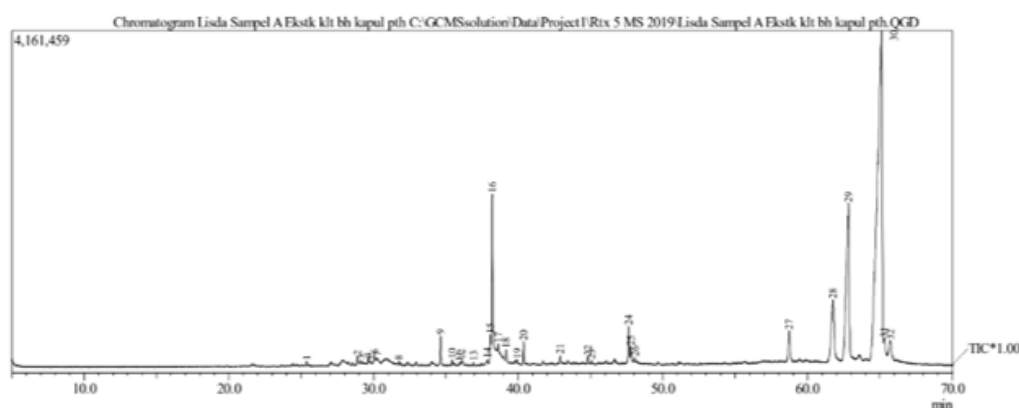


Figure 5. GC chromatogram of ethyl acetate extract of white Kapul fruit rind

Ginoluton is the main progestational steroid compound secreted mainly by the corpus luteum and placenta. Ginoluton acts on the uterus, mammary glands, and brain. Function in embryo implantation, pregnancy maintenance, and milk tissue development for milk production. Ginoluton is converted from pregnenolone. It also functions as an intermediate in the biosynthesis of gonadal steroid hormones and adrenal corticosteroids. Ginoluton is a progestin or synthetic form of the female sex hormone, namely progesterone. Ginoluton tricks the body into thinking that ovulation has occurred by maintaining high levels of synthetic progesterone. It prevents the release of the egg from the ovary. Ginoluton is used as a contraceptive. It shows that white Kapul fruit rind has the potential as a natural contraceptive drug.

The compound 15-chloro-4-pentadesuna shows potential activity in therapy against various diseases (Sivakrishnan, 2019). 15-chloro-4-pentadesuna also has anti-metastatic or anti-cancer effects (Kokila, 2014). The compound 17-(acetyloxy)-2-methyl-, (2.α.,5. .,17. .)-estra-3-on has an antioxidant effect (Erukainure, 2018).

Methyl dodecanoate, commonly called methyl laureate, is used as a raw material for methyl ester sulfonate (MES) detergents. MES is widely used in agricultural products to prevent the development of mosquito larvae. Methyl laurate or methyl esters are generally found in transesterification products in vegetable oils, such as the process of using alcohol (ethanol and methanol) with the help of a catalyst to break vegetable oil molecules into ethyl or methyl esters with glycerol as

a by-product (Arbianti, 2008). In the body, methyl laurate functions as an antiviral, antiprotozoal, and antimicrobial, improving the body's immune system, such as protection from HIV, herpes, and pathogenic bacteria (Adyana, 2017).

4. CONCLUSION

This study revealed that the ethyl acetate extract of white Kapul fruit rind was the most toxic to the BSLT test, with an LC₅₀ value of 350.87 ppm. The TLC chromatogram of each extract showed a different stain pattern according to the polarity of the solvent used. GC-MS analysis of the ethyl acetate extract of Kapul fruit rind showed the presence of 32 peaks, with the main compound being ginoluton (58.09%).

ACKNOWLEDGEMENT

Acknowledgments are conveyed to the Dean of FMIPA ULM for financing this research with DIPA-PNBP FMIPA ULM for the 2019 Fiscal Year according to the Dean's Decree No. 1139/UN8.1.28/SP/2019.

LIST OF REFERENCES

- Adyana, D., Daniel & C. Saleh. (2017). Sintesis Askorbil Laurat dari Metil Laurat dan Asam Askorbat melalui Reaksi Transesterifikasi dengan Katalis Lipase serta Uji Aktivitas Antioksidan. *Jurnal Kimia Mulawarman*. 2(14), 71-76.
- Anindya, D. (2012). *Efek Ekstrak Kulit Buah Manggis (Garcinia mangostana L.) Terhadap Pertumbuhan Bakteri Shigella dysenteriae dan Escherichia coli*. Skripsi. Fakultas Kedokteran dan Ilmu Kesehatan UIN Syarif Hidayatullah, Jakarta.
- Antarlina, S. (2009). Identifikasi Sifat Fisik dan Kimia Buah-buahan Lokal Kalimantan. *Buletin Plasma Nutfah*. 15(2), 80-90.
- Arbianti, R., T. S. Utami & N. Astri. (2008). Isolasi Metil Laurat dari Minyak Kelapa sebagai Bahan Baku Surfaktan *Fatty Alcohol Sulfate* (FAS). *Makara Teknologi*. 2(12), 61-64.
- Arwan, B. (2017). *Uji Toksisitas Fraksi Ekstrak Etanol 70% Akar Parang Romang (Boehmeria virgata (Forst) Guill.) terhadap Larva Udang (Artemia salina Leach) dengan Menggunakan Metode Brine Shrimp Lethality Test (BSLT)*. Skripsi. Fakultas Kedokteran dan Ilmu Kesehatan Universitas Islam Negeri Alauddin, Makassar.
- Astuti, MD, W. F/ Ana, K/ Rosyidah, Rodiansono. The antioxidant activity of white kapul (*Baccaurea macrocarpa*) fruit rinds. IOP Conf. Series: Materials Science and Engineering 980. (2020) 012040 IOP Publishing, doi:10.1088/1757-899X/980/1/012040

- Dwijayanti, E. A., H. Alimuddin & M. A. Wibowo. (2014). Skrining Fitokimia dan Uji Aktivitas Sitotoksik pada Kulit Batang Tampoi (*Baccaurea macrocarpa*) terhadap *Artemia salina* Leach dengan Metode BSLT. *Jurnal Kimia Khatulistiwa*. 4(1), 6-10.
- Kokila, K., S. D. Priyadharshini & V Sujatha. (2014). Antioxidant, Antibacterial and GC-MS Analysis of *Albizia amara* Leaves and Seed Extract – A Comparison. *Indo American Journal of Pharmaceutical Research*. 1928-1939.
- Maharani, R., A. Fernandes., M. Turjaman., G. Lukmandaru & H. Kuspradini. (2016). The Characterization of Phytochemical and GC-MS Analysis on Borneo Agarwood (*Aquilaria malaccensis* Lamk) Leaves and Its Utilization as an Anti-Browning in Apple Juice. *International Journal of Pharmacognosy and Phytochemical Research*. 8(10),1576-1582.
- Meyer, B. N., N. R. Ferrigni., J. E. Putnam., L. B. Jacobsen., D. E. Nichols & J. L. McLaughlin. (1982). *Brine Shrimp*: A Convenient General Bioassay for Active Plant Constituent. *Drug Information Journal*. 32, 513-524.
- Rasyid, A. (2016). Analisis Metabolit Sekunder, Aktivitas Antibakteri dan Komposisi Golongan Senyawa dalam Ekstrak Teripang *Bohadschia sp*. *Jurnal Ilmu dan Teknologi Kelautan Tropis*. 8(2), 645-653.
- Rizqillah, N. (2013). *Uji Toksisitas Akut Ekstrak N-heksana Daun Garcinia benthami Pierre Terhadap Larva Artemia salina Leach dengan Metode Brine Shrimp Lethality Test (BSLT)*. Skripsi. Program Studi Pendidikan Dokter Fakultas Kedokteran dan Ilmu Kesehatan Universitas Islam Negeri Syarif Hidayatullah, Jakarta.
- Sivakrishnan, S & D. Pradepraj. (2019). Gas Chromatography-Mass Spectroscopy Analysis of Ethanolic Extract of Leaves of *Cordia obliqua* Willd. *Assian Journal of Pharmaceutical and Clinical Research*. 12(6), 110-112.
- Susi. (2014). Potensi Pemanfaatan Nilai Gizi Buah Eksotik Khas Kalimantan Selatan. *Zira'aah*. 39(3), 144-150.
- Tirtana, E., N. Idiawati., Warsidah & A. Jayuska. (2013). Analisa Proksimat, Uji Fitokimia dan Aktivitas Antioksidan pada Buah Tampoi (*Baccaurea macrocarpa*). *Jurnal Kimia Khatulistiwa*. 2(1), 42-45.
- Yunus R., A. H. Alimuddin & P. Ardiningsih. (2014). Uji Aktivitas Antibakteri Ekstrak Kulit Buah Tampoi (*Baccaurea macrocarpa*) terhadap Bakteri *Escherichia coli* dan *Staphylococcus aureus*. *Jurnal Kimia Khatulistiwa*. 3(3), 19-2

The Effect of Hydrolysis Time Using Microwave on Bioethanol Production from Sorghum Waste (*Sorghum Bicolor L.*)

Pengaruh Waktu Hidrolisis Menggunakan *Microwave* Terhadap Produksi Bioetanol Dari Ampas Sorgum (*Sorghum Bicolor L.*)

Sefrinus Maria Dolfi Kolo^{1,*}, Lukas Pardosi², Anita Ensiana Baru¹

^{1,3}Chemistry Study Program, University of Timor

²Biology Study Program, University of Timor
Kefamenanu, TTU- NTT, 85613, Indonesia

*Email: sefrichem@unimor.ac.id

ABSTRACT

*In this study, the production of bioethanol from sorghum bagasse was carried out to understand the surface morphology of sorghum bagasse before and after hydrolysis, the effect of hydrolysis time using a microwave, and the concentration of inoculum on the ethanol content produced. A total of 10 grams of sorghum bagasse was suspended with 250 mL of 2% H₂SO₄ solution and then heated using a microwave at a temperature of 150°C with variations in heating time of 20, 30, 40, and 50 minutes. The heated hydrolyzate was analyzed for reducing sugar content using UV-Vis. The morphology of sorghum bagasse before and after hydrolysis was analyzed using SEM and quantitative analysis of fermented ethanol using a pycnometer and GC. The results showed that there were differences in the surface of sorghum bagasse before and after hydrolysis, the highest reducing sugar content was obtained at 30 minutes of hydrolysis, which was 30.4 g/L, and the highest concentration of *Saccharomyces cerevisiae* was 8% which resulted in 5.325% ethanol content using a pycnometer and 9.05% using GC.*

Keywords: Sorghum bagasse, Hydrolysis, Microwave, Bioethanol

ABSTRAK

*Pada penelitian ini dilakukan produksi bioetanol dari ampas sorgum dengan tujuan untuk mengetahui morfologi permukaan ampas sorgum sebelum dan sesudah hidrolisis, pengaruh waktu hidrolisis menggunakan microwave dan konsentrasi inokulum terhadap kadar etanol yang dihasilkan. Sebanyak 10 gr ampas sorgum disuspensi dengan 250 mL larutan H₂SO₄ 2% lalu dipanaskan menggunakan microwave pada suhu 150 °C dengan variasi waktu pemanasan 20, 30, 40 dan 50 menit. Hidrolisat hasil pemanasan dianalisis kadar gula pereduksi menggunakan UV-Vis, morfologi ampas sorgum sebelum dan sesudah hidrolisis dianalisis menggunakan SEM dan analisis kuantitatif etanol hasil fermentasi menggunakan piknometer dan GC. Hasil penelitian menunjukkan adanya perbedaan pada permukaan ampas sorgum sebelum dan sesudah hidrolisis, kadar gula pereduksi tertinggi diperoleh pada waktu hidrolisis 30 menit yaitu sebesar 30,4 g/L dan konsentrasi tertinggi *saccharomyces cerevisiae* adalah 8% yang menghasilkan kadar etanol sebesar 5,325% menggunakan piknometer dan 9,05% menggunakan GC.*

Kata Kunci: Ampas sorgum, Hidrolisis, Microwave, Bioetanol

Submitted: August 23, 2021; **Accepted:** February 18, 2022; **Available online:** March 8, 2022

1. INTRODUCTION

The current energy crisis is caused by dependence on fossil fuels which are non-renewable sources. Therefore, it is critical to developing new alternative energy, namely bioethanol. Bioethanol can be produced from starch- or carbohydrate-containing plants such as corn (*Zea mays* L.), sweet sorghum (*Sorghum bicolor* L.), sugarcane (*Saccharum officinarum* L.), cassava (*Manihot esculenta* C.), and sugar beet (*Beta vulgaris*) (Ray et al., 2019). However, the current bioethanol production is from starch derived from food. It may have a detrimental effect on food supply due to the conflict between food and energy. To address this issue, it is required to perform research using non-food raw materials, including sorghum bagasse. Sorghum pulp has 72.05 % carbohydrates, making it suitable for bioethanol production (Arif et al., 2018). The redevelopment of the sorghum plant is deemed necessary because apart from being used as food, this plant can also be used as an energy source.

In general, there are three stages in producing bioethanol from starch, namely hydrolysis, fermentation, and distillation. Hydrolysis is one of the critical processes in bioethanol production. This process uses acids or enzymes catalyst (Rani et al., 2019). Various studies on bioethanol using the acid hydrolysis method have been carried out. One of them was by Kolo et al. (2020), who reported that bioethanol concentration from elephant grass with microwave irradiation at the optimum concentration of 2% sulfuric acid (H_2SO_4) with a hydrolysis time of 30 minutes and a temperature of $90^\circ C$ was 10.79 g/L. One factor affecting the bioethanol concentration is the amount of reducing sugar produced from the hydrolysis process. Kolo et al. (2021) found that under the optimum conditions of dilute acid hydrolysis using microwave irradiation was $150^\circ C$, 50 minutes, the concentration of reducing sugar was 33.41 g/L, and the hydrolysis efficiency reached 83.52% (v/v).

Research by Ahmed El-Imam et al. (2019) found that the glucose level from the hydrolysis of sorghum pulp using a 3% H_2SO_4 concentration was 34.53 g/L.

In this study, sorghum bagasse taken from North Central Timor Regency (TTU) was converted into bioethanol through a hydrolysis process using dilute acid. Before and after the hydrolysis process, the carbohydrate texture was analyzed by SEM (Scanning Electron Microscopy). Furthermore, the reducing sugar content was analyzed using UV-Vis Spectro, and the bioethanol content was measured using a pycnometer and GC (Gas Chromatography). This study aimed to study the surface morphology of sorghum bagasse before and after hydrolysis to determine the optimum hydrolysis time and the highest bioethanol content of sorghum bagasse based on variations in inoculum concentration.

2. MATERIALS AND METHODS

2.1. Materials

The materials used were sorghum taken from North Central Timor (TTU) Regency, yeast, pure isolate of *Saccharomyces cerevisiae* taken from Gadjah Mada University Yogyakarta, NaOH (Merck), H_2SO_4 (Merck), aluminum foil, wrapping, tissue, cotton, glucose (pro analysis), distilled water, alcohol, PDA media, inoculum medium (Glucose 10 g/L (pro analysis), yeast extract 0.1 g/L (pro analysis), KH_2PO_4 0.1 g/L (pro analysis), $MgSO_4 \cdot 7H_2O$ 0.1 g/L (pro analysis), $(NH_4)_2SO_4$, 0.1 g/L (pro analysis), and fermentation media. The tools used were petri dish, beaker, Erlenmeyer flask, graduated cylinder, funnel, stirrer, test tube, and dropper, pH meter analytical balance, oven, GC instrument, UV-Vis, microwave, SEM, magnetic stirrer, cuvette, wire loop, hot plate, autoclave, thermometer, and distillation apparatus.

2.2. Sample preparation

The sorghum seeds were dried and ground. Then the pulp was taken and sieved using a 100 mesh sieve to obtain uniform size. Milling and sifting aimed to expand the surface of sorghum to facilitate the hydrolysis process.

2.3. Hydrolysis

A total of 10 grams of sorghum powder with a size of 100 mesh was suspended with 250 ml of 2% H₂SO₄ solution and then heated using a microwave at 150°C with variations in time (20, 30, 40, and 50 minutes). The heating results were filtered and neutralized using a 2% NaOH solution, then analyzed for glucose content using UV-Vis at a wavelength of 540 nm. The surface of the hydrolyzed powder was analyzed using SEM (Scanning Electron Microscopy).

2.4. Stock breeding and rejuvenation of *Saccharomyces cerevisiae*

S. cerevisiae breeding stock and rejuvenation were carried out by inoculating *Saccharomyces cerevisiae* in 250 ml of PDA media (9.75 g of PDA) and incubated for 48 hours. Furthermore, the rejuvenated *S. cerevisiae* was inoculated in 50 mL of inoculum media (Glucose 10 g/L; Yeast extract 0.1 g/L; KH₂PO₄ 0.1 g/L; MgSO₄·7H₂O 0.1 g/L; and (NH₄)₂SO₄, 0.1 g/L in an Erlenmeyer, then incubated for 48 hours using an orbital shaker at 120 rpm (Samsuri et al., 2007).

2.5. Preparation of fermentation media

The fermentation medium was prepared by mixing 10 g/L glucose, 0.1 g/L yeast extract, 0.1 g/L KH₂PO₄, 0.1 g/L MgSO₄·7H₂O, and 0.1 g/L (NH₄)₂SO₄ in 50 mL aquadest. It was then sterilized using an autoclave at 121°C for 30 minutes.

2.6. Bioethanol production

Fermentation with yeast *Saccharomyces cerevisiae* used variations in inoculum concentrations of 4, 6, and 8%. A total of 100 ml of the hydrolyzate was put into an

Erlenmeyer and neutralized using 2% NaOH. The fermentation medium was added and sterilized at 121°C for 30 minutes. Then it was cooled, and the inoculum medium was added, then covered with cotton and aluminum foil. Fermentation was carried out anaerobically for 7 days.

2.7. Destillation

The sample to be distilled was put into a distillation flask and heated. Observations were made on the time and temperature of the product's boiling point that dripped from the first to the end. The volume of the distillate obtained was measured using a graduated cylinder. Density was measured using a pycnometer and ethanol content using GC.

2.8. Characterization and analysis

A. Texture analysis of powder surface

The surface texture of sorghum powder was analyzed using SEM before and after hydrolysis. The sorghum bagasse before and after hydrolysis were put into the SEM chamber for position setting and image recording. SEM images were taken at 800x magnification.

B. Analysis of reducing sugar

The reducing sugar content of the hydrolyzed sorghum pulp was analyzed using the DNS (Dinitrosalicylate) method. A total of 1.5 ml of standard glucose solution with concentrations of 1000, 2000, 3000, 4000, 5000 ppm was put into a test tube, and then 1.75 ml of DNS reagent was added. The standard solution and the sample were put in a 100°C water bath for 20 minutes and allowed to stand until room temperature. The absorbance was measured at a wavelength of 540 nm. The hydrolysis efficiency (EH) is calculated using the following equation:

$$EH (\%) = \frac{[Glucose]_{gr/L}}{[Biomass]_{gr/L}} \times 100\%$$

C. Analysis of ethanol concentration

1. Qualitative analysis of ethanol

Distilled ethanol was added with 2 mL of 2% $K_2Cr_2O_7$ and 5 drops of concentrated H_2SO_4 . Then the solution was homogenized and added with 1 mL of distillate until the color changed from orange to greenish.

b. Quantitative Analysis of Ethanol

Quantitative analysis was carried out in two ways, namely:

- a. The pycnometer with known volume was activated in the oven for 10 minutes at $105^\circ C$ and then cooled. Then the empty pycnometer was weighed, and the weight was recorded. Water was added to the pycnometer until it was filled and then weighed. The same procedure was carried out by replacing the distilled water with the sample (Saleh et al., 2016). The following equation calculates the density of ethanol:

$$\rho_1 = \frac{W_1}{W_2} \times \rho_2$$

description:

W_1 = weight of ethanol

W_2 = weight of aquades

= density of the sample

= density of the sample

Density obtained from the measurement using a pycnometer was then used to calculate the ethanol concentration, yield (Y), fermentation efficiency (EF), and conversion efficiency (EK) using the following equation:

$$Y (\%) = \frac{\text{ethanol concentration (g/L)}}{\text{sugar concentration (g/L)}} \times 100$$

EF (%)

$$= \frac{\text{ethanol concentration (g/L)}}{0,51 \times \text{sugar concentration (g/L)}} \times 100$$

$$EK (\%) = \frac{\text{ethanol concentration (g/L)}}{\text{biomassa (g/L)}} \times 100$$

b. Analysis of Ethanol Concentration Using Gas Chromatography (GC)

The concentration of fermented ethanol was analyzed using GC. A total of 1 μL of sample solution was injected into the column. The area of the ethanol peak from the chromatogram was then calculated. The ethanol concentration was determined using the standard curve equation.

3. RESULTS AND DISCUSSION

3.1. Surface Texture Analysis Using Scanning Electron Microscopy (SEM)

Before and after hydrolysis, sorghum starch was characterized using Scanning Electron Microscopy (SEM). SEM analysis aims to determine the morphological structure of sorghum starch before and after the hydrolysis. The results of the SEM analysis are depicted in Fig. 1.

Based on Figure 1, there are differences between Figures 1a and Figure 1b, where Figure 1a shows sorghum starch which is still tightly arranged, regular, and rigid. It is due to the presence of wax, hemicellulose, lignin, and other binder components that bind to each other in sorghum starch that has not been hydrolyzed (Umagiliyage et al., 2015). While in Figure 1b, there is a change in the structure of the sorghum starch fiber, which looks more crushed and makes a uniform structure and small size. Microwave hydrolysis accelerates the reduction and degradation of cellulose, resulting in a solid structure with reduced size (Riazi et al., 2015). The low contact time and energy consumption of the microwave reaction will reduce the formation of unwanted secondary products. Microwave heating can rapidly convert starch to sugar. Compared with conventional heating, the reaction rate of starch hydrolysis into glucose increases 100 times with the use of microwave irradiation (Nikolic et al., 2010)

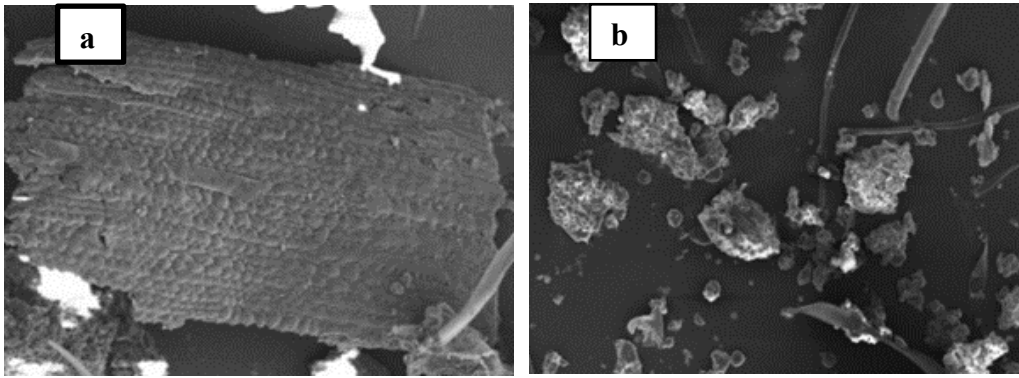


Figure 1. Results of SEM Analysis

Notes: (a) Before Hydrolysis, (b) After Hydrolysis (Source: ITS Energy Laboratory Surabaya)

3.2. Analysis of reducing sugar

Sorghum bagasse was hydrolyzed by microwave at 150°C with variations in heating time of 20, 30, 40, and 50 minutes and using 2% sulfuric acid as a catalyst. Based on the time variation, it was seen that there was a color change with increasing heating time on the sorghum starch hydrolyzate (Fig. 2). The longer the heating time, the darker the color of the hydrolyzate produced. It indicates that there has been a

complete degradation of hemicellulose and cellulose into glucose (Widyastuti, 2019), but if the hydrolysis process is continued, charcoal will form on the Erlenmeyer wall. It implies that the glucose produced is damaged or burned. The microwave method is more profitable than the standard reflux method because of the shorter reaction time (in minutes), fewer solvent, and higher yield (Chen *et al.*, 2012).

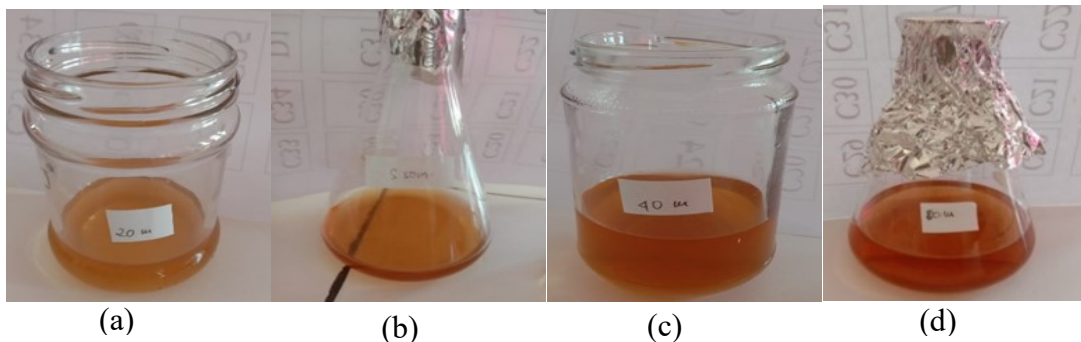


Figure 2. Hydrolysis results from sorghum bagasse (a) 20 minutes, (b) 30 minutes, (c) 40 minutes, (d) 50 minutes

The reducing sugar content of the hydrolyzed filtrate was analyzed using the DNS (Dinitrosalicylic Acid) method with 3,5-dinitrosalicylic acid reagent. The reducing sugar concentration was determined based on the formation of a red-brown reduced product when the sugar in the sample reduced 3,5-dinitrosalicylic to 3-amino-5-nitrosalicylic acid during heating. Glucose testing was carried out at a wavelength of 540 nm because the brownish-red color was absorbed maximally

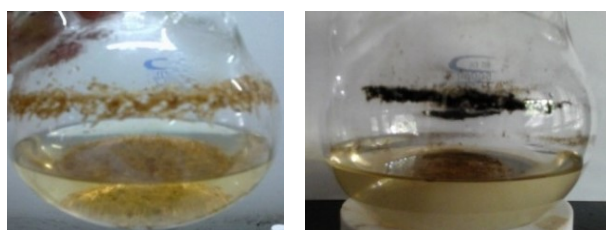
at that wavelength. Glucose can react with DNS so that by processing absorbance values, its levels can be measured spectrophotometrically (Galung, 2021). The measurement results of reducing sugar content are presented in Table 1.

Table 1. Measurement Results of Reducing Sugar Levels

Time (minute)	Reducing Sugar Level (g/L)	Hydrolysis Efficiency (%)
20	29.2	73
30	30.4	76
40	24.3	60
50	22.2	55

Measurement of reducing sugar content using the DNS method in Table 1 shows an increase in reducing sugar content at a hydrolysis time of 20-30 minutes, from 29.2-30.4 g/L, and hydrolysis efficiency from 73-76%. The increase in reducing sugar levels is caused by the hydrolysis process, which takes longer to cause more H⁺ ions to break the cellulose polymer chain, resulting in high free radicals that will bind to OH⁻ ions to form glucose monomers (Melwita et al., 2014). Suppose the hydrolysis process is allowed to continue continuously. In that case, it will cause reducing sugar content, as shown in Table 1, where the hydrolysis time of 40 and 50 minutes had reduced sugar content from 24.3-22.2 g/L. Susansti et al. (2013) reported that the decrease in reducing sugar content was due to a too long

hydrolysis time, causing the converted glucose to be damaged (sugar caramelization) due to excessive heating (Figure 3). Another factor causing the decrease in reducing sugar levels is the hydrolysis of glucose into hydroxymethylfurfural (HMF) and further reaction to form formic acid (Sukowati et al., 2014). The maximum production of reducing sugar was obtained at 30 minutes of heating, which was 30.4 g/L with a hydrolysis efficiency of 76%. This result is higher than Kolo & Sine (2019) on the hydrolysis of sorghum pulp which produces a reducing sugar content of 34.3 mg/L at a hydrolysis time of 40 minutes.


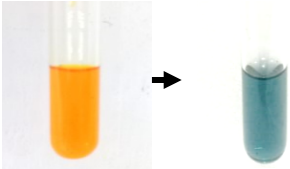
**Figure 3.** The appearance of Microwave Hydrolyzed Solution

3.3. Qualitative analysis of ethanol

Fermentation of glucose hydrolyzate in 2% sulfuric acid treatment was carried out at 150°C for 30 minutes. Fermentation in this study used sorghum bagasse hydrolyzate as a substrate fermented using *Saccharomyces cerevisiae*. The yeast *Saccharomyces cerevisiae* was chosen because it possesses various advantages, including a high rate of survival and the ability to produce an

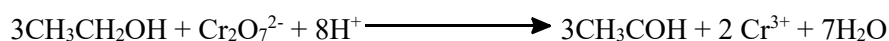
adequate amount of alcohol (Jayus et al., 2016). Before proceeding with Gas Chromatography analysis, a qualitative analysis using potassium dichromate (K₂CrO₇) was performed to verify that the sample from the stepwise distillation produced ethanol. The results of the analysis are presented in Table 2.

Table 2. Qualitative results of ethanol analysis

Sample	Results	Image
Pure ethanol	Positif (+)	
Sorghum ethanol	Positif (+)	

The images in Table 2 show the color change from orange to blue. It proves the presence of ethanol in the distillate (Saleh et al., 2016). Color change due to oxidized

alcohol. Cr^{6+} , which is yellow, is reduced to Cr^{3+} , which is blue, according to the following reaction (Sania et al., 2015):



3.4. Quantitative analysis of ethanol

a. Analysis results of ethanol concentration using pycnometer

The fermentation process in this study was carried out with various inoculum concentration treatments, namely 4, 6, and 8%. Analysis using a pycnometer was carried out to determine the density of fermented ethanol. The ethanol density results obtained were matched with the specific gravity conversion table to determine the ethanol concentration. Conversion of specific gravity of ethanol concentration for each treatment (inoculum concentration 4, 6, and 8%) is depicted in Table 3.

Based on the ethanol results and the parameters of the three variations of inoculum concentration, it can be concluded that the highest ethanol concentration was obtained from fermentation with 8% inoculum, namely 5.325%. These results indicated that the ethanol concentration increased with increasing inoculum

concentration. It is because the percentage concentration of inoculum is inversely proportional to the lag phase, where the higher the inoculum concentration, the shorter the lag phase so that it quickly reaches the exponential phase. The exponential phase occurs when the yeast fully grows and adapts, allowing for maximum sugar conversion and the formation of a product (ethanol). The purpose of inoculum preparation is to shorten the lag phase (adaptation) of fermentation, resulting in a shorter fermentation time and a higher alcohol content produced (Pramita et al., 2014). The highest values obtained from a pycnometer examination of ethanol content were used for GC analysis, namely fermentation with 8% inoculum (Table 4). The quantitative test of ethanol using a pycnometer and GC showed that the ethanol concentration increased with the increase in the inoculum concentration.

Table 3. Substrate Parameters and Experimental Results

Yeast Concentration %	Ethanol Concentration (%)	Y (%)	EF%	EK%
4	0.465	1.52	2.98	1.15
6	5.034	16.33	32.03	12.41
8	5.325	17.25	33.86	13.12

*Description: Y: Yield, EF: Fermentation Efficiency, EK: Conversion Efficiency

b. Analysis of ethanol concentration using GC

Standard chromatograms and sample analysis using GC are presented in Fig. 4 and Fig. 5.

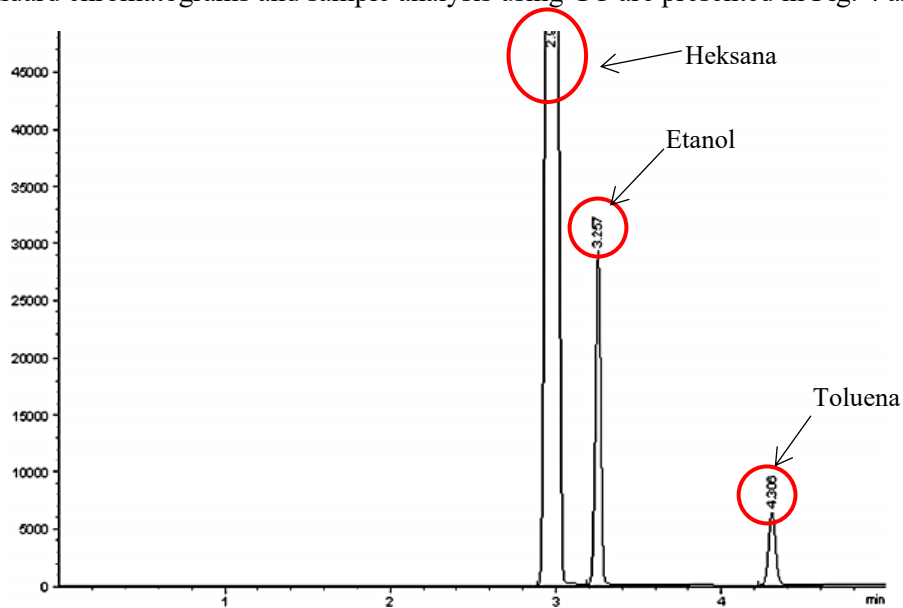


Figure 4. Ethanol standard chromatogram

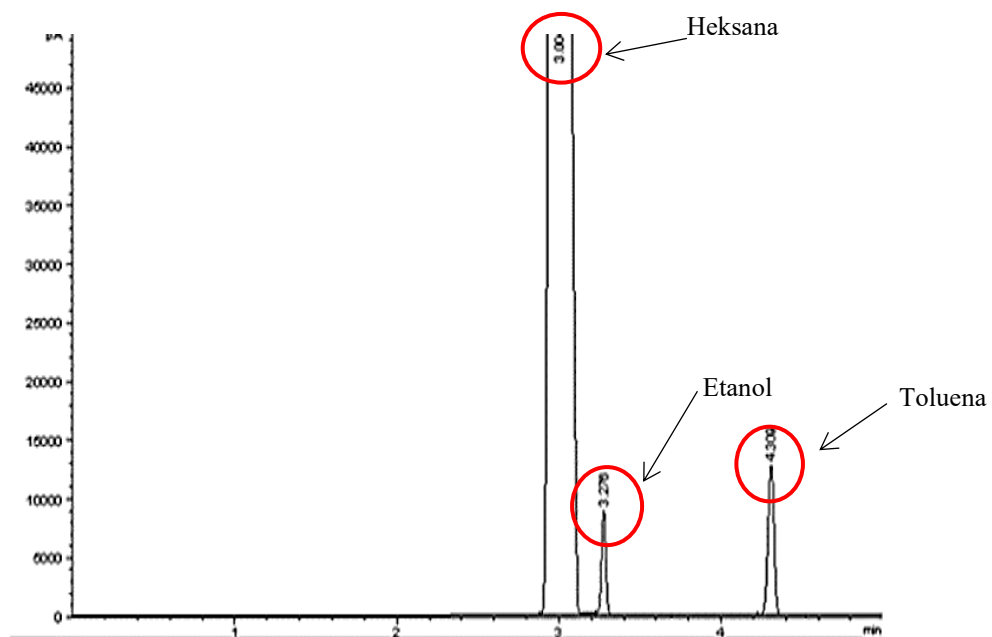


Figure 5. Bioethanol Chromatogram of Sorghum Bagasse

The presence of ethanol in the fermentation product was determined by comparing the sample's retention time to the standard, as seen in Figures 4 and 5. The chromatogram results showed no significant difference between the standard solution and the sample. Retention time on standard ethanol is 3.257 minutes and on the sample is 3.276 minutes. It indicates that the analysis results contain pure ethanol. At the same time, the toluene that comes out at a retention time of 4.306 minutes on the standard and 4.309 minutes on the sample is the internal standard used in the analysis

using GC. This study chose toluene as the internal standard because toluene has a molecular formula similar to ethanol. Due to the similarities of the two structures, it is simple to determine the solubility of the two solutions (like dissolves like) (Solikha, 2017). Quantitatively, the measurement of ethanol content using GC was performed by comparing the area of the ethanol peak with the area of the standard and multiplied by the standard concentration. The calculation results of bioethanol concentration, yield, fermentation efficiency, and conversion efficiency are presented in Table 4.

Table 4. Substrate Parameters of GC Analysis

Ethanol Concentration %	Y (%)	EF%	EK%
9,05	29,35	57,56	22,31

***Description:** Y: Yield, EF: Fermentation Efficiency, EK: Conversion Efficiency

The highest ethanol yield was obtained at an inoculum concentration of 8%, namely 9.05 % with a yield of 29.35 %, fermentation efficiency of 57.56 %, and conversion efficiency of 22.31 %. The ethanol yield value indicates the amount of ethanol produced from the substrate. The efficiency of fermentation is used to determine the success of the fermentation. The higher the fermentation efficiency, the higher product is produced, and the conversion efficiency reflects how many substrates are converted to ethanol products. According to the GC analysis results presented in the table, the fermented sorghum bagasse contained 9.05 % ethanol. This result is lower than that of Sarongallo *et al.* (2017), who purified bioethanol from sweet sorghum juice at a concentration of 43%. This difference could be explained by the fact that prior investigations used sorghum juice, but this

study used sorghum bagasse. Other possible explanations for the low ethanol content in this investigation include the absence of an ethanol purification step. The distillation results still contain water and inhibitor chemicals that prevent the creation of ethanol. It is supported by Roni (2015), who states that inhibitor compounds formed in the hydrolysis process using dilute acid can inhibit the fermentation process.

4. CONCLUSION

Based on the findings of the investigation, the following conclusion could be drawn:

1. SEM analysis revealed that the sample's surface was flat, rough, and rigid prior to hydrolysis, but after hydrolysis, the surface was damaged, appearing crushed with a smaller size.
2. The optimum hydrolysis time using a microwave at 150°C was 30 minutes, resulting in the highest reducing sugar content of 30.4 g/L.
3. The highest ethanol content obtained from sorghum bagasse fermentation using an inoculum concentration of 8% was 5.325% (pycnometer) and 9.05% (GC).

LIST OF REFERENCES

- Arif, A. Bin, Budiyanto, A. ., Diyono, W. ., & Richana, N. (2018). Optimasi Waktu Fermentasi Produksi Bioetanol Dari Dedak Sorghum Manis (*Sorghum Bicolor* L) Melalui Proses Enzimatis. *Jurnal Penelitian Pascapanen Pertanian*, 14(2), 67. <https://doi.org/10.21082/jpasca.v14n2.2017.67-78>
- Galung, F. S. (2021). Analisis Kandungan Karbohidrat (Glukosa) Pada Salak Golla – Golla *Salacca Edulis*. *Journal Of Agritech Science*, 5(1), 10–14.
- Kolo, S.M.D, & Sine, Y. (2019). *Produksi Bioetanol Dari Ampas Sorgum Lahan Kering Dengan Perlakuan Awal Microwave Irradiasi*. 2(2622), 39–40.
- Kolo, S.M.D., Presson, J., & Amfotis, P. (2021). Produksi Bioetanol Sebagai Energi Terbarukan Dari Rumpuk Laut Ulva *Reticulata* Asal Pulau Timor. *Alchemy Jurnal Penelitian Kimia*, 17(2), 159. <https://doi.org/10.20961/alchemy.17.2.45476.159-167>
- Kolo, S.M.D., Wahyuningrum, D., & Hertadi, R. (2020). The Effects Of Microwave-Assisted Pretreatment And Cofermentation On Bioethanol Production From Elephant Grass. *International Journal Of Microbiology*, 2020, 1–11. <https://doi.org/10.1155/2020/6562730>
- Melwita, E., & Kurniadi, E. (2014). Pengaruh Waktu Hidrolisis Dan Konsentrasi H₂so₄ Pada Pembuatan Asam Oksalat Dari Tongkol Jagung. *Teknik Kimia*, 20(2), 55–63.
- Rani, D. A., Yuniar, & Sofiah. (2019). Pembuatan Bioetanol Dari Umbi Singkong Karet (*Manihot Glaziovii*) Yang Dihidrolisis Asam Dan Enzim. *Prosiding Seminar Nasional Ii Hasil Litbangyasa Industri*, 174–180.

- Ray, R. C., Uppuluri, K. B., Trilokesh, C., & Lareo, C. (2019). Sweet Sorghum For Bioethanol Production: Scope, Technology, And Economics. In *Bioethanol Production From Food Crops*. Elsevier Inc. All Rights Reserved. <https://doi.org/10.1016/B978-0-12-813766-6/00005-9>
- Riazi, S., Rahimnejad, M., & Najafpour, G. D. (2015). Hydrolysis Of Sorghum (Broomcorn) In Diluted Hydrochloric Acid. *International Journal Of Engineering, Transactions B: Applications*, 28(11), 1543–1551. <https://doi.org/10.5829/idosi.ije.2015.28.11b.01>
- Roni, K. A. (2015). Pembuatan Bioethanol Dari Tanah Gambut Dengan Proses Hidrolisis Asam Kuat. *Berkala Teknik*, 5(1), 801–813.
- Saleh, H. A., Saokani, J., & Rijal, S. (2016). Penentuan Nilai Kalor Serta Pengaruh Asam Klorida (Hcl) Terhadap Kadar Bioethanol Bonggol Pisang (Musa Paradisiacal). *Al-Kimia*, 4(1), 68–77. <https://doi.org/10.24252/Al-Kimia.V4i1.1458>
- Samsuri, M., Gozan, M., Mardias, R., Baiquni, M., Hermansyah, H., Wijanarko, A., Prasetya, B., & Nasikin, M. (2007). Pemanfaatan Sellulosa Bagas Untuk Produksi Ethanol Melalui Sakarifikasi Dan Fermentasi Serentak Dengan Enzim Xylanase. *Makara Teknologi*, 11(1), 17–24. <https://doi.org/10.7454/mst.v11i1.437>
- Sania, Eleny., S. (2015). Pemanfaatan Limbah Tandan Kelapa Untuk Pembuatan Bioethanol Melalui Proses Hidrolisis Dan Fermentasi. *Indonesian Journal Of Chemical Science*, 4(3).
- Solikha, D. F. (2017). Analisis Kandungan P-Xilena Pada Pertamina Dan Pertamina Plus Dengan Teknik Kromatografi Gas (Gc-Pu 4600) Menggunakan Standar Internal. In *Jurnal Ilmiah Indonesia* (Vol. 2, Issue 8).
- Sukowati, Asih., Sutino., Rizal, S. (2014). Produksi Bioethanol Dari Kulit Pisang Melalui Hidrolisis Asam Sulfat. *Jurnal Teknologi Dan Industri Hasil Pertanian Volume*, 19(3), 274–288.
- Susanti, Ari Diana, Puspito Teguh Prakoso, H. P. (2013). Pembuatan Bioethanol Dari Kulit Nanas Melalui Hidrolisis Dengan Asam. *Ekulibrium*, 12(1), 11–16. <https://doi.org/10.20961/Ekulibrium.V12i1.2170>
- Umagiliyage, A. L., Choudhary, R., Liang, Y., Haddock, J., & Watson, D. G. (2015). Laboratory Scale Optimization Of Alkali Pretreatment For Improving Enzymatic Hydrolysis Of Sweet Sorghum Bagasse. *Industrial Crops And Products*, 74, 977–986. <https://doi.org/10.1016/J.Indcrop.2015.05.044>
- Widyastuti, P. (2019). Pengolahan Limbah Kulit Singkong Sebagai Bahan Bakar Bioethanol Melalui Proses Fermentasi. *Jurnal Kompetensi Teknik*, 11(1), 41–46.

Study on Adsorption Kinetics of Methylene Blue by Modified Sago Frond Waste

Kajian Kinetika Adsorpsi Metilena Biru oleh Limbah Pelepah Sagu Termodifikasi

Seniman Gempur Tirani^{1,2,*}, Sunardi^{1,2,3,*}

¹Chemistry Study Program, Faculty of Mathematics and Natural Sciences,
Lambung Mangkurat University, Banjarbaru, Indonesia

²Ecomaterials Research Group, Faculty of Mathematics and Natural Sciences,
Lambung Mangkurat University, Banjarbaru, Indonesia

³Wetland-Based Materials Research Group, Lambung Mangkurat University, Banjarbaru, Indonesia

*Email: sunardi@ulm.ac.id

ABSTRACT

The modified sago frond waste (PSM) using the Fast Microwave-Assisted Acid method, which has several characteristic changes, was tested to determine its adsorption ability to a cationic textile dye. PSM samples as adsorbents have variations in the modification of oxalic acid addition at 0; 1,5; 3,0 and 4,5% (w/v) were used for the adsorption of Methylene Blue (MB) dye on several parameters. This study was conducted to determine the adsorption kinetics through the effect of the ratio of the adsorbent and the contact time and the acid variation of the adsorbent as additional variables. Optimum MB absorption was obtained at a ratio of 0,6 g/L and a contact time of 120 minutes. The data results were analyzed using four general kinetic models: pseudo-first-order, pseudo-second-order, intra-particle diffusion, and Elovich equation. Adsorption followed the pseudo-second-order reaction rate with a coefficient of determination (R^2) 0.9996-0.9999 in all variations of PSM. The theoretical adsorption capacity was 25.58 to 27.32 mg/g, and the effect of increasing acid on PSM increased the adsorption and absorption capacity of MB.

Keywords: sago frond waste, adsorption, kinetic models, methylene blue.

ABSTRAK

Limbah pelepah sagu hasil modifikasi (PSM) dengan metode Fast Microwave-Assisted Acid yang memiliki beberapa perubahan karakteristik diuji untuk mengetahui kemampuan adsorpsinya terhadap suatu zat warna tekstil kationik. Sampel PSM sebagai adsorben memiliki variasi modifikasi penambahan asam oksalat pada 0; 1,5; 3,0 dan 4,5% (b/v) digunakan untuk adsorpsi zat warna Metilena Biru (MB) pada beberapa parameter. Studi ini dilakukan untuk mengetahui tinjauan kinetika adsorpsi melalui pengaruh dari rasio adsorben dan waktu kontak serta variasi asam dari adsorben juga menjadi variabel tambahan. Penyerapan optimum MB didapat pada rasio 0,6 g/L dan waktu kontak 120 menit. Untuk memperkirakan model kinetika adsorpsi MB pada PSM, empat model kinetika umum yaitu orde pertama semu, orde kedua semu, difusi intra-partikel dan persamaan Elovich telah digunakan. Adsorpsi diketahui mengikuti laju reaksi orde kedua semu dengan tingkat koefisien determinasi (R^2) 0,9996-0,9999 pada semua variasi PSM. Kapasitas adsorpsi maksimum teoritis diketahui sebesar 25,58 hingga 27,32 g/mg dan peningkatan asam pada PSM juga diketahui dapat meningkatkan kapasitas adsorpsi serta penyerapan dari MB.

Kata Kunci: pelepah sagu, adsorpsi, model kinetika, metilena biru.

Submitted: November 26, 2021; **Accepted:** February 22, 2022; **Available online:** March 8, 2022

1. INTRODUCTION

The continuous development of the industry has led to a massive increase in the release of excess synthetic dyestuffs into water sources. According to Mittal et al. (2010), Saleh and Gupta (2014), and Anwar and Mulyadi (2015), more than 15% of synthetic dyestuffs are lost or separated during the manufacturing and operational processes as industrial waste. Many industries waste contains dyes as a by-product of the process. This dye is present as a pollutant that is difficult to degrade naturally, has a high level of toxicity, and is carcinogenic (Oladipo et al., 2014). Industries that produce plastics, cosmetics, rubber, printing, leather, pharmaceuticals, food, and textiles are the most dominant industries that produce dye waste during their operations (Mittal et al., 2009). The ability of dyes to spread quickly causes these pollutants to change the color of polluted water easily. When dissolved in water, the dye will block sunlight from penetrating the water's surface and inhibit the photochemical and biological activity of the aquatic life. Therefore, removing or reducing synthetic dyes as contaminants in wastewater is of particular concern (Malik et al., 2007, Balarak et al., 2015).

Dyes are generally classified into cationic and anionic. Cationic dyes are more toxic than anionic dyes. One example of a cationic dye is methylene blue ($C_{16}H_{18}N_3S$, C.I. No. 52015). This dye is generally applied as dyes for cotton, wool, silk, leather, and coatings for paper stocks (Ghaedi et al., 2014). Although methylene blue is not very dangerous, long-term exposure could cause serious health problems such as increased heart rate, vomiting, shock, cyanosis, jaundice, quadriplegia, mental confusion, eye burns, tissue necrosis, and methemoglobinemia (Rafatullah et al., 2010, Kushwaha et al., 2014).

Removing contaminants from synthetic dyes is known to be quite tricky because of its resistance to aerobic and anaerobic decomposition. It is also stable to light, heat,

and moderate oxidizing agents (Crini, 2006, Vimonses et al., 2009). One of the most effective technologies for removing dyes from waste is the adsorption process (Demirbas, 2009). Although the activated carbon adsorption method has been proven to be the most effective adsorbent (Mall et al., 2005, Namasivayam and Kavitha, 2002), its widespread application is hampered by the relatively high production cost of up to \$1.3-20/kg (Gupta et al., 2009). Therefore, various studies have been conducted to obtain other alternatives to develop low-cost adsorbents using lignocellulosic biomass and natural minerals (clay, zeolite).

Modified sago frond (PSM) has several changed characteristics, such as darker color, reduced adsorbent mass, reduced lignin composition, and changes in the crystallinity of the lignocellulosic structure (Tirani et al., 2021). This research was conducted to determine the adsorption capacity of the modified biomass source, especially in terms of its kinetics. In addition, the research results are expected to provide a deeper understanding of the MB adsorption mechanism on PSM.

2. MATERIALS AND METHODS

2.1. Materials

The materials used were Methylene Blue ($C_{16}H_{18}N_3S$, CAS.NO. 61-73-4) from PUDAK SCIENTIFIC and PSM samples from previous studies. The tools used were a series of glassware, Fujitsu FSR-A Analytical balance, UV-Visible spectrophotometer LGS 53 BEL® Photonics., and Orbital Shaker KJ-201BD OREGON. This research was conducted at the Forestchem Workshop, Banjarbaru.

2.2. Methods

The initial preparation was crushing and milling the sago frond into powder and small pieces, then drying in direct sunlight. The dried samples were filtered to a 40-60 mesh size and dried in an oven at 105°C for 30 minutes and then stored in an airtight container at room temperature. A total of 3

grams of prepared sago frond were added with water as a solvent; oxalic acid 0; 1.5; 3.0; & 4.5 % (w/v) with a 1:25 ratio of sample powder and solvent. The sample was then irradiated in a microwave with a power of 450 W for 10 minutes. After completion, the samples were rinsed and neutralized. The neutral sample was then placed in an oven at 105°C for 5 hours. This procedure was carried out in the previous studies (Tirani et al., 2021).

The 1000 ppm MB stock solution was prepared by dissolving 0.5 grams of MB in 500 mL of deionized water. MB standard solution was prepared by diluting stock solution up to 2; 3; 4; 5; 6, and 7 ppm. Determination of the maximum wavelength was carried out by measuring the absorption of 4 ppm MB solution in the range of 600-700 nm. The absorption of each standard solution was measured, and a calibration curve was made to determine the final concentration of the MB sample.

The first test parameter was the effect of PSM ratio (0.2; 0.3; 0.4; 0.5 and 0.6 g/L). PSM adsorbent with oxalic acid variation 0; 1.5; 3.0 and 4.5% of the previous study were taken (4; 6; 8; 10 and 12 mg), and a 20 ppm MB solution was prepared from the dilution of the stock solution, respectively. A total of 20 mL of the MB solution was put into an Erlenmeyer, and PSM adsorbent was added and then stirred with an Orbital Shaker for 120 minutes at 120 rpm. The adsorbed MB solution was taken, and the absorption was measured at a wavelength of 665 nm. The

second parameter was the effect of contact time (10, 20, 40, 80, and 120 minutes). A total of 12 mg PSM of all variations was tested at 20 mL MB 20 ppm at a predetermined time range, and the final absorption was measured. The adsorption and adsorption capacities of MB were then calculated.

3. RESULTS AND DISCUSSION

Modification of the biomass source (sago frond waste) was carried out using the Fast Microwave-Assisted Acid method. Samples of sago frond with variations in oxalic acid (0; 1.5; 3.0 and 4.5%) were irradiated by microwave at 450 W for 10 minutes. This pretreatment method has been used in previous studies, where the lignocellulosic structure was crushed to release cellulose and remove hemicellulose and lignin components (Tirani et al., 2021). The modified adsorbent was then used for the MB adsorption test by taking into account the adsorption capacity and percent absorption of MB, which was calculated through the following equation:

$$q_e = \frac{(C_0 - C_e) \times V}{m} \quad (1)$$

$$\% \text{ absorption} = \frac{(C_0 - C_e)}{C_0} \quad (2)$$

Where q_e as adsorption capacity (mg/g), C_0 and C_e as initial concentration and final concentration/equilibrium (mg/L), V as volume MB (L), and m is the mass of adsorbent used (g). PSM adsorbent is showed in Fig. 1.

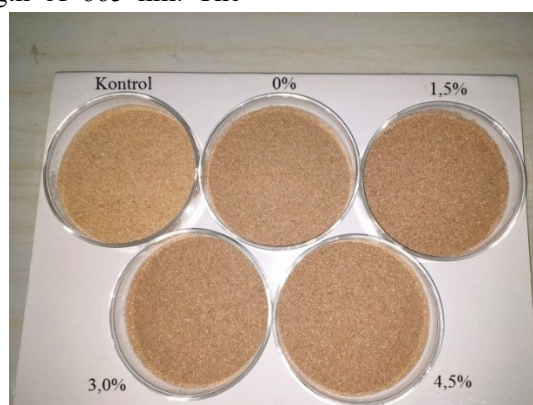


Figure 1. PSM adsorbent (Tirani et al., 2021).

Table 1. MB concentration data before and after the adsorption

Parameter	Ratio (g/L)	Contact Time (minute)	Initial Concentration (ppm)	Final Concentration (ppm)			
				0%	1,5%	3,0%	4,5%
Effect of adsorbent ratio	0.2	120	20	10.91	10.41	10.16	9.92
	03	120	20	9.08	8.71	8.50	8.35
	0.4	120	20	7.12	6.83	6.58	6.38
	0.5	120	20	5.06	4.82	4.58	4.48
	0.6	120	20	4.40	4.14	3.99	3.85
Effect of contact time	0.6	10	20	7.74	7.71	7.69	7.66
	0.6	20	20	6.96	6.73	6.41	6.64
	0.6	40	20	6.19	5.54	5.08	4.84
	0.6	80	20	5.45	4.83	4.48	4.24
	0.6	120	20	5.00	4.72	4.44	4.13

3.1. Effect of PSM Adsorbent ratio on adsorption ability for MB

The effect of the ratio and variation of acid on the adsorption and absorption capacity is presented in Fig. 2. These results indicate that the percentage of MB adsorption increases with the increase in the ratio of the adsorbent used. However, as it approaches 0.6 g/L, there is a smaller increase than before, which is predicted to approach the maximum absorption for the following parameters. An increase in the ratio also means an increase in the amount of adsorbent used. Therefore, the surface site for adsorption also increases, and the interaction between adsorbent-adsorbate increases the absorption percentage. Meanwhile, the adsorption capacity showed a decrease as the ratio increased. According to El Qada et al. (2006), increasing the amount of adsorbent while maintaining the same volume and concentration of MB may

take longer to attain the maximal adsorption capacity. The sample with a lower ratio has more adsorption sites and thus a larger adsorption capacity. In addition, other studies also showed similar results when using activated carbon from corn husks (biomass) as MB adsorbent. According to Khodaie et al. (2013), decreased adsorption capacity at higher ratios could occur for two reasons. First is the unsaturation of the adsorption site that occurs during the adsorption process. Second, particulate interactions such as aggregation at high ratios lead to a decrease in the surface area of the adsorbent and an increase in the length of the diffusion path. Overall, the effect of acid variations on the adsorbent indicates that the increase in the concentration of oxalic acid used will increase the adsorption ability of PSM. The highest absorption occurred at 4.5% PSM adsorbent with a ratio of 0.6 g/L, 80.76% with an adsorption capacity of 26.92 mg/g.

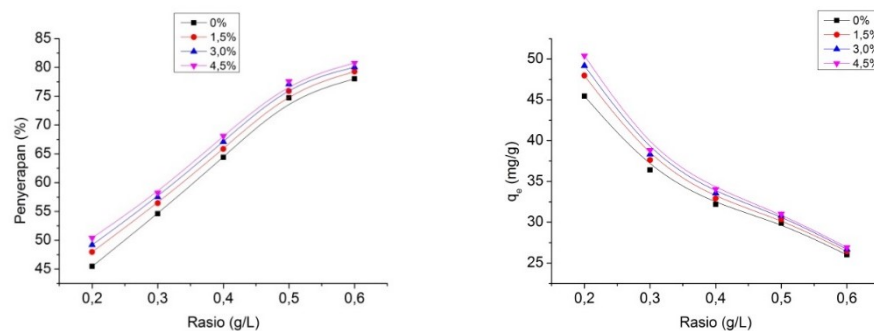


Figure 2. Effect of adsorbent ratio on MB absorption and adsorption capacity ($C_0 = 20$ ppm, contact time = 120 minutes, stirring speed = 120 rpm).

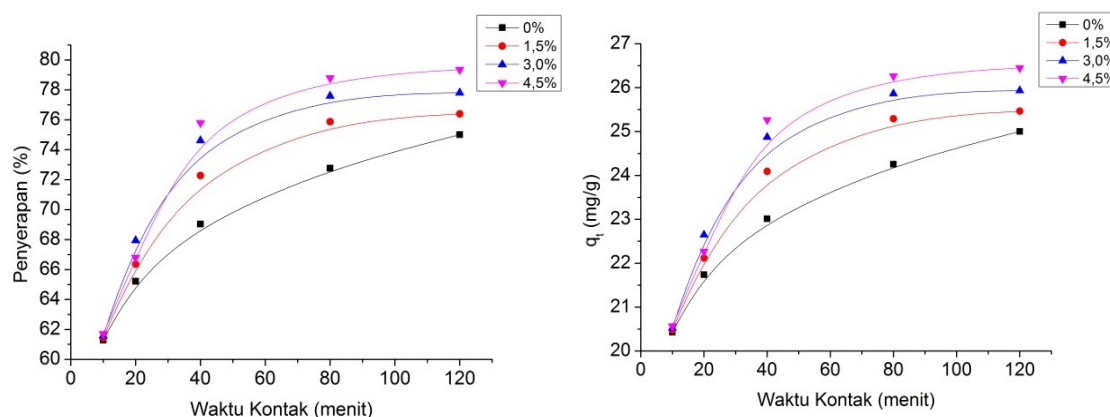


Figure 3. Effect of contact time on MB absorption and adsorption capacity ($C_0 = 20$ ppm, adsorbent ratio = 0.6 g/L, stirring speed = 120 rpm).

3.2. Effect of contact time on adsorption ability for MB

By optimizing the previous adsorbent ratio, an adsorbent ratio of 0.6 g/L was taken

to maximize the absorption of MB. Fig. 3 illustrates the effect of the contact time for the adsorbent-adsorbate interaction on the adsorption and adsorption capacity.

In general, the pattern of increasing adsorption capacity with MB absorption is nearly identical to the trend of increasing contact time. A significant increase occurred at a time of up to 40 minutes, and after that, the increase was relatively small. This not-too-significant increase can be indicated as a time towards equilibrium. Judging from the

effect of the PSM acid variation itself, as the concentration of the acid used increases, it can accelerate the adsorption process to its equilibrium state and also slightly increase the adsorption capacity at the equilibrium state.

3.3. Kinetic Model

Determination of the appropriate model is needed to determine the adsorption mechanism. Several models that can be used are pseudo-first-order (Lagergren, 1898), intra-particle diffusion (Ho and McKay, 1998), and the Elovich equation (Wu et al., 2009). The four models are based on Table 2 below.

Table 2. Kinetic model of reaction rate mechanism

Model	Equation	Plot
pseudo-first-order	$\ln(q_{e,exp} - q_t) = \ln q_e - k_1 t$ (3)	$\ln(q_{e,exp} - q_t)$ vs t
pseudo-second-order	$\frac{t}{q_t} = \frac{1}{k_2 q_e^2} + \frac{1}{q_e} t$ (4)	t/q_t vs t
intra-particle diffusion	$q_t = k_{id} t^{1/2} + C$ (5)	q_t vs $t^{1/2}$
Elovich equation	$q_t = \left(\frac{1}{\beta}\right) \ln(\alpha\beta) + \left(\frac{1}{\beta}\right) \ln(t)$ (6)	q_t vs $\ln(t)$

The model validity can be seen from each plot. The most suitable model is determined from the correlation coefficient (r) and/or the coefficient of determination (R^2). Each model has its variable parameters such as $q_{e,exp}$, namely adsorption capacity at experimental equilibrium (mg/g), q_t , namely adsorption capacity at time t (mg/g), q_e , namely theoretical adsorption capacity (mg/g), k_1 and k_2 are the rate constants for the pseudo-first-order ($l \text{ min}^{-1}$) and pseudo-second-order ($g \cdot mg^{-1} \cdot min^{-1}$) reactions, respectively. For the diffusion model, k_{id} is the rate constant of the intra-particle diffusion model ($mg \cdot g^{-1} \cdot min^{-1/2}$), and C represents the thickness of the boundary layer (mg/g). For the Elovich equation, a represents the chemisorption rate at zero coverage ($mg \cdot g^{-1} \cdot min^{-1}$) and b corresponds to the level of surface coverage and the chemisorption activation energy (g/mg).

Through the plot graphs of the four models, the coefficient of determination (R^2), normalized standard deviation (Dq), and sum squared errors (SSE) will become the reference for determining the most suitable model. Among all the types of kinetic models tested, the pseudo-second-order had the highest coefficient of determination, namely 0.9996-0.9999. Besides that, the Dq value of the model ranged from 0.019-0.044%. Another similar study was by Foo and Hameed (2012), which used industrial solid waste prepared by microwave for MB adsorption. The adsorption kinetics are also in line with the

pseudo-second-order model. The parameters obtained from this kinetic model are theoretical adsorption capacity which increases as the concentration of oxalic acid increases from the previous pretreatment process. This value was calculated at 25,576;

26,178; 26.667 and 27.322 mg/g with a pseudo-second-order reaction rate constant of 0.011135; 0.011854; 0.012133 and 0.010034 ($l \text{ min}^{-1}$) respectively. The adsorption capacity shown in the pseudo-second-order model is also close to the experimental adsorption capacity value, compared to the pseudo-first-order model, which has a significant difference in the value of the theoretical adsorption capacity to the experiment. Therefore, the mechanism that occurs during the adsorption of MB by PSM based on a pseudo-second-order kinetic model explains the presence of a corresponding chemisorption by sharing and exchanging electrons between MB and the PSM structure (Ho and McKay, 1998). Although not as good as the pseudo-second-order, the pseudo-first-order kinetic model also shows a relatively high fit to the experimental data. The mechanism that occurs based on this model is adsorption which is influenced by the adsorbate so that the interactions that occur are limited to physical adsorption (Foo and Hameed, 2012).

The fundamental difference between the two Lagergren models lies in their basic properties, namely physisorption for pseudo-first-order and chemisorption for pseudo-second-order (Lagergren, 1898). As a conclusion from the consensus between the experimental data and the model, the mechanism that occurs during MB adsorption by PSM based on a pseudo-second-order kinetics model explains the existence of corresponding chemisorption by sharing and exchanging electrons between MB and the PSM structure (Ho and McKay, 1998), but does not mean that adsorption is physically absent or not involved in the process. Chemisorption (adsorption) can be assumed to act more dominantly as a rate-determining step of the reaction.

Table 3. Comparison of pseudo-first-order and pseudo-second-order kinetic model parameters of MB adsorption by several variations of PSM

PSM (b/v)	q _{e,exp} (mg/g)	Pseudo-firstorder				Pseudo-second-order				
		k ₁ (1/sec)	q _{e,cal} (mg/g)	R ²	Dq (%)	k ₂ (1/sec)	q _{e,cal} (mg/g)	h (mg ² /g ² sec)	R ²	Dq (%)
0%	25.002	-0.0254	5.634	0.9977	0.086	0.011135	25.576	7.283	0.9996	0.044
1.5%	25.463	-0.0485	8.676	0.9975	0.167	0.011854	26.178	8.124	0.9999	0.019
3.0%	25.934	-0.0626	11.226	0.9967	0.247	0.012133	26.667	8.628	0.9999	0.020
4.5%	26.449	-0.0505	10.111	0.9953	0.255	0.010034	27.322	7.491	0.9998	0.027

Table 4. Comparison of the parameters of the intra-particle diffusion kinetics model and the Elovich equation

PSM (b/v)	Difusi intra-partikel				Persamaan Elovich			
	C (mg/g)	k _{id}	R ²	Dq	a	b	R ²	Dq
0%	19.02	0.5711	0.9695	5.850	12747.49	0.545167	0.9999	0.986
1.5%	19.179	0,6364	0.8941	63.638	4065.815	0.476872	0.9708	21.001
3.0%	19.411	0.673	0.8429	16.775	2518.834	0.444425	0.9423	32.141
4.5%	19.013	0.7604	0.8601	17.708	971.494	0.396715	0.9450	35.100

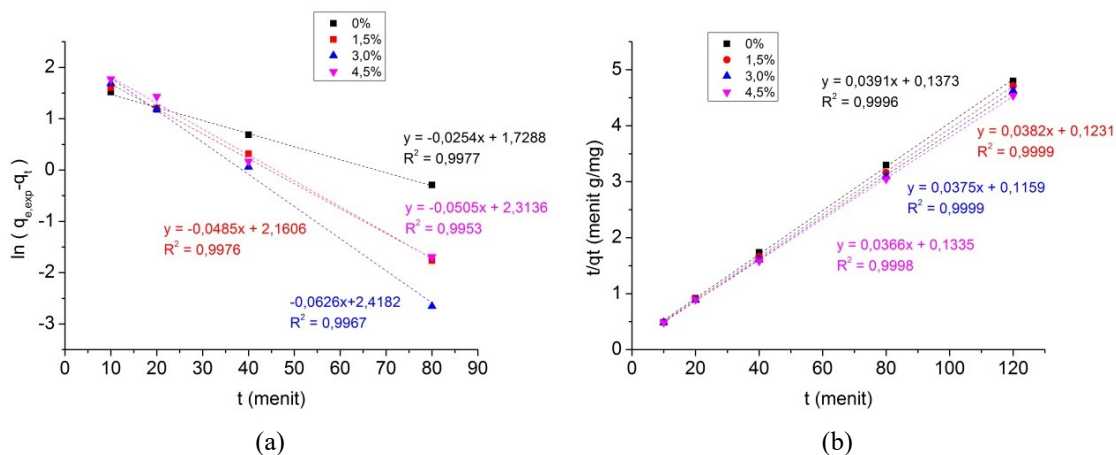


Figure 5. Comparison of pseudo-first-order plots (a) and pseudo-second-order plots (b)

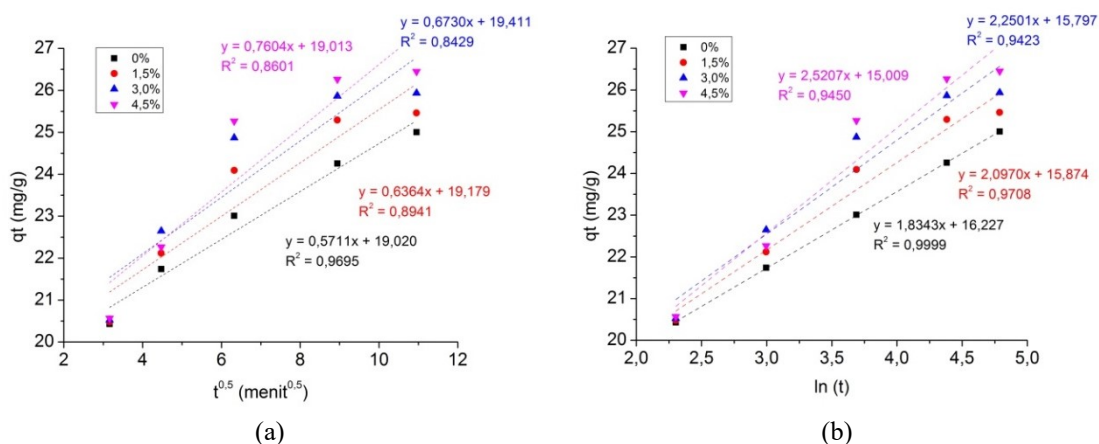


Figure 6. Intra-particle diffusion kinetics model plot (a) and Elovich equation (b)

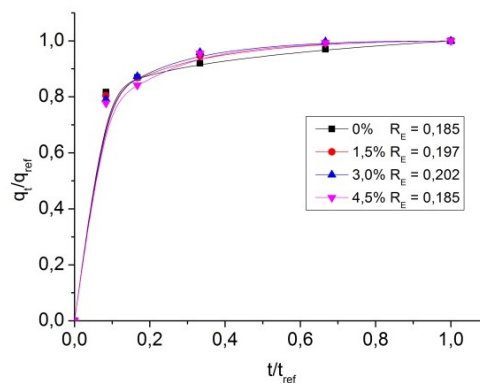


Figure 7. Curves characteristics based on the dimensionless Elovich equation

Another graph also exhibits samples with a kinetic model that matches the Elovich equation, namely 0% PSM. The Elovich equation describes a reaction involving the adsorption of a chemical substance on a solid surface without any product desorption. The reaction rate decreases with time due to increased surface coverage (Wu et al., 2009). Characteristics that can explain the type of reaction that occurs are indicated by the RE value of the equation:

$$\left(\frac{q_t}{q_{ref}}\right) = R_E \ln\left(\frac{t}{t_{ref}}\right) + 1 \quad (7)$$

The RE value at 0% PSM, which was 0.185, is in zone III, which ranges from 0.02 to 0.1, and this type of reaction means a rapid rise. According to Elovich's equation, the majority of adsorption systems are in zone II, while zones I and IV are very few (Wu et al., 2009). The intra-particle diffusion plot has a relatively low fit with the experimental data (except 0% PSM). With some of the available data, it can be assumed that the effect of chemisorption on determining the rate of a reaction is greater than that of physisorption or diffusion.

4. CONCLUSIONS

The experimental results of the treatment of sago frond by increasing the concentration of oxalic acid could increase the adsorption and absorption capacity of MB. The optimal adsorption process occurred at an adsorbent ratio of 0.6 g/L for 120 minutes, focusing on the highest MB absorption of 79.346% at 4.5% PSM with an adsorption capacity of 26.449 mg/g. The experimental data follow the pseudo-second-order kinetic model based on the dominant chemisorption as determining the reaction rate. This process has the advantage of fast and efficient adsorption.

LIST OF REFERENCES

- Anwar, D. I. & Mulyadi, D. (2015). Synthesis of Fe-TiO₂ composite as a photocatalyst for degradation of methylene blue. *Procedia Chemistry*, 17, 49-54.
- Balarak, D., Jaafari, J., Hassani, G., Mahdavi, Y., Tyagi, I., Agarwal, S. & Gupta, V. K. (2015). The use of low-cost adsorbent (Canola Residues) for the adsorption of methylene blue from aqueous solution: isotherm, kinetic and thermodynamic studies. *Colloids and Interface Science Communications*, 7, 16-19.
- Crini, G. (2006). Non-conventional low-cost adsorbents for dye removal: a review. *Bioresource technology*, 97, 1061-1085.
- Demirbas, A. (2009). Agricultural based activated carbons for the removal of dyes

- from aqueous solutions: a review. *Journal of hazardous materials*, 167, 1-9.
- El Qada, E. N., Allen, S. J. & Walker, G. M. (2006). Adsorption of basic dyes onto activated carbon using microcolumns. *Industrial & engineering chemistry research*, 45, 6044-6049.
- Foo, K. & Hameed, B. (2012). Adsorption characteristics of industrial solid waste derived activated carbon prepared by microwave heating for methylene blue. *Fuel Processing Technology*, 99, 103-109.
- Ghaedi, M., Pakniat, M., Mahmoudi, Z., Hajati, S., Sahraei, R. & Daneshfar, A. (2014). Synthesis of nickel sulfide nanoparticles loaded on activated carbon as a novel adsorbent for the competitive removal of methylene blue and safranin-O. *Spectrochimica Acta Part A: Molecular and Biomolecular Spectroscopy*, 123, 402-409.
- Gupta, V. K., Carrott, P., Ribeiro Carrott, M. & Suhas. (2009). Low-cost adsorbents: growing approach to wastewater treatment—a review. *Critical reviews in environmental science and technology*, 39, 783-842.
- Ho, Y.-S. & McKay, G. (1998). Kinetic models for the sorption of dye from aqueous solution by wood. *Process Safety and Environmental Protection*, 76, 183-191.
- Khodaie, M., Ghasemi, N., Moradi, B. & Rahimi, M. (2013). Removal of methylene blue from wastewater by adsorption onto ZnCl₂ activated corn husk carbon equilibrium studies. *Journal of Chemistry*, 2013.
- Kushwaha, A. K., Gupta, N. & Chattopadhyaya, M. (2014). Removal of cationic methylene blue and malachite green dyes from aqueous solution by waste materials of *Daucus carota*. *Journal of Saudi Chemical Society*, 18, 200-207.
- Lagergren, S. (1898). Zur theorie der sogenannten adsorption gelöster stoffe.
- Malik, R., Ramteke, D. & Wate, S. (2007). Adsorption of malachite green on groundnut shell waste based powdered activated carbon. *Waste management*, 27, 1129-1138.
- Mall, I. D., Srivastava, V. C., Agarwal, N. K. & Mishra, I. M. (2005). Removal of congo red from aqueous solution by bagasse fly ash and activated carbon: kinetic study and equilibrium isotherm analyses. *Chemosphere*, 61, 492-501.
- Mittal, A., Mittal, J., Malviya, A. & Gupta, V. (2009). Adsorptive removal of hazardous anionic dye “Congo red” from wastewater using waste materials and recovery by desorption. *Journal of colloid and interface science*, 340, 16-26.
- Mittal, A., Mittal, J., Malviya, A., Kaur, D. & Gupta, V. (2010). Decoloration treatment of a hazardous triarylmethane dye, Light Green SF (Yellowish) by waste material adsorbents. *Journal of colloid and interface science*, 342, 518-527.
- Namasivayam, C. & Kavitha, D. (2002). Removal of Congo Red from water by adsorption onto activated carbon prepared from coir pith, an agricultural solid waste. *Dyes and pigments*, 54, 47-58.
- Oladipo, A. A., Gazi, M. & Saber-Samandari, S. (2014). Adsorption of anthraquinone dye onto eco-friendly semi-IPN biocomposite hydrogel: equilibrium isotherms, kinetic studies and optimization. *Journal of the Taiwan Institute of Chemical Engineers*, 45, 653-664.
- Rafatullah, M., Sulaiman, O., Hashim, R. & Ahmad, A. (2010). Adsorption of methylene blue on low-cost adsorbents: a review. *Journal of hazardous materials*, 177, 70-80.
- Saleh, T. A. & Gupta, V. K. (2014). Processing methods, characteristics and adsorption behavior of tire derived carbons: a review. *Advances in colloid and interface science*, 211, 93-101.
- Tirani, S. G., Yasrifa, M. A. & Sunardi. (4 September 2021). Karakterisasi Limbah Pelepeah Sagu (Metroxylon sagu) Hasil

Modifikasi dengan Metode Fast Microwave-Assisted Acid. SEMINAR NASIONAL SAINS, TERAPAN & PENDIDIKAN KIMIA, Banjarmasin. (in process).

Vimonses, V., Lei, S., Jin, B., Chow, C. W. & Saint, C. (2009). Kinetic study and equilibrium isotherm analysis of Congo Red

adsorption by clay materials. *Chemical Engineering Journal*, 148, 354-364.

Wu, F.-C., Tseng, R.-L. & Juang, R.-S. (2009). Characteristics of Elovich equation used for the analysis of adsorption kinetics in dye-chitosan systems. *Chemical Engineering Journal*, 150, 366-373.

The Effect of Activated Charcoal Coffee Grounds (*Coffea Sp.*) as an Adsorbent on the Quality of the Liquid Sugar of Siwalan

Pengaruh Adsorben Arang Aktif Ampas Kopi (*Coffea Sp.*) Terhadap Kualitas Gula Cair Siwalan

Eufronius Darus^{1,*}, Imanuel Gauru¹, Febri O. Nitbani¹, Philiphi De Rozari¹

¹ Chemistry Study Program, Faculty of Science and Engineering, Nusa Cendana University
Jl. Adisucipto, Penfui, Kupang

*Email: rhyodarus98@gmail.com

ABSTRACT

*This study aimed to determine the adsorbent characteristics of coffee grounds activated charcoal (*Coffea Sp.*), optimum adsorption contact time, and differences in the quality of siwalan liquid sugar through adsorption and without adsorption. The characteristics of coffee grounds activated charcoal were determined by FTIR and SAA. FTIR characterization showed that activated coffee grounds charcoal contained functional groups of O-H, Csp²-H, Csp³-H, C-H₂ methylene, C-O, and C=C-H. Characterization with SAA showed that the surface area of activated charcoal was 27.70 m²/g with a pore volume of 0.02 ml/g and an adsorption pore size of 1.63 nm. The optimum contact time of the adsorbent in the adsorption of impurities in the palm sap was 60 minutes. The siwalan liquid sugar, which went through adsorption, had a reducing sugar content of 6.70%, and the one without adsorption was 10.18%. While the ash content of siwalan liquid sugar through adsorption was 4.73%, and without adsorption was 6.5%. This value indicates that the quality of siwalan liquid sugar through adsorption is higher than that which does not go through the adsorption stage.*

Keywords: adsorption, activated charcoal, siwalan liquid sugar

ABSTRAK

*Telah dilakukan penelitian dengan judul pengaruh adsorben arang aktif ampas kopi (*coffea sp.*) terhadap kualitas gula cair siwalan yang bertujuan untuk mengetahui karakteristik adsorben arang aktif ampas kopi (*Coffea Sp.*), waktu kontak optimum adsorpsi dan perbedaan kualitas gula cair siwalan yang melalui adsorpsi dan tanpa adsorpsi. Penentuan karakteristik arang aktif ampas kopi menggunakan FTIR dan SAA. Hasil karakterisasi dilakukan menggunakan FTIR menunjukkan arang ampas kopi yang sudah diaktivasi mengandung gugus fungsi O-H, Csp²-H, Csp³-H, C-H₂ metilen, C-O, C=C-H. Sedangkan karakterisasi menggunakan SAA menunjukkan luas permukaan arang aktif yang diperoleh sebesar 27,70 m²/g dengan volume pori sebesar 0,02 ml/g dan ukuran pori adsorpsi yang terbentuk sebesar 1,63 nm. Waktu kontak optimum adsorben dalam mengadsorpsi zat pengotor pada nira siwalan adalah 60 menit. Hasil penentuan kualitas gula cair siwalan yang meliputi kadar gula pereduksi yaitu 6,70 % kadar gula pereduksi yang melalui adsorpsi dan 10,18 % tanpa adsorpsi dan kadar abu yang melalui adsorpsi sebesar 4,73 % dan tanpa adsorpsi sebesar 6,5% yang menunjukkan kualitas gula cair siwalan yang melalui adsorpsi lebih baik dari pada gula cair tanpa adsorpsi.*

Kata Kunci: adsorpsi, arang aktif, gula cair siwalan

Submitted: December 13, 2021; **Accepted:** February 18, 2022; **Available online:** March 8, 2022

1. INTRODUCTION

Sugar is a source of carbohydrates in the human body and is added to food or beverages. Indonesia's national sugar consumption continues to increase every year. This increase is due to the high projected growth of the food and beverages industry and changes in the quality of life, which is equivalent to the increase in population. The most widely traded sugar is solid sucrose crystals, used to sweeten foods or beverages. In Indonesia, besides cane sugar, there is also brown sugar (palm sugar) in both solid and liquid forms. Apart from being a sweetener, brown sugar contains mineral salts and is rich in nutrients beneficial for the body. One type of palm sugar that is widely used is siwalan sugar (Sahroel, 2009). According to Sahroel (2009), siwalan sap is obtained from tapping the male flowers of the siwalan tree. Siwalan sap is usually clear, slightly cloudy, and contains between 10-15% sugar. The potential production of siwalan sap in East Nusa Tenggara per tree per year with a tapping period of 184 days is 726.84 liters. When multiplied by the average number of trees of 1516,500 trees, the total production of siwalan sap is 110,498,256,000 per year (Journal of forest policy analysis, vol.7, no.1, 2010:27-45). One of the centers for siwalan sugar production is in the province of NTT.

The production of siwalan sugar in East Nusa Tenggara generally uses traditional methods resulting in a low-quality product. The production of siwalan sugar goes through several systematic stages. Filtering is one of the processes. However, this filtering process does not guarantee that the filtrate or siwalan sap is free from impurities, meaning that impurities pass through the filter, such as heavy metals or other dyes that cause a non-clear/cloudy sugar. Therefore, it is necessary to develop innovation in producing higher quality siwalan sugar. Several methods can be used to improve the quality of the sugar, including coagulation, filtration, electrodecolorization, and adsorption. According to Setyaningtias and Roy (2007),

one of the most widely used methods for purification is adsorption. Adsorption using activated carbon is a potential way of separating a substance.

Coffee grounds are the final waste of the coffee brewing and are one of the raw materials for producing carbon. Coffee grounds contain carbon, nitrogen, lipophilic compounds, ethanol, lignin, alkaloids, polyphenolic compounds, tannins, polysaccharides, and chlorogenic acid (Pujol et al., 2013). The hydrocarbon content in coffee beans is relatively high (19.9%). This high hydrocarbon content can produce carbon when coffee beans are roasted or heated. Therefore, ground coffee that have been brewed can be used as activated charcoal.

Research on activated carbon from coffee grounds as an adsorbent has been carried out by Nasution et al. (2002), namely the use of coffee grounds activated charcoal as an adsorbent of iron and mercury ions in drinking water with an absorption yield of 90.34%. Baryatik et al. (2016) used coffee grounds activated charcoal as an adsorbent for chromium (Cr) metal in batik liquid waste with an absorption yield of 95%. Moelyaningrum et al. (2019) reported the utilization of coffee grounds activated charcoal as cadmium adsorbent in well water with an absorption yield of 95%. Asutik et al. (2015) used coffee grounds as an adsorbent to reduce BOD and COD in domestic wastewater with an absorption yield of 99%. Coffee grounds have not been widely used in the community, where coffee grounds are usually seen as waste, garbage, or compost for plants. Coffee grounds can also be used for air freshener/anti-odor, ink for painting, and coffee oil for grooming products. In addition, studies on the use of coffee grounds as adsorbents for dyes or impurities have not been carried out.

2. MATERIALS AND METHODS

2.1 Materials

The materials used were coffee grounds, siwalan sap, distilled water, Luff Schrool solution, 0.1M HCl, Na₂S₂O₃, 20% KI, 25% H₂SO₄, Al(OH)₃, and 5% starch indicator. The tools used were Surface Area Analyzer (SSA) to determine the surface area of coffee grounds activated charcoal, Fourier Transform Infrared Spectroscopy (FTIR) to determine the functional groups of coffee grounds activated charcoal, kiln to carbonize coffee grounds charcoal, magnetic stirrer, shaker, 60 mesh sieve, oven, funnel, Whatman filter paper no.40, analytical balance, pH meter, and various glassware.

2.2 Preparation of the adsorbent

This research begun with preparing the adsorbent by collecting brewed coffee grounds. The collected coffee grounds were dried in the oven. The dried coffee grounds were then carbonized in a kiln at 400°C for 3 hours. The charcoal were ground and sieved through a 60 mesh sieve. The charcoal powder was chemically activated. A total of 50 grams of coffee grounds charcoal was mixed with 100 mL of 0.1 M HCl. The immersion results were filtered, washed with distilled water until the pH was neutral, filtered, and dried in an oven at 110°C for 3 hours. The obtained charcoal was characterized using a Surface Area Analyzer (SAA) and Fourier Transform Infrared Spectroscopy (FTIR) characterization.

2.3 Determination of optimum adsorption contact time in reducing sugar content

Fresh siwalan sap that was tapped for 12 hours from the siwalan tree was put in a bottle and stored in a cool box containing ice cubes to prevent fermentation during transportation to the laboratory. A total of 10 grams of activated charcoal of coffee grounds and 500 mL of siwalan sap were put into an Erlenmeyer flask and stirred using a shaker with variations of 30, 60, and 90 minutes. The solution was filtered with filter paper, and

the filtrate was cooked to obtain liquid palm sugar.

A total of 2 mL of siwalan sap was put into a 100 mL volumetric flask and added with 50 mL of distilled water. Al(OH)₃ was added until the effect was no longer there (no cloudy solution and other impurities were formed). Furthermore, distilled water was added to the mark and filtered. A total of 20 mL of the filtered filtrate was added with 20 mL of Luff Schrool solution in an Erlenmeyer. The blank solution was made by mixing 20 ml of Luff Schrool solution with 20 mL of distilled water. The sample and blank solutions were heated for 10 minutes while stirring using a magnetic stirrer. Then cooled and added with 10 mL of KI 20% and 25% H₂SO₄. The solution was then titrated with 0.1 N Na₂S₂O₃ solution using a 5% starch indicator.

2.4 Determination of optimum contact time against ash content of siwalan liquid sugar

A total of 2 grams of samples from each time variation and samples without adsorption were burned in a kiln at 550°C to a constant weight, then cooled and weighed as ash content.

3. RESULTS AND DISCUSSION

3.1 Characteristics of coffee ground activated charcoal

a. Characteristics based on Fourier Transform Infrared Spectroscopy (FTIR) analysis

The results of the FTIR spectrum of the activated carbon of coffee grounds (Fig.1) showed an absorption with strong intensity at a wavelength of 3464.15 cm⁻¹, which was side by side with absorption at a wavelength of 3425.58 cm⁻¹ due to the absorption of the O-H group from phenol. The absorption at wavelengths of 3070.68 cm⁻¹ and 3001.24 cm⁻¹ was due to the absorption of the Csp²-H group. The absorption at wavelengths of 2900.94 cm⁻¹ and 2862.36 cm⁻¹ was due to the absorption of the Csp³-H group. The absorption at a wavelength of 1465.90 cm⁻¹ was due to C-H₂ methylene groups. There

was also absorption at wavelength 1265.30 cm^{-1} and 1165.00 cm^{-1} , which was side by side with absorption at wavelength 1080.14 cm^{-1} due to absorption of C-O groups from carboxyl. Furthermore, there was an

absorption band at wavelengths of 925.83 cm^{-1} , 856.39 cm^{-1} , 748.38 cm^{-1} , 694.37 cm^{-1} , which was the absorption of aromatic C=C-H groups. FTIR analysis data of coffee grounds activated carbon presented in Table 1.

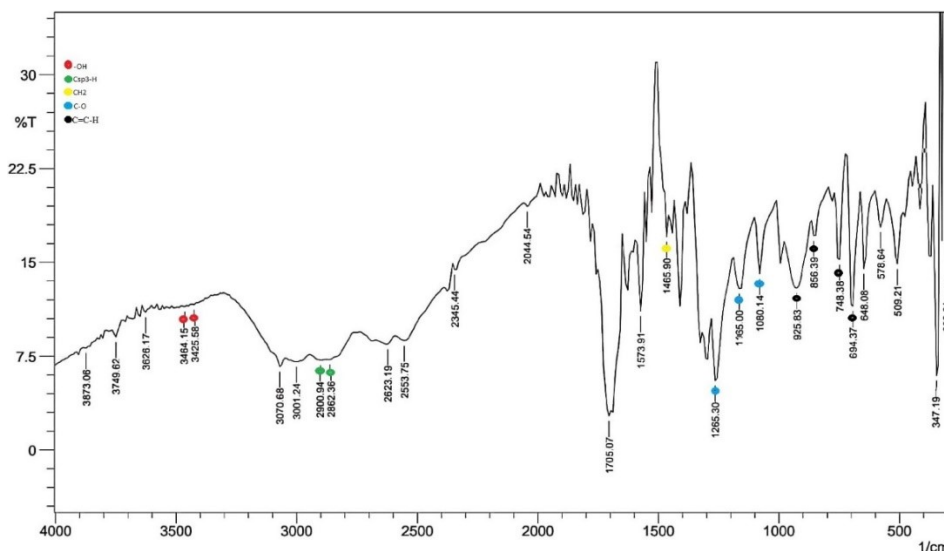


Figure 1. FTIR spectrum of coffee grounds activated charcoal after activation

Table 1. FTIR analysis data of coffee grounds activated carbon

Wavelength cm^{-1}		Functional Group
Literature	Coffee Ground Activated Carbon	
3473.3 (Sari,2017)	3464.15, 3425.58	OH
2924.09-2854.65 (Sari,2017)	2900.94, 2862.36	C-H
1442.75-1381.03 (Sari,2017)	1465.90	C-H Bending
1165.00-1118.71 (Sari,2017)	1265.90, 1165, 1080.14	C-O
1000-675 (Sari,2017)	925.83, 856.39, 748.38, 694.37	C=C-H Bending

b. Characteristics Based on Surface Area Analyzer (SAA)

Table 2 shows that the surface area of the coffee grounds activated charcoal obtained was 27.70 m^2/g with a pore volume of 0.023 mL/g and an adsorption pore size of 1.63 nm.

Based on these results, the pore size of coffee grounds activated charcoal is classified as microporous. It is based on the classification of pore size according to the International Union of Pure and Applied

Chemistry (IUPAC), namely micropore size $d < 2$ nm. The smaller the particle size of the adsorbent, the larger the surface area. The micropore type indicates that in adsorption, the adsorbate particles will stick around the adsorbent wall to form a strong bond (Sugesti, 2018).

Table 2. SAA karakter characterization data

Surface Area (m ² /g)	Pore Volume (cc/g)	Pore Size (nm)
27.70	0.023	1.63

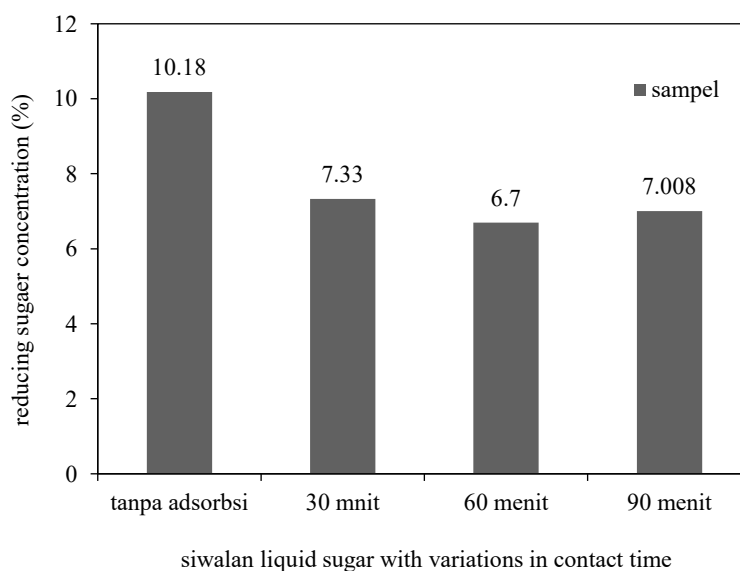
3.2 Optimum adsorption contact time on reducing sugar content

According to Baharudin *et al.* (2007), the higher the reducing sugar content in brown sugar, the lower the quality of the sugar. And vice versa, the lower the reducing sugar content, the higher the quality. High levels of reducing sugar might be caused by

contaminated raw materials (sap) with microbes during tapping and production. The maximum quality standard for reducing sugar according to SNI is 6%. The reducing sugar level in palm sugar liquid using the Luff Schoorl method are presented in Table 3. Graph of reducing sugar concentration from siwalan liquid sugar presented in Fig. 2.

Table 3. Data analysis of reducing sugars using the Luff Schoorl method

No	Siwalan liquid sugar	Volume Na ₂ S ₂ O ₃ 01 N (mL)		Reducing Sugar (%)
		Sample	Blanko	
1	Contact time 30 minutes	19.3	31	7.33
2	Contact time 60 minutes	20.3	31	6.70
3	Contact time 90 minutes	19.7	31	7.008
4	Without adsorption	13.2	29	10.18

**Figure 2.** Graph of reducing sugar concentration from siwalan liquid sugar

The titration of Luff Schoorl's solution on siwalan liquid sugar through adsorption with variations in contact time and without adsorption showed that the four samples contained reducing sugars. There were differences in reducing sugar content in the samples that went through the adsorption process and those that did not. The liquid sugar of siwalan through adsorption had reducing sugar content which decreases with the increasing of contact time. At the contact time of 30 minutes, the reducing sugar content was higher than other contact times, 7.33%. It is caused by the presence of empty spaces on the carbon that has not been occupied by impurities that affect the increase in reducing sugar in the siwalan liquid sugar.

At the contact time of 60 minutes, there was an increase in adsorption, indicated by a decrease in the reducing sugar content, which was 6.70%. It indicates that the empty spaces in the activated charcoal of coffee grounds have been filled with impurities of the liquid sugar of siwalan. Meanwhile, at the contact time of 90 minutes, the absorption of activated charcoal from coffee grounds decreased, as indicated by an increase in reducing sugar content, which was 7.008%. It happens because the prolonged contact time between the adsorbent and the adsorbate resulting in a reduce adsorption rate. Longer

contact time can also result in desorption, namely the release of impurities that the adsorbent has bound. It is in accordance with Bernard et al. (2013), who states that after the adsorption reaches an equilibrium state at the optimum contact time, the addition of the contact time between the adsorbent and the adsorbate will not have a significant effect on the absorption process.

Siwalan liquid sugar without adsorption has a higher reducing sugar content than siwalan liquid sugar that undergo adsorption. It proves that adsorption can improve the quality of palm sugar liquid by decreasing the reducing sugar content by 3.48%. The adsorption mechanism is that the activated charcoal of the coffee grounds releases water molecules from the surface cavity and then interacts with the molecules to be adsorbed from the siwalan sap in the form of unwanted impurities. Impurities in siwalan sap might come from the air, the bamboo container for tapping, or other contaminants during the tapping process. These impurities can stimulate the growth of the yeast *Saccharomyces cerevisiae* and bacteria of the acetobacter genus (Mulyawanti et al., 2011). According to Marsigit (2005), *Saccharomyces cerevisiae* can hydrolyze sucrose to produce reducing sugars (fructose and glucose).

Table 4. Ash content

Adsorption contact time	Sample weight (gram)	Cup weight (gram)	Weight of cup + ash (gram)	% Ash content
Contact time 30 minutes	2	13.3	13.397	4.85
Contact time 60 minutes	2	13.3	13.395	4.73
Contact time 90 minutes	2	13.3	13.396	4.8
Without adsorption	2	13.3	14.6	6.5

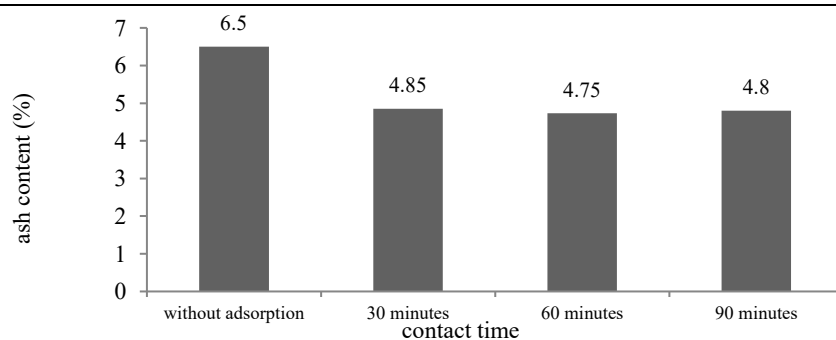


Figure 3. Graph of ash content of siwalan liquid sugar

3.3 Effect of optimum adsorption contact time on ash content

The ash content of siwalan liquid sugar through the adsorption process and without adsorption is presented in Fig. 3. Analysis of the ash content of the siwalan liquid sugar through adsorption with variations in contact time and without adsorption (Table 4) showed that the four samples had different ash content. Samples that went through the adsorption process showed that as the adsorption contact time increased, the ash content decreased until the adsorption reached a state of equilibrium. At the 30 minutes contact time, the adsorption was still low at 4.85%. At the 60 minutes contact time, there was an increase in absorption, which was indicated by a decrease in the ash content of the liquid sugar of palm sugar, which was 4.73%. Meanwhile, at the 90 minutes contact time, the absorption of activated charcoal from coffee grounds decreased, which was indicated by an increase in the ash content of the siwalan liquid sugar, which was 4.8%. It proves that adsorption can reduce the ash content in the siwalan liquid sugar by 1.7%.

The decrease in ash content occurred due to decreasing of reducing sugar in the liquid sugar due to adsorption. The increase in reducing sugar can increase the ash content in liquid sugar, which results in a decrease in sugar quality. The mechanism of adsorption of activated charcoal carbon from coffee grounds releases water molecules from the surface cavity. It effectively interacts with organic acid molecules that will be adsorbed from the siwalan sap. Organic acids are formed due to the hydrolysis of sucrose into reducing sugars (Waluyo, 2005). Organic acids significantly affect the increase in ash content during the cooking of sap so that the quality of the sugar produced decreases.

4. CONCLUSIONS

On the basis of the study's findings, it can be concluded that:

1. FTIR analysis showed that the charcoal after activation contained functional groups O-H, Csp²-H, Csp³-H, C-H₂ methylene, C-O, C=C-H. Analysis of activated charcoal with SAA showed that the surface area obtained was 27.70 m²/g with a pore volume of 0.02 mL/g, and the adsorption pore size formed was 1.63 nm.
2. The optimum condition of the adsorbent to adsorb impurities in the water cave occurs at a contact time of 60 minutes.
3. Siwalan liquid sugar that went through the adsorption process had a higher quality than without adsorption. It can be seen from the smaller content of reducing sugar and ash content than siwalan liquid sugar without adsorption.

LIST OF REFERENCES

- Anonim. (1991). The Standard Laboratory Manual for Australian Sugar Mills. Volume 2: Analytical Methods and Tables. Bureau of Sugar Experiment Stations, Brisbane.
- Anonim. (1995). Standard Industri Indonesia (SNI) Gula Palma 01-3743-1995. Dewan Standarisasi Nasional, Jakarta.
- Anonim. (2015, February 21). *Kongres KMITB Beri Kepastian Soal Pemira*. ganecapos.com. <http://ganecapos.com/2015/02/kongres-km-itb-beri-kepastian-soal-pemira/>
- Muin, M., & Bandaso, H. (2007). PEMANFAATAN NIRA AREN (Arenga pinnata Merr) SEBAGAI BAHAN PEMBUATAN GULA PUTIH KRISTAL. *PERENNIAL*, 3(2), 40-43.
- Bansal, R. C., & Goyal, M. (2005). *Activated carbon adsorption*. CRC press, USA.
- Baryatik, P., S. R. Pujiati, & Ellyke. (2016). Pemanfaatan Arang Aktif Ampas Kopi sebagai Adsorben Logam Kromium (Cr) pada Limbah Cair Batik (Studi Kasus Industri Batik UD. Pakem Sari Desa Sumberpakem Kecamatan Sumberjambe Kabupaten Jember). *Artikel Ilmiah Hasil Penelitian Mahasiswa 2016*, 1-6.
- Hessler, J.W. (1951). *Active Carbon*. Chemical Publishing Co Inc., New York.
- Badan Pusat Statistik. (2020). <https://www.bps.go.id>. Diakses pada tanggal 11 Oktober 2020.
- Pubchem NCBI. (2020). <http://pubchem.ncbi.nlm.nih.gov/compound/coffe>. diakses pada tanggal 30 maret 2020.
- Lubis, S., & R. Nasution. (2002). Pemanfaatan Limbah Bubuk Kopi sebagai Adsorben pada Penurunan Kadar Besi (Fe anorganik) dalam Air Minum. *Jurnal Natural*, 2(2), 12-16.
- Mulyana, D. (2007). Pembuatan Gula Siwalan. Penerbit Bina Sumber Daya MIPA.
- Mulyawanti, I., N. Setyawan, Syah, A. N. A., & R. Risfaheri. (2011). Evaluasi mutu kimia, fisika dan mikrobiologi nira aren (Arenga pinnata) selama penyimpanan. *Agritech*, 31(4).
- Pontoh, J. (2007). Analisa Komponen Kimia dalam Gula dan Nira Siwalan. *Laporan pada Yayasan Masarang*. Tomohon.
- Pujol D, C. Liu, J. Gominho, M.A. Olivella, N. Fiol, Villaescusa I, & H. Pereira. (2013). The Chemical Composition of Exhausted Coffee Waste. *J Ind Crops Prod*. 50, 423-429.
- Rasdiansyah. (2014). Optimasi Proses Pembuatan Karbon Aktif Dari Ampas Bubuk Kopi Menggunakan Activator ZnCl₂. 6(3).
- Rattnapan, S., J. Srikrum, & P. Kongsune. (2017). Adsorption of Methyl Orange on Coffee Grounds Activated Carbon. *Energy Prodecia*. 138, 949-954.
- Sahroel. (2009). *Aren Indonesia*. Wikipedia. <http://id.wikipedia.org/wiki/enu>. Diakses pada tanggal 10 November 2009.
- Sembiring, M.T., dan Tuti, S.S. (2003). *Arang Aktif (Pengenalan dan Proses Pembuatan)*. Jurusan Teknik Industri Fakultas Teknik, Universitas Sumatra Utara.
- Setyaningsih, H. (1995). *Pengolahan Limbah Batik dalam Proses Kimia dan Adsorpsi Karbon Aktif*. Tesis. Program Pascasarjana, Universitas Indonesia. Jakarta.
- Utomo, H.D., R.Y.N. Phoon, Z. Shen, L.H. Lim. (2015). Removal of Methylen Blue Using Chemical Modified Sugarcane Bagasse. *Natural Resources*, 6, 209-220
- Waluyo, L. (2005). *Mikrobiologi Umum*. UMM Press, Malang.
- Winarno, F. G. (2008). *Kimia Pangan dan Gizi*. Gramedia, Jakarta.
- Yanuanda, & M. Febrianto. (2014). *Pengaruh Penambahan Adsorben pada Pengolahan Gula Semut Siwalan*. Universitas Brawijaya, Malang.

Design of Vaccines Candidate Based on Ebola Virus Epitop with In-Silico Approach

Perancangan Kandidat Vaksin Berbasis Epitop Virus Ebola dengan Pendekatan *In-Silico*

Erwin Prasetya Toepak¹, Sari Namarito Simarmata^{1,*}, Sudarman Rahman¹,
Stevin Carolius Angga¹

¹Chemistry Study Program, Faculty of Mathematics and Natural Sciences, University of Palangka Raya
Kampus UPR Tunjung Nyaho, Palangka Raya, 73111, Indonesia

*Email: sarinamarito@gmail.com

ABSTRACT

The World Health Organization (WHO) recorded as many as 2,299 cases of death with a case percentage of 66% during 2018 to 2020 in the Democratic Republic of the Congo due to the Ebola virus. Ebola virus is a member of the Filoviridae family. One of the viro cores consists of glycoprotein (GP). Messenger RNA (mRNA) generates long GP chains for the attachment protein (GP 1) and the fusion protein (GP 2). Epitope-based vaccines are a promising approach because epitopes represent immunogenic regions that elicit immunity specifically. Epitope prediction was performed based on the GP EBOV sequence available in the Data Bank. The designed vaccine could be one of the candidates for the Ebola virus vaccine. The design of the virus with access to NCBI AAB81004 was carried out by testing such as B cell epitope, T cell, and their antigenicity using the VaxiJen v2.0 server and IEDB. The T cell epitope prediction results showed that 20 T cell epitopes interacted with the Major Histocompatibility Complex (MHC) with the highest score of 2.8069. B cell epitope by linear BepiPred assay had 77 candidate epitope peptides from sequence 401-477. Karplus and Schulz's flexibility predictions showed a predictive value of 1.119 with a threshold of 1.008, with the analyzed area having an antigenic tendency where the threshold area was yellow.

Keywords: Ebolavirus; Vaccine; Epitope B Cell; Epitope T Cell; In Silico

ABSTRAK

World Health Organization (WHO) mencatat sebanyak 2.299 kasus meninggal dengan persentase kasus 66% pada tahun 2018-2020 di Republik Demokrasi Kongo akibat virus Ebola. Ebolavirus merupakan salah satu anggota family Filoviridae. Inti viron salah satunya terdiri dari glikoprotein (GP). RNA messenger (mRNA) menghasilkan rantai panjang GP untuk protein pelekat (GP 1) dan protein fusi (GP 2). Vaksin berbasis epitop sebagai salah satu pendekatan yang menjanjikan dikarenakan epitop mewakili wilayah imunogenik yang dapat secara khusus memunculkan kekebalan. Prediksi epitop dilakukan berdasarkan urutan GP EBOV yang tersedia pada Bank Data. Vaksin yang dirancang dapat dijadikan salah satu kandidat vaksin virus Ebola. Perancangan virus dengan akses NCBI AAB81004 dilakukan dengan pengujian seperti epitop sel B, sel T, serta antegenitasnya menggunakan server VaxiJen v2.0 dan IEDB. Hasil prediksi epitop sel T memperlihatkan terdapat 20 epitop sel T yang berinteraksi dengan Major Hystocompatibility Complex (MHC) dengan skor tertinggi 2.8069, epitop sel B dengan pengujian BepiPred linier memiliki kandidat epitop banyak 77 peptida dari urutan 401-477. Prediksi Karplus dan Schulz flexibility menunjukkan nilai prediksi 1,119 dengan ambang batas 1,008 dengan daerah yang dianalisis memiliki kecenderungan antigenik dimana daerah ambang batasnya berwarna kuning.

Kata Kunci: Ebolavirus; Vaksin; Epitop Sel B; Epitop Sel T; In Silico

Submitted: December 22, 2021; **Accepted:** February 22, 2022; **Available online:** March 8, 2022

1. INTRODUCTION

Based on data from the World Health Organization (WHO), there were 3,481 cases and 2,299 deaths with a case percentage of 66% in 2018-2020 in the Democratic Republic of Congo due to the Ebola virus and continues to this day. The Ebola virus is one of the largest outbreaks, with many deaths and a significant increase in cases compared to other outbreaks. The first Ebola virus disease was discovered in 1976 by Dr. Peter Piotin in Zire, Africa. In tropical Saharan Africa, additional Ebola virus disease (EVB) outbreaks have occurred between humans (Moghadam, Omidi, Bayrami, Moghadam, & SeyedAlinaghi, 2015; Rajak, Jain, Singh, Sharma, & Dixit, 2015; Zawilińska & Kosz-Vnenchak, 2014).

Ebola virus is a member of the order Mononegavirales, the Filoviridae family consisting of five species, including Zaire Ebolavirus, Bundibugyo Ebolavirus, Sudan Ebolavirus, Reston Ebolavirus, and Tai Forest Ebolavirus (Sridhar, 2015; Zawilińska & Kosz-Vnenchak, 2014). The negative RNA genome encodes 7 proteins. The viron core consists of an RNA-independent genome, RNA-polymerase (L), nucleoprotein (NP) binding to genomic RNA, and viral nucleocapsid proteins (VP35, VP40, VP30, and VP24) surrounded by a lipid envelope with surface projections consisting of glycoproteins. GPs have multimeric surfaces derived from single structural GPs that function in cell attachment, fusion, and cell entry (Dash et al., 2017; Sridhar, 2015; Zawilińska & Kosz-Vnenchak, 2014).

The GP gene performs different transcriptions of glycoproteins. RNA messenger (mRNA) generates long GP chains for the attachment protein (GP1) and the fusion protein (GP2) containing additional adenosine. RNA transcription results in synthesized soluble GP (sGP). In contrast, small soluble GP (ssGP) added 2 adenosine residues during the process (Dash et al., 2017). GP is virally described as a

virion surface that has the role of catalyzing membrane fusion and amalgamation into host cells. It indicates this component's importance for vaccines and as a potential target for developing attachment inhibitors and antibodies (Dash et al., 2017).

The development of the Ebola vaccine is carried out by inactivating the virus. Several methods can be used to manufacture vaccines, such as DNA vaccine, viral recombination, protein subunits, protein recombination, and VLP. All vaccines manufactured must undergo clinical trials to evaluate their reactogenicity and immunogenicity. Several vaccines in clinical trials target the GP of the Ebola virus and provide a dominant immune response (Sridhar, 2015).

Vaccines are antigenic given to stimulate the immune system to prevent viral infections. Immune system stimulation involves T cell epitopes and B cell epitopes. Both of these epitopes have responsibilities in cellular and humoral immunity (Patronov & Doytchinova, 2013; Sanchez-Trincado, Gomez-Perosanz, & Reche, 2017).

Epitope vaccines refer to alternative vaccine strategies that use peptide fragments to elicit a strong immune response against a pathogen instead of using the whole organism. The application of epitope vaccines is growing with advances in biotechnology due to *in silico* tools and databases that provide safe and promising results (Garg, Srivastava, & Srivastava, 2020). Despite the tremendous progress in the last few decades, there is no generally accepted strategy for implementing a vaccine design approach. From different methods, epitope-based vaccines have been developed to provide promising results for prophylactic and therapeutic aspects of pathogen-specific immunity. This strategy offers several advantages, including eliminating unwanted immune responses by designing specific constructs, establishing prolonged immunity with the required response, and cost and time

effectiveness (Parvizpour, Pourseif, Razmara, Rafi, & Omid, 2020).

Epitope-based vaccines are a promising approach. Epitopes represent protein sequences' immunogenic regions that elicit accurate immunity (Dash et al., 2017). Epitope prediction was carried out based on the GP Ebov sequence available in the in silico-based National Center for Biotechnology Information (NCBI) Data Bank. Epitope vaccine designed based on this glycoprotein could be used as a candidate for the Ebola virus vaccine through several testing parameters such as prediction of B cell epitope, T cell epitope, and antigenicity.

2. MATERIALS AND METHODS

2.1. Materials

The GP EBOV protein sequences were taken from the National Center for Biotechnology Information (NCBI) database (<https://www.ncbi.nlm.nih.gov/>) glycoprotein [Zaire ebolavirus], GenBank: AAB81004.1. The protein sequences were created in FASTA format. Epitope prediction tests for B cells, T cells, and antigenicity were carried out using the VaxiJen v2.0 server (<https://www.ddg-pharmfac.net/vaxijen/VaxiJen/VaxiJen.html>) and IEDB (<https://www.iedb.org/>). B cell epitope was tested with BepiPred 2.0 and Karpluz and Schulz Flexibility, while T cell epitope was tested with NetCTL v1.2 server (<https://services.healthtech.dtu.dk/service.php?NetCTL-1.2>).

2.2. Methods

In the NCBI, the protein was selected, and the Zaire Ebolavirus glycoprotein was entered, then the GenBank access number: AAB81004.1 was selected. The glycoprotein [Zaire ebolavirus] sequence, GenBank: AAB81004.1, was prepared in FASTA format then tested using VaxiJen v2.0 to determine antigenicity with a threshold of 0.5.

The protein sequences were then tested using the IEDB. On the IEDB web server, select B Cell Epitope Prediction, protein sequences in FASTA format were entered, and then predictions were selected using BepiPred. The same steps were carried out for testing with Karplus and Schulz Flexibility. T cell epitopes were assayed with NetCTL to predict binding between T cells and MHC.

3. RESULTS AND DISCUSSION

The Zaire Ebolavirus GP sequence is shown in Fig. 1. The antigenicity test was performed using the VaxiJen v2.0 server with the FASTA format protein sequence. The test was carried out with a threshold value of 0.5. Determination of this value aims to see the accuracy and sensitivity of the test. Fig. 2 shows the predictive value of 0.4946 antigenicity. Prediction of MHC-bound T cell epitope was performed with NetCTL. The test results presented in Table 1. B cell epitope prediction was performed using IEDB with linear BepiPred prediction to determine B cell epitope (Table 2) and Karpluz and Schulz Flexibility (Fig. 3). This prediction was chosen because it displays the results of the flexibility of the B cell epitope region. The maximum predicted value was 1.119 with a threshold of 1.008.

The general idea behind peptide vaccines is based on a chemical approach for synthesizing B cell and T cell epitopes which were identified as being immunodominant and able to induce a specific immune response. The B cell epitope of the target molecule can be conjugated with the T cell epitope to form immunogenic. T cell epitopes bind to MHC to induce an immune response. T cells can trigger specific adaptive immunity for pathogens. Epitope recognition by T cells and induction of immune response have key roles for the individual immune system.

NCBI Resources How To

Protein Protein Advanced

FASTA

glycoprotein [Zaire ebolavirus]

GenBank: AAB81004.1

[GenPept](#) [Identical Proteins](#) [Graphics](#)

>AAB81004.1 glycoprotein [Zaire ebolavirus]
 MGVTGILQLPDRFRKRTSFLLWVILFQRTFSIPLGVIHNSTLQVSDVDKLVCRDKLSSTNQLRSVGLNL
 EGNVATVDPVSATKRWGFSGVPPKVVNVEAGEWAENCYNLEIKKPDGSECLPAAPDGIRGFPRCRYVHK
 VSGTGPCAGDFAFHKEGAFLLYDRLASTVIYRGTTFAGVVAFLILPQAKKDFSSHPLREPVNATEDPS
 SGYYSTTIRYQATGFGTNETEYLFVDNLTIVVQLESRFTQFLQLNETIYTSGKRSNTTGKLIWKVNP
 IDTTIGEWAFWETKKNLTRKIRSEELSFTVVSNGAKNISGQSPARTSSDPGTNTTEDHKIMASENSAM
 VQVHSGREAAVSHLTLTATISTPQSLTTKPGPDNSTHNTPVYKLDISEATQVEQHRRTDNDSTASDT
 PSATTAAGPPKAENTNTSKSTDFLDPATTTSPQNHSETAGNNTHHQDTGEESASSGKLGILITNTIAGVA
 GLITGRRTRREAIVNAQPKCNPNLHYWTTQDEGAAIGLAWIPYFGPAAEGIYIEGLMHNQDGLICGLRQ
 LANETTQALQLFLRATTELRFTSILNRKAIDFLLQRWGGTCHLGPDCCIEPHDWTKNITDKIDQIHF
 VDKTLPDQDNDNMTGWRQWIPAGIVGTGVIIVIALFCKICKVF

Figure 1. [Zaire ebolavirus] glycoprotein sequence, GenBank: AAB81004.1

(a)

(b)

Figure 2. Protein sequence input (a), and GP sequence antigenic test results with a threshold of 0.5 using VaxiJen v2.0 (b)

Table 1. Prediction results of T cell epitope interacting with MHC using NetCTL

Peptide	Skor	Peptide	Skor
ATEDPSSGY	2.8069	STSPQSLTT	0.8530
NSTHNTPVY	1.6532	NTSKSTDFL	0.8769
TEDPSSGYY	1.5503	RTSFFLWI	0.8393
ITDKIDQII	1.0729	LLQLNETIY	0.9753
SSDPGTNTT	0.9700	TTGKLIWKV	0.8119
LFEVDNLTY	1.1224	RSEELSFTV	0.8030
TTQALQLFL	0.9347	ATDVPSATK	0.8179
RTDNDSTAS	0.7621	KIDQIHF	0.8565
ASESSAMV	0.9823	GTNETELYF	0.8084
HKEGAFFLY	1.0887	AIGLAWIPY	0.8453

T cell epitope prediction aims to identify the shortest peptide in the antigen capable of inducing CD4 or CD8 T cells. MHC-peptide binding is the most selective in determining T cell epitopes. Data-driven methods for predicting MHC-peptide binding are based on peptide sequences known to bind to MHC molecules. Antigen processing forms a

repertoire of peptides available for T cell binding (Sanchez-Trincado *et al.*, 2017). In Table 1, data on glycoprotein peptides bound to MHC are presented. The results showed that 20 peptides could bind to MHC. Among the T cell epitopes produced by the ATEDPSSGY peptide with a value of 2.8069 is a candidate peptide for the Ebola vaccine because it has the highest value.

Table 2. Prediction of B cell epitope using BepiPred Linear

No	Initiall	End	Peptide	Wavelength
1	14	14	F	1
2	57	59	LSS	3
3	73	106	NGVATDVPSATRWGFRSGVPPKVVNYEAGEWAE	34
4	114	131	KKPDGSECLPAAPDGIRG	18
5	141	148	VSGTGPCA	8
6	175	176	TF	2
7	191	193	KDF	3
8	198	215	PLREPVNATEDPSSGYYS	18
9	223	229	TGFGTNE	7
10	261	270	YTSGKRSNTT	10
11	279	285	PEIDTTI	7
12	296	296	N	1
13	313	339	NGAKNISGQSPARTSSDPGTNTTTEHD	27
14	341	342	IM	2
15	344	348	SENSS	5
16	355	360	SQGREA	6
17	371	393	ISTSPQSLTTKPGPDNSTHNTPV	23
18	401	477	ATQVEQHRRRTDNDSTASDTPSATTAAAGPPKAENTNTSKSTDFLDPATTSP QNHSETAGNNNTHHQDTGEESASSG	77
19	497	500	RRTR	4
20	506	513	NAQPKCNP	8
21	518	526	WTTQDEGAA	9
22	536	540	GPAAE	5
23	563	564	NE	2
24	566	566	T	1
25	609	611	CIE	3
26	613	618	HDWTKN	6
27	620	621	TD	2
28	633	646	KTLPDQGDNDNWWT	14

B cell epitope prediction aims to facilitate the identification of B cell epitope for antibody production. Linear B cell epitopes consist of sequential peptide residues. Antibodies that recognize linear B cell epitopes can recognize antigens. Although B cell epitopes are in the minority, this prediction has received significant attention because B cell epitopes have a role in binding antibodies produced. Epitope prediction by computation is based on a simple amino acid propensity scale that describes the physicochemical features of B cells (Sanchez-Tricando et al., 2017).

In the B cell epitope test with the prediction of BepiPred linear B cells with a threshold of 0.35, the maximum value was 2.514. The peptide residues constituting the B cell epitope are presented in Table 2. Tests

with Karpluz and Schulz predictions showed the flexibility of the B cell epitope presented in Fig. 3 with a maximum value of 1119 and a more dominant yellow region. The yellow color indicates an antigenic tendency in the region above the threshold. B cell epitopes induce minimal immunity that is strong enough to provide a humoral immune response and does not cause harmful side effects to the body. Epitope-based vaccine manufacture also has the advantage of eliciting an accurate immune response because the epitope is considered an immunogenic region (Dash et al., 2017). The flexibility of the peptide is correlated with the antigenicity. Therefore, Karpluz and Schulz were used to show the flexibility of the peptide. In Fig. 3, the Y-axis represents the score, and the X-axis represents the length of the sequence.

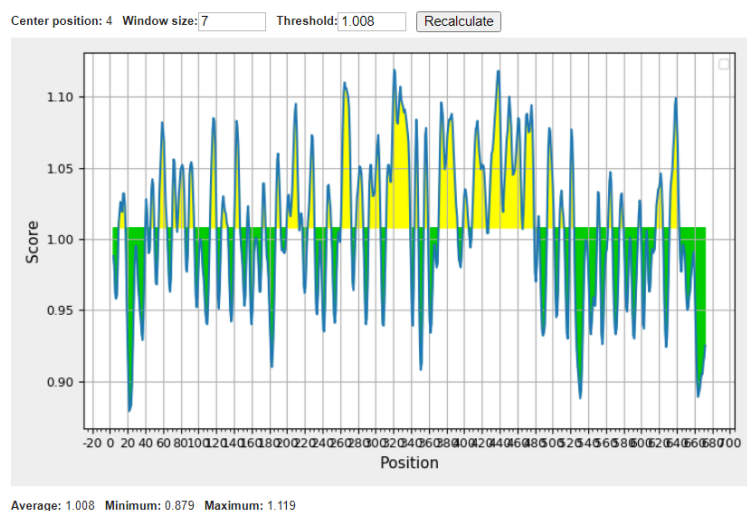


Figure 3. Prediction results of B cell epitope using IEDB with Karpluz and Schulz Flexibility prediction. The yellow color indicates the antigenic area, while the green indicates the peptide that does not cross the threshold.

4. CONCLUSIONS

Antigenicity test showed a prediction of antigen on glycoprotein with a value of 0.4946. There were 20 T cell epitopes with a score of 2.8069 with the peptide sequence ATEDPSSGY. B cell epitope with Karpluz and Schulz Flexibility test showed a predictive result of 1,119. In the BepiPred test, there were 77 candidate B cell epitopes of the order 401-477 (ATQVEQHRRRTDNDSTASDTPSATTA AGPPKAENTNTSKSTDFLDOATTTSPQN HSETAGNNNTHHQDTGEESASSG). Flexibility test results have an antigenic tendency that is above the yellow threshold. Between the epitope of B cells and T cells produced, there is the same peptide, namely SSG, making it a candidate for vaccine design for the Ebola virus.

LIST OF REFERENCES

- Dash, R., R. Das, M. Junaid, M. F. C. Akash, A. Islam, & S. M. Z. Hosen. (2017). In silico-based vaccine design against Ebola virus glycoprotein. *Advances and Applications in Bioinformatics and Chemistry*, 10(1), 11–28. <https://doi.org/10.2147/AABC.S115859>
- Garg, P., N. Srivastava, & P. Srivastava. (2020). An Integrated In-Silico Approach to Develop Epitope-Based Peptide Vaccine against SARS-CoV-2. *Coronaviruses*, 02(May). <https://doi.org/10.2174/2666796702666210208142945>
- Moghadam, S. R. J., N. Omid, S. Bayrami, S. J. Moghadam, & S. A. SeyedAlinaghi. (2015). Ebola viral disease: A review literature. *Asian Pacific Journal of Tropical Biomedicine*, 5(4), 260–267. [https://doi.org/10.1016/S2221-1691\(15\)30341-5](https://doi.org/10.1016/S2221-1691(15)30341-5)
- Parvizpour, S., M. M. Pourseif, J. Razmara, M. A. Rafi, & Y. Omid. (2020). Epitope-based vaccine design: a comprehensive overview of bioinformatics approaches. *Drug Discovery Today*, 25(6), 1034–1042. <https://doi.org/10.1016/j.drudis.2020.03.006>

Patronov, A., & I. Doytchinova. (2013). T-cell epitope vaccine design by immunoinformatics. *Open Biology*, 3(JAN). <https://doi.org/10.1098/rsob.120139>

Rajak, H., D. K. Jain, A. Singh, A. K. Sharma, & A. Dixit. (2015). Ebola virus disease: Past, present and future. *Asian Pacific Journal of Tropical Biomedicine*, 5(5), 337–343. [https://doi.org/10.1016/S2221-1691\(15\)30365-8](https://doi.org/10.1016/S2221-1691(15)30365-8)

Sanchez-Trincado, J. L., M. Gomez-Perosanz, & P. A. Reche. (2017). Fundamentals and Methods for T- and B-Cell Epitope Prediction. *Journal of Immunology Research*. <https://doi.org/10.1155/2017/2680160>

Sridhar, S. (2015). Clinical development of Ebola vaccines. *Therapeutic Advances in Vaccines*, 3(5–6), 125–138. <https://doi.org/10.1177/2051013615611017>

Zawilińska, B., & M. Kosz-Vnenchak. (2014). General introduction into the Ebola virus biology and disease. *Folia Medica Cracoviensia*, 54(3), 57–65.

Moringa leaf (*Moringa oleifera* L) flavonoids utilization in suppressing growth of *Aedes aegypti* larvae

Pemanfaatan Flavonoid Daun Kelor (*Moringa oleifera* L) dalam Menekan Pertumbuhan Larva Nyamuk *Aedes aegypti*

Vinsensius Manek Ati^{1,*}, Ermelinda D. Meye¹, Refli¹, Alfred O. M. Dima¹, Djefry Amalo¹, Ursula Luhur Jebatu¹

¹Biology Study Program, Faculty of Science and Engineering, Nusa Cendana University
Jl. Adi Sucipto Penfui, Kupang

*Email: vinsenmanekati@gmail.com

ABSTRACT

The study was conducted to determine the potential use of Moringa leaf flavonoids as biolarvicides in suppressing the growth of *Aedes aegypti* mosquito larvae. The design used was a completely randomized design (CRD) with six flavonoid treatments including P0 (0 ppm flavonoids as a negative control), P1 (12.5 ppm flavonoids), P2 (25 ppm flavonoids), P3 (50 ppm flavonoids), P4 (flavonoids 75 ppm), and P5 (flavonoids 100 ppm). Each treatment was repeated three times. The results of the analysis of diversity (Anova) revealed that Moringa leaf flavonoids had a very significant effect ($P = 0.000$) on the mortality of *A. aegypti* mosquito larvae. The administration of 50 ppm flavonoids of Moringa leaf extract caused the mortality of *A. aegypti* larvae to reach 95%, and at a concentration of 75 ppm, it increased the mortality percentage to 100%. The results of the probit analysis showed that the lethal concentration 50 (LC₅₀) was achieved at a concentration of 7.96 ppm with exposure for 24 hours, while the lethal concentration-time 50 (LT₅₀) at a concentration of 75 ppm was achieved in a shorter time (2.08 hours).

Keywords: flavonoids, moringa leaf, *Aedes aegypti*, biolarvacide

ABSTRAK

Penelitian dilakukan untuk mengetahui potensi pemanfaatan flavonoid daun kelor sebagai biolarvasida dalam menekan pertumbuhan larva nyamuk *Aedes aegypti*. Rancangan yang digunakan adalah Rancangan Acak Lengkap (RAL) dengan enam perlakuan flavonoid meliputi P0 (flavonoid 0 ppm sebagai kontrol negatif), P1 (flavonoid 12,5 ppm), P2 (flavonoid 25 ppm), P3 (flavonoid 50 ppm), P4 (flavonoid 75 ppm), dan P5 (flavonoid 100 ppm). Setiap perlakuan diulang sebanyak tiga kali. Hasil analisis keragaman (Anova) menunjukkan bahwa flavonoid daun kelor berpengaruh sangat nyata ($P = 0,000$) terhadap mortalitas larva nyamuk *A. aegypti*. Pemberian 50 ppm flavonoid ekstrak daun kelor menyebabkan kematian larva *A. aegypti* mencapai 95% dan pada konsentrasi 75 ppm meningkatkan persentase kematian hingga 100%. Hasil analisis probit menunjukkan bahwa lethal concentration 50 (LC₅₀) dicapai pada konsentrasi 7,96 ppm dengan pemaparan selama 24 jam sedangkan lethal concentration time 50 (LT₅₀) pada konsentrasi 75 ppm dicapai dalam waktu lebih singkat (2,08 jam).

Kata Kunci: flavonoid; daun kelor; *Aedes aegypti*; biolarvasida

Submitted: January 2, 2022; **Accepted:** February 22, 2022; **Available online:** March 8, 2022

1. INTRODUCTION

The *Aedes aegypti* mosquito is a biological vector that aids in spreading dengue fever. The dengue fever cases in East Nusa Tenggara (NTT) as of April 1, 2020, were 4,518 cases, with 48 deaths. The four regencies/cities in NTT with the highest cases were Sikka 1,548 cases, Kupang City 578 cases, Belu Regency 569 cases, and Alor Regency 401 cases (Bere, 2020). Data from the Indonesian Ministry of Health shows that cases of DHF between January to July 2020 in Indonesia reached 71,633 cases, with the number of deaths reaching 459 (Maulana et al., 2021).

Djojosumarto concluded that eradication attempts involving the killing of adult mosquitoes were ineffective compared to the use of larvicides to destroy mosquito larvae (Yasi et al., 2018). Synthetic larvicides have always been the preferred method of preventing the spread of the *Aedes aegypti* mosquito due to their ease of use, availability, and effectiveness. However, the use of conventional insecticides to control mosquitoes, such as organochlorine, carbamates, pyrethroids, malathion, DDT, and organophosphorus, has raised concerns about environmental pollution, residual effects, and resistance of certain mosquito populations, as well as adverse effects on human health (Gautam et al. 2013; Ferreira et al., 2009). The investigation of alternative controllers that are safer and derived from plants is motivated by the adverse effects of chemical pesticides on non-target creatures, human health concerns, and the environment. The use of ecologically acceptable bioactive compounds that are readily biodegradable and have specific targets that are poisonous to nuisance insects is a viable alternative.

Plants contain bioactive organic chemicals, which are superior to synthetic pesticides because they are less toxic, less susceptible to the development of resistance, and are easily biodegradable (Prabhu et al., 2011). Research and development of natural larvicides derived from plants have been

widely carried out. Nwankwo et al. (2015) showed that the seed oil extracts of *M. oleifera* and *Anona muricata* were beneficial as larvicides to control *A. aegypti* in eradicating yellow fever outbreaks and reducing the impact of conventional insecticides on the environment.

Nature provides a variety of medicinal plants that are useful in controlling infectious disease vectors (Prabhu et al., 2011). Moringa leaves are widely known as medicinal plants. Moringa leaf extract can be used directly on mosquito habitats for effective control (Sharma et al., 2013).

Moringa oleifera, according to Coppin et al. (2013), is a multipurpose tropical plant that is underutilized as a medicinal and nutritional ingredient. However, this plant contains high concentrations of flavonoids, which could be a new bioactive source in developing natural commercial products. Flavonoids are polyphenolic compounds that are abundant in nature. Flavonoids consist of several hydroxyl groups attached to an aromatic ring structure (Mohammed and Manan, 2015) and are generally soluble in water (Lin et al., 2018). Its antioxidant properties are determined through the mechanism of chelation formation or scavenging (Astuti et al., 2021). Gautam et al. (2013) proved that the flavonoid extracts of *Vitex negundo* and *Andrographis paniculata* had larvicidal activity against *Anopheles stephensi* and *A. aegypti* mosquitoes. Phytochemicals derived from plant materials can act as larvicides, insect growth regulators, repellants, and oviposition attractants (Prabhu et al., 2011).

Moringa leaf extract from the Giri Banyuwangi area can kill *A. aegypti* mosquito larvae with an LC50 of 3953.17 ppm and an LT50 of 18.98 hours (Yasi and Harsanti, 2018). Hikmah and Ardiansyah (2018) showed that Moringa leaf extract (*M. oleifera*) combined with fig leaf (*Ficus carica*) at a ratio of 75%: 25% was effective in triggering the mortality of *A. aegypti* larvae. With this combination, larval

mortality reached 62% after 10 hours of exposure.

Moringa plants contain various bioactive chemicals, such as alkaloids, saponins, tannins, and phenols, that have the potential as larvicides (Putra et al., 2016). Meye et al. (2021) proved that the alkaloid and tannin compounds of Moringa leaf extract are toxic to *A. aegypti* larvae, indicating that they have the potential to be developed as natural pesticides or biolarvicides. However, little data show the application of flavonoid compounds from Moringa leaf extract directly to *A. aegypti* larvae. This research was conducted to study the potential use of Moringa leaf flavonoids as biolarvicides in suppressing the growth of *A. aegypti* mosquito larvae.

2. MATERIALS AND METHODS

2.1. Materials

The materials used were Moringa leaves (*Moringa oleifera* L) obtained from Baumata Timur Village, Kupang Regency (semi-arid region), *A. aegypti* eggs (Waikabubak Health Research and Development Center NTT), aquadest, 70% ethanol, n-hexane (Sigma), ethyl acetate (Merck), chloroform (Sigma), magnesium powder, concentrated HCl (Sigma), 10% NaOH, acetic acid (Sigma), n-butanol (Merck), 1% AlCl₃ detector, and methanol (Merck). The tools used were graduated cylinder, Erlenmeyer, test tube racks, tongs, beakers, blenders (National), UV-Vis spectrophotometer (Genesys 10S UV-Vis Spectrophotometer), filter paper, oven, medium-sized plastic containers, sifter trays, filter cloth, rotary vacuum evaporator (Buchi Rotavapor R-210), stirring rod, analytical balance (Digital SF400), glass plate, Thin Layer Chromatography (TLC) plate, water bath, silica Gel G60F254, spray bottle, ultraviolet lamp, coverslip, syringe, funnel, dropper, sieve, knife, glass jar, static, test tube, volume pipette, loop, and digital camera.

2.2. Maceration

The Moringa leaves were used from stalks number 2-5. The leaves were dried, mashed with a blender, and filtered. A total of 400 grams of Moringa leaf powder was macerated with 800 mL of 70% ethanol and stirred twice a day. After 24 hours, it was filtered and separated between the dregs and the filtrate. The dregs were macerated again with new ethanol and repeated until the clear filtrate was obtained. The filtrate obtained was concentrated with an evaporator at 40°C (Yasi and Harsanti, 2018). The yield was calculated using the following formula:

$$\%Yield = \frac{\text{weight of extract}}{\text{weight of moringa leaf powder use}} \times 100\%$$

2.3. Extract fractionation

A total of 5 g of Moringa leaf extract was dissolved in 100 mL of water, stirred until it was runny and homogeneous, and then put into a separating funnel. Fractionation was carried out with 10 mL of n-hexane solvent. The solvent was put into a separating funnel and then shaken 3 times to form 2 layers, namely n-hexane and a layer of water. The n-hexane layer and the aqueous layer were further separated. The water layer was fractionated with 10 mL of chloroform to form 2 layers: the chloroform and the water. The chloroform layer and the aqueous layer were separated. The aqueous layer was fractionated with 10 mL of ethyl acetate to obtain an ethyl acetate and a water layer. The ethyl acetate layer and the aqueous layer were separated. The above process was repeated 5 times. This process produced n-hexane fraction, chloroform fraction, and ethyl acetate fraction. Furthermore, the three fractions were evaporated by heating using a water bath for 15 minutes at 100°C (Simanjuntak, 2008).

2.4. Flavonoid phytochemical test

As much as 1 mL of the three fractions were put into 3 test tubes. The first tube was reacted with magnesium powder and 2-4 drops of concentrated HCl and shaken. The formation of red color indicates the presence of flavonoids from the flavonol and flavanone

groups. The second tube was dropped with concentrated HCl and heated for 15 minutes on a bath. The orange color formed indicates the presence of anthocyanidin group flavonoids. The third tube was dripped with 10% NaOH solution, and the color change indicated the presence of phenolic flavonoids (Zirconia et al., 2015).

2.5. Separation of flavonoid compounds with TLC

The stationary phase used 4 G60F254 silica plates measuring 7 x 1 cm, which were marked with a line 1 cm from the bottom edge of the plate to indicate the initial position of the spots and 1 cm from the top edge of the plate to indicate the boundaries of the elution process. The TLC plate was activated by heating in an oven at 105°C for 15 minutes to remove moisture, then removed and cooled.

The mobile phase (eluent) used several mixed eluents, including n-hexane: ethyl acetate (16: 4), acetic acid: H₂O: concentrated HCl (15: 5: 1.5), n-butanol: acetic acid: water (8: 2: 10), methanol: ethyl acetate (16: 4). Each eluent was put into a beaker. The positive ethyl acetate fraction containing flavonoids was taken as much as 5 mL using a syringe, and then it was spotted on a plate that had been marked and put into a beaker containing the eluent. The elution process was stopped when a predetermined limit was reached. The plate was removed, dried, and then wrapped in aluminum foil (Rahmawati, 2015; Zirconia et al., 2015). The silica plate was then observed under UV light at a wavelength of 366 nm. The visible spots were marked with a pencil, and the distance traveled by each spot and the R_f (Retardation factor) value were calculated.

$$RF = \frac{\text{the distance traveled by the substance}}{\text{distance traveled by the mobile phase}}$$

(Sari, 2011).

2.6. Larva preparation

A. aegypti eggs were incubated in water media. Larvae were reared for 3-5 days to reach instar III and IV larvae with complete and clear anatomical characteristics, there

were parts of the head (cephal), chest (thorax), abdomen, spines on the chest begin to be clearly visible, and breathing funnel (siphon) which was blackish brown. Larvae were fed with dog food (Buni, 2013).

2.7. Research design

This study used a completely randomized design (CRD) consisting of 6 treatments with 3 replications. The treatments applied were variations in flavonoid concentrations (0 ppm (P0), 12.5 ppm (P1), 25 ppm (P2), 50 ppm (P3), 75 ppm (P4), and 100 ppm (P5). Into each container, flavonoid compounds were added according to the predetermined concentration and added water until it reached 100 mL. The solution was then stirred until it was runny and homogeneous. 20 *A. aegypti* larvae were placed into each container, and the larval mortality was observed every 2 hours for 24 hours (Imanta and Hidajati, 2017) using the formula:

$$M = \frac{Mt}{M0} \times 100\%$$

Where M is the percentage of larval mortality (%), Mt is the number of dead larvae, and M0 is the number of early larvae.

In addition, the Lethal Concentration 50 (LC50) was determined, which is the concentration of the extract that can cause 50% larval death, and the Lethal Concentration Time 50 (LT50) is the time needed to kill up to 50% of the larvae.

The percentage of larval mortality was analyzed using analysis of variance (ANOVA) to determine the effectiveness of flavonoid compounds in *A. aegypti* larvae. Significant differences between treatments were tested using Duncan MRT (Multiple Range Test), while LC50 and LT50 were analyzed using the Minitab version 16 program.

3. RESULTS AND DISCUSSION

3.1. Phytochemical test

The phytochemical test proved that the ethyl acetate fraction gave positive results of containing flavonoid compounds, whereas the chloroform and n-hexane fractions gave negative results (Fig.1). The first flavonoid test used magnesium powder and added with concentrated HCl. The polyhydroxy flavonols will be reduced by magnesium metal in hydrochloric acid, resulting in red benzopyrylium or flavilium salts and foaming. The second flavonoid test used concentrated HCl then heated. HCl hydrolyzes and breaks down anthocyanins into anthocyanidins, heating accelerates the reaction until an orange color was formed. The third flavonoid test with 10% NaOH produced a red to brown color because flavonoid compounds formed acetophenone which reacted with NaOH. Phytochemical tests conducted by Yasi and Harsanti (2018) proved that Moringa leaf extract contains flavonoid compounds. In this study, the ethyl acetate fraction was positive for flavonoids, so it was continued with Thin Layer Chromatography (TLC) (Zirconia, 2015).

The eluent mixture of n-butanol: acetic acid: water (8:2:10) in TLC provided the best separation by producing two stains with Rf values of 0.42 and 0.9, respectively (Fig. 1). In contrast, a mixture of n-hexane: ethyl acetate (16:4) eluent, concentrated acetic acid:water: HCl (15:5:1,5), and methanol: ethyl acetate (16:4) resulted in only one stain. The separation occurs because the eluent used is polar so that it can separate flavonoid compounds which are also polar. According to Latif et al. (2018), a good eluent is an eluent that can separate compounds in large quantities marked by the appearance of stains. Yuda (2017) used the mobile phase of n-butanol: acetic acid: water (1:4:5) for the flavonoid TLC test and produced six spots.

The appearance of a light blue color on the two TLC stains observed under UV light proved that the Moringa leaf extract was positive for flavonoids which were thought to be from the isoflavone flavonoid compound group. Yuda (2017) proved that the blue fluorescence at UV 366 nm with a length of Rf 0.76 is a type of isoflavone flavonoid containing a free 5-OH group.

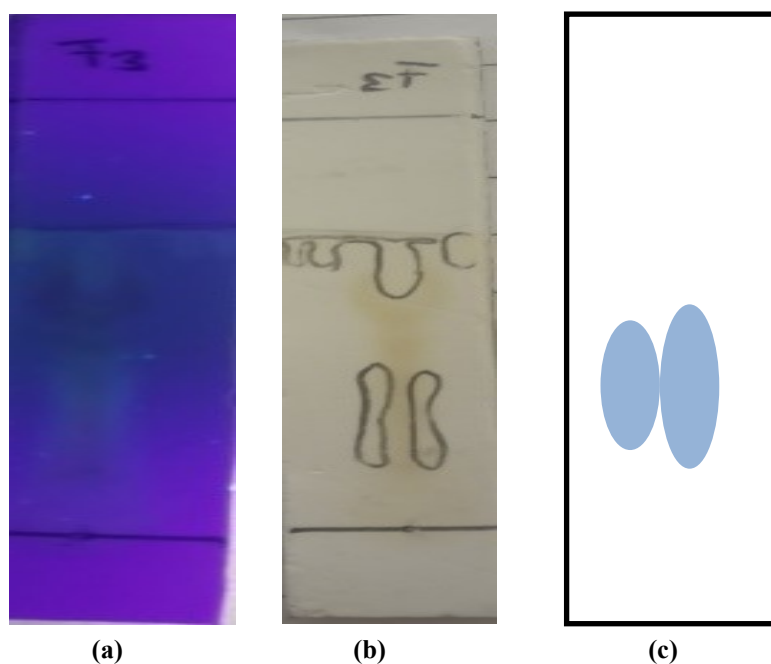


Figure 1. TLC results of the ethyl acetate fraction of Moringa leaf extract with n-butanol as eluent: acetic acid: water (8:2:10). Observations under UV light (λ 366 nm) (a), without UV light (b), and picture illustrations (c).

Table 1. Mortality percentage of *A. aegypti* larvae after 24 hours of treatment

Treatment (ppm)	Repetition			Total Deaths	Average	Percentage
	1	2	3			
P0 (0)	0	0	0	0	0	0 ^a
P1 (12.5)	14	14	15	43	14.3	72 ^b
P2(25)	17	18	17	52	17.3	87 ^{bc}
P3(50)	19	18	20	57	19.0	95 ^c
P4 (75)	20	20	20	60	20.0	100 ^c
P5 (100)	20	20	20	60	20.0	100 ^c

* Numbers in columns with the same superscript are not significantly different

3.2. Effects of Moringa leaf extract flavonoids

Moringa leaf flavonoids are very potential as larvicides of *A. aegypti*. The results of the larvicidal test of Moringa leaf flavonoids are presented in Table 1. Table 1 shows that the higher the flavonoid concentration, the higher the mortality percentage of *A. aegypti* larvae. The analysis of variance (ANOVA) showed that the flavonoids of Moringa leaf extract had a very significant effect ($p = 0.000$) on the mortality of *A. aegypti* larvae. The use of flavonoids with concentrations of 75 ppm and 100 ppm can trigger larval death up to 100%. However, the two treatments were not statistically significant ($P > 0.05$) in larval mortality compared to concentrations of 50 ppm and 25 ppm. This study showed that the application of Moringa leaf flavonoids at a dose of 25 ppm could initiate larval death, although it was 13% lower than the application of 75 ppm. Increasing the concentration of flavonoids to 50 ppm could initiate an increase in mortality 5% lower than the 75 ppm application. The toxic effects caused by larval mortality ranged from 87%-100%, proving that Moringa leaf flavonoids become toxic loads and are very potential as natural larvicides when applied at adequate concentrations.

A. aegypti larvae treated with flavonoids showed poisoning symptoms such as restlessness, up and down movements in water media (telescopic), and death marked by floated mosquito larvae on the surface of the media and did not respond when stimulated by touch. Flavonoids are plant secondary metabolites with various metabolic

functions (Makita et al., 2016). Harith et al. (2018) stated that in plants, flavonoids act as attractants or excitants, repellents or feed deterrents, and also as oviposition inhibitors. The toxicity of flavonoids triggers larvicidal activity. In this study, flavonoids with a concentration of 75 ppm caused death up to 100% after exposure for 24 hours. In contrast, using moringa leaf extract tannins at a concentration of 75 ppm after 72 hours of exposure could only kill larvae with a mortality percentage of 67% (Meye et al., 2021).

Flavonoids work as respiratory toxins that enter the body through the respiratory system (Cania and Setyaningrum, 2013). Moringa leaf flavonoid compounds are thought to affect and damage the respiratory system and cause nervous wilting, resulting in larvae not being able to breathe and ending in death. Moringa leaf flavonoids stimulate cytoplasmic membrane damage at the cellular level, causing cells to leak and cause the enzyme system to inactivate. As a result, phospholipids cannot maintain the shape of the cytoplasmic membrane so that the membrane breaks and causes the death of *A. aegypti* larvae (Hebert and Hamidah, 2018).

3.3. Lethal concentration 50 (LC₅₀) of Moringa leaf flavonoids

LC₅₀ was determined by probit analysis to determine the effective concentration that could kill 50% of the total larvae of the test. The relationship curve between flavonoid concentration and the number of larval mortality is presented in Fig. 2.

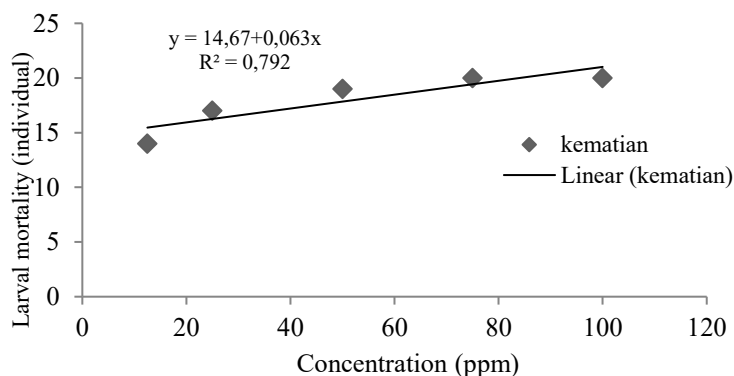


Figure 2. The relationship curve between flavonoid concentration and the number of deaths of *A. aegypti* mosquito larvae

Fig. 2 shows that the percentage of mortality of *A. aegypti* mosquito larvae and the concentration of Moringa leaf flavonoids follow the equation $Y = 14.67 + 0.063x$. Each increase in flavonoid concentration of Moringa leaf extract by one unit will increase the mortality of 0.063 individual larvae of *A. aegypti* with a coefficient of determination (R^2) of 0.792. It means that 79.2% of mosquito larvae mortality was caused by the contribution of flavonoid compounds from Moringa leaf extract and the rest by other factors not observed in this study. Coelho et al. reported that sulfate flavonoids in the Sterculiaceae family showed strong larvicidal activity against *A. aegypti* larvae so that they have the potential to be developed as domestic larvicides in combating *A. aegypti*, which is an insect vector for several viral diseases such as dengue fever and Zika (Fernandes et al., 2018). According to Haditomo, flavonoids are stomach poisons that interfere with the digestive system of *A. aegypti* larvae and cause failure to grow and then die (Utami et al., 2016). Flavonoids such as furanoflavonoid karanjin, pyranoflavonoid karanjachromene, and oleic acid from *Milletia pinnata* were very effective against larvae of *A. aegypti* and *Culex pipiens pallens*. The flavonoids karanjachromene, pongamol, and pongarotene have strong inhibitory effects on mosquito larvae acetylcholinesterase but do not affect cAMP levels (Perumalsamy et al., 2015).

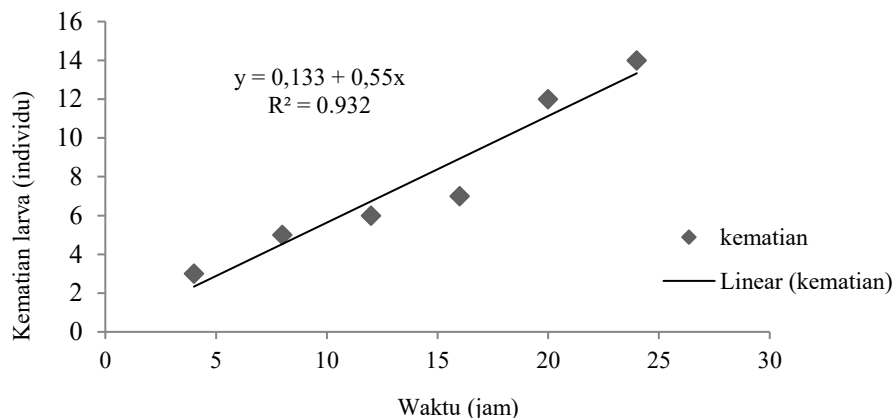
Probit analysis showed that the LC_{50} of Moringa leaf flavonoids in *A. aegypti* larvae was reached at a concentration of 7.96 ppm. It means that Moringa leaf flavonoids (*Moringa oleifera* L) could kill 50% of test larvae at 7.96 ppm application. The relatively small LC_{50} value proves that flavonoid compounds have the potential as biolarvicides in mosquito larvae (Rumengan, 2010). The LC_{50} value for the toxicity test is classified as very high if <1 mg/L, high if it ranges from 1-10 mg/L, moderate if $>10-100$ mg/L, and low if >100 mg/L (Hendri et al., 2010).

3.4. Lethal concentration time (LT_{50}) of Moringa leaf flavonoids

LT_{50} was determined by probit analysis to determine the effective time in killing 50% of the test larvae. The LT_{50} values for each concentration are shown in Table 2. Table 2 shows that the application of 75 ppm flavonoids gave a shorter LT_{50} value of 2.083 hours compared to other treatments. It means that after 2.08 hours of administration of 75 ppm flavonoids, 50% of *A. aegypti* larvae will die. Cania and Setyaningrum (2013), who used legundi leaf extract, found that the higher the concentration of the extract, the shorter the LT_{50} . The linear regression equation curve of the relationship between time and number of larval mortality after being treated with flavonoids from Moringa leaf extract is presented in Fig. 3.

Table 2. LT₅₀ Value of Moringa Leaf Flavonoids

Treatment	LT ₅₀ Value
12.5 ppm	17.4357
25 ppm	6.32661
50 ppm	2.62772
75 ppm	2.08281
100 ppm	3.45742

**Figure 3.** Relationship curve of time and number of larvae mortality treated with flavonoid

The pattern of the relationship between the time and the number of deaths of *A. aegypti* larvae given flavonoids as shown in Fig 3 shows that each time increase of one unit will increase the mortality of larvae by 0.55 individuals following the equation, $Y = 0.133 + 0.55x$ with a coefficient of determination (R^2) of 0.932. It indicates that 93.2% of larval mortality was triggered by the length of time the larvae were exposed to Moringa leaf flavonoids, while the rest was caused by other factors not observed in this study. This study confirms Gautam et al. (2013), who stated that the larvicidal activity of *Vitex negundo* and *Andrographis paniculata* against *Anopheles stephensi* and *A. aegypti* was a synergistic effect of phenolic compounds, including flavonoids. However, further research is needed before the commercial use of the flower bud flavonoid extract of *V. negundo*. Likewise, the flavonoids of Moringa leaf extract in this study need to be studied further before being applied commercially.

4. CONCLUSIONS

The application of 75 ppm Moringa leaf flavonoids could increase the mortality of *A. aegypti* larvae up to 100% with a shorter Lethal Concentration Time (LT₅₀) (2.08 hours) than other treatments. However, the administration of flavonoids with a concentration of 7.96 ppm could cause larval mortality up to 50% (LC₅₀).

ACKNOWLEDGEMENT

Acknowledgments are conveyed to the Biology Study Program, Faculty of Science and Engineering, Nusa Cendana University for funding this research.

LIST OF REFERENCES

- Astuti, M.D., M. Wulandari, K. Rosyidah, & R. Nurmasari. (2021). Analisis proksimat dan fitokimia buah pedada (*Sonneratia ovate* Back). *Jurnal Sains dan Terapan Kimia*. 15(2), 154-163.
- Bere, S.M. (2020, April 3). *Jumlah penderita DBD di NTT bertambah jadi 4.518 orang, 48 meninggal*. [Halaman web]. Diakses dari <https://regional.kompas.com/read/2020/04/03/07304521/jumlah-penderita-dbd-di-ntt-bertambah-jadi-4518-orang-48-meninggal?page=all>.
- Buni, V. A. (2013). Efektivitas daya bunuh ekstrak daun kirinyu (*Chromolaena odorata* L.) terhadap larva nyamuk *Aedes aegypti*. Skripsi. *Jurusan Biologi Fakultas Sains dan Teknik Universitas Nusa Cendana*.
- Cania, E., & E.Setyaningrum. (2013). Uji efektifitas larvasida ekstrak daun legundi (*Vitex trifolia*) terhadap larva *Aedes aegypti*. *Medical Journal of Lampung University*. 2(4), 52-60.
- Coppin, J.P., Yanping Xu, Hong Chen, Min-Hsiung Pan, Chi-Tang Ho, R. Juliani, J.E. Simon, & Qingli Wu. (2013). Determination of flavonoids by lc/ms and anti-inflammatory activity in *Moringa oleifera*. *Journal of Functional Foods*. 5, 1892-1899.
- Fernandes, D.A., M.S.R. Souza, Y.C.F. Teles, L.H.G. Oliveira, J.B. Lima, A.S.Conceicao, F.C. Nunes, T.M.S. Silva, & M.de Fatima V. de Souza. (2018). New sulphated flavonoids and larvicidal activity of *Helicteres velutina* K. Schum (Sterculiaceae). *Molecules*. 23, 2784-2795.
- Ferreira, P.M.P., A.E.U Carvalho, D.F. Farias, N.G. Cariolano, V.M.M. Melo, M.G.R. Queiroz, A.M.C. Martins dan J.G. Machado-Neto. (2009). Larvicidal activity of water extract of *Moringa oleifera* seeds against *Aedes aegypti* and its toxicity upon laboratory animals. *Anais da Academia Brasileira de Ciencias*. 81(2), 207-216.
- Gautam, K., P. Kumar dan S. Poonia. (2013). Larvicidal activity and gc-ms analysis of flavonoid of *Vitex negundo* and *Andrographis paniculata* against two vektor mosquitoes *Anopheles stephensi* and *Aedes aegypti*. *J Vector Borne. Dis* 50 September, 171-178.
- Harith, S.S., S.N.A.S. Mohd, N.A. Aziz, M.M. Mydin, & N.T.S. Nasir. (2018). Phytochemical screening and larvicidal activity of *Murraya koenigii* leaves extracts against mosquito larvae. *Malaysian Journal of Analytical Science*. 22(3), 471-476.
- Hebert, A. dan Hamidah. (2018). Evaluasi toksisitas ekstrak metanol daun jeruk nipis (*Citrus aurantifolia*) terhadap kematian larva nyamuk *Aedes aegypti*. *Aspirator*. 10(1), 57-64.
- Hendri, M., G. Diansyah, & J.Tampubulon. (2010). Konsentrasi lethal (LC₅₀-48 jam) logam tembaga (Cu) dan logam kadmium (Cd) terhadap tingkat mortalitas juwana kudo laut (*Hippocampus* sp). *Jurnal Penelitian Sains*. 13(1D), 1310726 – 1310730.
- Hikma, S.R. dan S. Ardiansyah. (2018). Kombinasi ekstrak daun kelor (*Moringa oleifera*) dengan ekstrak daun tin (*Ficus carica* L) sebagai larvasida terhadap larva *Aedes aegypti*. *Medica*. 1(2), 94-102.
- Imanta, E., & N. Hidajati. (2017). Uji biolarvasida nyamuk *Aedes aegypti* dari hasil isolasi ekstrak metanol tanaman sambilotto (*Andrographis paniculata* NESS). *UNESA Journal of Chemistry*. 6(1), 36-41.
- Latif, R.A., M.A. Mustapa, & S. Duengo. D. (2018). Analisis kadar senyawa flavonoid ekstrak metanol kulit batang waru (*Hibiscus tiliaceus* L) dengan menggunakan metode spektrofotometri UV-VIS. [Halaman web]. Diakses dari <https://repository.ung.ac.id>.
- Lin, M., J. Zhang, & X. Chen. (2018). Bioactive flavonoids in *Moringa oleifera* and their health-promoting properties. *Journal of Functional Foods*. 47, 469-479.

- Makita, C., L. Chimuka, P. Steenkamp, E. Cukrowska, & E. Madala. (2016). Comparative analyses of flavonoid content in *Moringa oleifera* and *Moringan ovalifolia* with the aid of UHPLC-qTOF-MS Fingerprinting. *South African Journal of Botany*. 105, 116-122.
- Maulana, S., F. Musthofa, A. Yamin, N. Juniarti, & A. Putri. (2021). Pengaruh biolarvasida daun tanaman sebagai kontrol vektor nyamuk *Aedes aegypti* penyebab demam berdarah: literature review. *Jurnal Medika Hutama*. 2(3), 978-989.
- Meye, E.D., F. Kia Duan, S.R. Toly, V.M. Ati, F.M. Ike Septa, A.N. Momo, & T. Hermanus. (2021). Uji efektivitas senyawa alkaloid dan tanin ekstrak daun kelor (*Moringa oleifera*) terhadap mortalitas larva nyamuk (*Aedes aegypti*). *Jurnal Biotropikal Sains*. 18(1), 24-35.
- Mohammed, S., & F. Abd Manan. (2015). Analysis of total phenolics, tannin and flavonoids from *Moringa oleifera* seed extract. *Journal of Chemical and Pharmaceutical Research*. 7(1), 132-135.
- Nwankwo, E.N., N.J. Okonkwo, C.U. Ogbonna, C.J.O. Akpom, C.M. Egbuche, & B.C. Ukonze. (2015). *Moringan oleifera* and *Annona muricata* seed oil extracts as biopesticides against the second and fourth larval instar of *Aedes Aegypti* L. (Diptera: Culicidae). *J.Biopest*. 8(1), 56-61.
- Perumalsamy, H., M.J. Jang, J.R. Kim, M. Kadarkarai, & Y.J. Ahn. (2015). Larvicidal activity and possible mode of action of four flavonoids and two fatty acids identified in *Milletia pinnata* seed toward three mosquito species. *Parasites dan Vectors*. 8, 237-250.
- Prabu, K., K. Murugan, A. Nareshkumar, N. Ramasubramanian, & S. Bragadeeswaran. (2011). Larvicidal and repellent potential of *Moringa oleifera* against malarial vector, *Anopheles stephensi* Liston (Insecta: Diptera: Culicidae). *Asian Pacisic Journal of Tropical Biomedicine*. 1(2), 124-129.
- Putra, I.D, A.G. Dharmayudha, & L.M. Sudimatini. (2016). Identifikasi senyawa kimia ekstrak etanol daun kelor (*Moringa oleifera* L) di Bali. *Medicus Veterinus Indonesia*. 5 (5): 464-473.
- Rahmawati, F. (2015). *Optimasi penggunaan kromatografi lapis tipis (KLT) pada pemisahan senyawa alkaloid daun pulai (Alstonia scholaris L.R.Br)*. Skripsi. Universitas Islam Negeri Maulana Malik Ibrahim. Malang.
- Rumengan, A.P. (2010). Uji larvasida nyamuk *Aedes aegypti* dari Ascidian (*Didemnum molle*). *Jurnal Perikanan dan Kelautan*. 6(2), 83-86.
- Sari, J.F. (2011). *Penerapan metode kromatografi lapis tipis (KLT) untuk membedakan Curcuma domestica Val, Curcuma xanthorrhiza Roxb, Curcuma zedoria Rosc, Curcuma manga Val dan Zipj, Curcuma aeruginosa Roxb dalam campuran*. Departemen Farmakognosi Dan Fitokimia Fakultas Farmasi Universitas Arlangga. Surabaya.
- Sharma, E., P Mathur, D. Kumar, M. Srivastava, & A. Prasad. (2013). *Larvicidal activity of Moringa oleifera leaves against human malaria vector Anopheles stephensi Liston (Insecta: Diptera: Culicidae)*. XII International Conference on Vector and Vector Borne Diseases Challenges in 21st Century: Their Global Impact and Strategic Management. 117-122.
- Simanjuntak, M.R. (2008). *Ekstraksi dan fraksinasi komponen ekstrak daun tumbuhan senduduk (Melastoma malabathricum L) serta pengujian efek sediaan krim terhadap penyembuhan luka bakar*. Skripsi. Fakultas Farmasi Universitas Sumatera Utara. Medan.
- Utami, W.W., A.R. Ahmad dan A. Malik. (2016). Uji aktivitas larvasida ekstrak daun jarak kepyar (*Ricinus communis* L) terhadap larva nyamuk *Aedes aegypti*. *Jurnal Fitofarmaka Indonesia*. 3(1), 141-145.

Yasi, M.R. dan R.S. Harsanti. 2018. Uji daya larvasida ekstrak daun kelor (*Moringa oleifera*) terhadap mortalitas larva *Aedes aegypti*. *Journal of Agromedicine and Medical Sciences*. 4(3), 159-164.

Yuda, P.E.S.K., E.C. Ningsih, N.L.P.Y. Winariyanthi. (2017). Skrinning fitokimia dan analisis kromatografi lapis tipis ekstrak tanaman patikan kebo (*euphorbia hirta* L). *Jurnal Ilmiah Medicamento*. 3 (2), 61-70.

Zirconia, A., N. Kurniasih dan V. Amali. (2015). Identifikasi senyawa flavonoid dari daun kembang bulan (*Tithonia diversifolia*) dengan metode pereaksi geser. *Al Kimia*. 2(1), 9-17.